Computers & Industrial Engineering 158 (2021) 107408

Contents lists available at ScienceDirect

Computers & Industrial Engineering

journal homepage: www.elsevier.com/locate/caie

African vultures optimization algorithm: A new nature-inspired metaheuristic algorithm for global optimization problems

Benyamin Abdollahzadeh [a], Farhad Soleimanian Gharehchopogh [a,*], Seyedali Mirjalili [b,c]

[a] Department of Computer Engineering, Urmia Branch, Islamic Azad University, Urmia, Iran
[b] Centre for Artificial Intelligence Research and Optimisation, Torrens University Australia, Fortitude Valley, Brisbane 4006, QLD, Australia
[c] Yonsei Frontier Lab, Yonsei University, Seoul, South Korea

ARTICLE INFO

Keywords:
Metaheuristic
Algorithm
Artificial vulture optimization algorithm
African vultures
Optimization
Artificial Intelligence
Benchmark
Soft Computing

ABSTRACT

Metaheuristics play a crucial role in solving optimization problems. The majority of such algorithms are inspired by collective intelligence and foraging of creatures in nature. In this paper, a new metaheuristic is proposed inspired by African vultures' lifestyle. The algorithm is named African Vultures Optimization Algorithm (AVOA) and simulates African vultures' foraging and navigation behaviors. To evaluate the performance of AVOA, it is first tested on 36 standard benchmark functions. A comparative study is then conducted that demonstrates the superiority of the proposed algorithm compared to several existing algorithms. To showcase the applicability of AVOA and its black box nature, it is employed to find optimal solutions for eleven engineering design problems. As per the experimental results, AVOA is the best algorithm on 30 out of 36 benchmark functions and provides superior performance on the majority of engineering case studies. Wilcoxon rank-sum test is used for statistical evaluation and indicates the significant superiority of the AVOA algorithm at a 95% confidence interval.

1. Introduction

The use of metaheuristic algorithms to solve various search problems, continuous and discrete optimizations has grown dramatically. Due to the complexity of continuous optimization problems and mathematical methods' inability to provide the optimal solution, metaheuristic algorithms are a reliable tool for continuous optimization problems. Mathematical methods have been used to solve many scientific and engineering problems and cover a wide range of different issues, but mathematical methods still face many difficulties in solving many optimization issues, despite their precision. Efforts and research by researchers in recent years have led to the development of algorithms inspired by natural phenomena, which investigate the evolution and behavior of nature creatures, which have led to the emergence of metaheuristic algorithms (Pršić, Nedić, & Stojanović, 2017). In addition to algorithms derived from nature, another evolutionary metaheuristic algorithm has been devised for optimization problems (Abualigah et al., 2021). Due to the inability of accurate optimization methods to solve complex and multidimensional problems, approximation algorithms have been proposed as a new approach to solving such problems. The approximation algorithms are divided into two major categories, including heuristic and metaheuristic methods. Heuristic algorithms have received less attention because they are trapped in the local trap and solve specific optimization problems (Benyamin, Farhad, & Saeid; Boussaïd, Lepagnot, & Siarry, 2013; Dokeroglu, 2019; Gharehchopogh & Gholizadeh, 2019; Gharehchopogh, Shayanfar, & Gholizadeh, 2019; Hussain et al., 2019; Nedić et al., 2017). Metaheuristic algorithms can find optimal solutions to various challenging and complex optimization problems (Stojanovic, He, & Zhang, 2020). Metaheuristic algorithms provide acceptable solutions reasonably, but they do not guarantee optimal solutions.

Several nature-inspired metaheuristic algorithms have been proposed lately. Despite the differences in inspiration and search mechanisms, they strive to balance exploitation and exploration. At the beginning of the generation, metaheuristic algorithms benefit from the exploration process to produce new solutions. It gradually transits to exploitation, in which the focus is on accuracy improvement of the solutions obtained in the exploration phase. The exploitation process produces a new solution based on the best solution available to the population. As a result, metaheuristic algorithms use two essential exploration and exploitation processes to avoid getting trapped in the local trap and converge toward the target (Abdollahzadeh & Gharehchopogh, 2021; Gharehchopogh, Maleki, & Dizaji, 2021; Mohmmadzadeh & Gharehchopogh, 2021; Rahnema & Gharehchopogh, 2020).

* Corresponding author.
E-mail address: farhad@iaurmia.ac.ir (F.S. Gharehchopogh).

https://doi.org/10.1016/j.cie.2021.107408
Received 16 January 2021; Received in revised form 12 May 2021; Accepted 17 May 2021
Available online 21 May 2021
0360-8352/© 2021 Published by Elsevier Ltd.

Nomenclature

AVOA	African Vultures Optimization Algorithm
GA	Genetic Algorithm
HS	Harmony Search
ABC	Artificial Bee Colony
FA	Firefly algorithm
GWO	Grey Wolf Optimizer
WOA	Whale Optimization Algorithm
GSO	Galactic Swarm Optimization
CSA	Crow Search Algorithm
IPO	Inclined Planes system Optimization
ABO	Artificial Butterfly Optimization
FFA	Farmland Fertility Algorithm
QSA	Queuing Search Algorithm
TSA	Tunicate Swarm Algorithm
AOA	Arithmetic Optimization Algorithm
JS	Jellyfish Search
ALSO	artificial lizard search optimization
TLBO	Teaching Learning Based Optimization
CS	Cuckoo Search
SA	Simulated Annealing
VPS	Vibrating Particles System
GSA	Gravitational Search Algorithm
BBO	Biogeography-Based Optimization
GbSA	Galaxy-based Search Algorithm
BMO	Bird Mating Optimizer
BB-BC	Big-Bang Big-Crunch
CBO	Colliding Bodies Optimization
SSO	Social Spider Optimization
IWD	Intelligent Water Drops
DE	Differential Evolution
CSS	Charged System Search
WEO	Water Evaporation Optimization
GSO	Glowworm Swarm Optimization
LCA	League Championship Algorithm
DEO	Dolphin echolocation Optimization
WCA	Water Cycle Algorithm
UM	Unimodal
UM	multi-modal
CM	composition model
CEC 2014	CEC 2014 competition benchmark
CEC 2011	CEC 2011 Real World Optimization Problems
S	Scalable
NS	Non-Separable
R	Rotated
MM	Multi-modal
UM	Unimodal
d	Dimension
SH	Shifted
N	Number of functions combined
STD	Standard Deviation
AVG	Average Results
CCD	central composite design
$population$	Number of vultures
$maxiterations$	Maximum number of iterations
$iteration$	Current number of iteration
$rand$	A random number between [0,1]
Sin	function of sine
cos	function of cosine
lb	The lower bound of search spaces
ub	The Upper bound of search spaces
$BestVulture_1$	First best vulture
$BestVulture_2$	Second best vulture
P_i	vulture position vector
$R(i)$	one of the best vultures selected
F	rate of starvation of vultures
L_1	Probability parameter for selecting the first best vulture
L_2	Probability parameter for selecting the second-best vulture
w	A parameter that determines the disruption of the exploration and exploitation phases
P_1	A parameter to determine the probability of selecting the mechanisms in the exploration phase
P_2	A parameter to determine the probability of selecting the mechanisms in the exploitation phase of the first part
P_3	A parameter to determine the probability of selecting the mechanisms in the exploitation phase of the second phase

Metaheuristic algorithms have been proposed more than other methods in solving optimization problems due to four main factors (Gharehchopogh & Gholizadeh, 2019; Gharehchopogh et al., 2019). First, the metaheuristic algorithms are inspired by simple concepts in nature that make them easy to implement. Simplicity helps computer scientists improve or hybrid metaheuristic methods and solve a vaudeville of problems quickly. It also makes it easy to learn these algorithms. Second, these algorithms' flexibility has made them useful in solving various optimization problems without altering the algorithm's structure. Third, most metaheuristic methods do not require derivation because these algorithms start to generate random solutions to the optimization problem. Therefore, we do not need to calculate the search space derivative to find the optimal solution. Finally, metaheuristic algorithms escape from local optimality compared to traditional methods.

Studies show that most of the proposed metaheuristic algorithms are inspired by natural foraging and hunting behaviors—however, there little on the modeling of vultures in nature to develop an optimization algorithm. The most recent work goes back to 2013, in which authors proposed a simple optimization algorithm inspired by Egyptian vultures (Sur, Sharma, & Shukla, 2013). This work proposes a different algorithm inspired by African vulture's lifestyles with a comprehensive model to develop a new metaheuristic optimization algorithm.

Some of the contributions of this paper are as follows:

- Creating a coefficient vector F with different random motions during the optimization operation and use this coefficient vector to change exploration and exploitation phases.
- Creating a different phase shift mechanism prevents premature convergence, escapes from local optimization, and balances the exploitation and exploration phases.
- Providing a new rotational search equation for optimization operations.
- Using the second-best solution in two different ways to simulate African vultures as much as possible.
- Using two different mechanisms in the exploration phase that increase the diversity of the solutions produced.
- Providing four diverse mechanisms in the exploration phase that have increased AVOA algorithm capability in the exploitation phase
- Utilizing LF-based patterns that make local search better with short, different jumps.
- Employing the vector coefficients F, r during the optimization operation, which has a significant impact on the exploitation potential of AVOA.
- Providing a powerful and efficient algorithm with shallow and good execution time and low computational complexity.
- Evaluating and testing AVOA performance using 36 standard benchmark functions and 11 highly complex engineering problems

and comparisons with various powerful and well-known optimization algorithms

In the remainder of the paper, Section 2 deals with nature-inspired metaheuristic algorithms. Section 3 shows the biological principles of African vultures and introduces the synthetic AVOA, which describes the theory, flowchart, and formulation of the proposed algorithm. So, in Section 4, the performance and efficiency of AVOA are tested by the use of standard test functions, and the results are recorded and displayed in separate graphs. The final section of the paper summarizes the conclusions and future works.

2. Related works

In the literature, there are different classifications of meta-heuristics. The majority of such algorithms are inspired by the creatures' collective behavior or evolutionary processes in nature. Genetic Algorithm (GA) has been used with the most essential combinatorial and mutational operators in most optimization problems and is considered a successful algorithm (Holland, 1992) with a large number of variations so far (Hussain & Iqbal, 2018). Another popular algorithm is the Harmony Search (HS) algorithm proposed by Gim et al. (Geem, Kim, & Loganathan, 2001), derived from searching for the best of the harmonics. After presenting the initial version of this algorithm, it was used in many optimization problems because of its simplicity (Manjarres et al., 2013).

In 2005, a bee-based group behavior algorithm called the artificial bee colony (ABC) optimization algorithm was proposed (Karaboga & Basturk, 2007). This algorithm simulated worker bees, prey bees, and searcher bees. In 2008, Yang introduced a Firefly Algorithm (FA) inspired by fireflies' light and radiance (Yang, 2008). In this algorithm, each firefly's light intensity and attractiveness were formulated so that each firefly was compared to the other firefly in terms of brightness or light, and dim fireflies moved to luminous fireflies. The fireflies occasionally flew in simple random order, resulting in an improved version of the algorithm.

Another popular swarm-based algorithm is Bat Algorithm (BA), proposed in 2010 (Yang, 2010). As its name implies, this algorithm mimics bat sound reflection behavior with different pulse diffusion and loudness rates. The Prey-predator algorithm is similar to BA and was introduced in (Tilahun & Ong, 2015). Spider monkey optimization algorithm (Bansal et al., 2014) is also a swarm-based algorithm benefiting from the division and composition of spider monkeys in nature. Some of the other popular algorithms in this class are Farmland Fertility Algorithm (FFA) (Shayanfar & Gharehchopogh, 2018); Grey Wolf Optimizer (GWO) (Mirjalili, Mirjalili, & Lewis, 2014), Whale Optimization Algorithm (WOA) (Mirjalili & Lewis, 2016), Crow Search Algorithm (CSA) (Askarzadeh, 2016), and Harris Hawk Optimization (HHO) (Heidari et al., 2019).

In (Rashedi, Nezamabadi-Pour, & Saryazdi, 2009), an optimization algorithm based on the law of gravity and mass interactions called the Gravitational Search Algorithm was introduced. In this algorithm, search agents are considered masses that interact with each other based

Table 1
Historical to state-of-the-art metaheuristic optimization algorithms.

Name	authors	year	classifications	mechanisms	objectives	Control Volumes
GA (Holland, 1992)	JH Holland	1992	Evolutionary-based	mutation, crossover	Global optimization	*Selection rate, Crossover rate, Mutation rate*
HS (Geem et al., 2001)	ZW Geem et al.	2001	Evolutionary-based	Harmony memory	Combinatorial optimization	*HMS, HMCR, PAR, Bandwidth*
ABC (Karaboga & Basturk, 2007)	D Karaboga et al.	2005	Nature-based	employed bee, onlooker bee and scout bee	constrained optimization	*Limit*
FA (Yang, 2008)	XS Yang	2008	Nature-based	Distance, attractiveness and limiting cases	Global optimization	α, β, γ
GSA (Rashedi et al., 2009)	E Rashedi et al.	2009	physics-based	Law of gravity, Law of motion	Global optimization	*Gravitational constant, Alpha coefficient, Rnorm, Rpower, K*
BA (Yang, 2010)	XS Yang	2010	Animal-based	Movement of Virtual Bats, Loudness and Pulse Emission	Global optimization	Q_{min}Frequency minimum, Q_{max}Frequency maximum, A Loudness, r Pulse rate
SMO (Bansal, 2014)	JC Bansal et al.	2014	Animal-based	Global Leader, Local Leader	*numerical optimization*	*perturbation rate*, *LLL*, *GLL* and maximum number of groups (*MG*)
GWO (Mirjalili et al., 2014)	S Mirjalili et al.	2014	Animal-based	Social hierarchy, Encircling prey, Hunting	Global optimization	Convergence constant a
PPA (Tilahun & Ong, 2015)	SL Tilahun et al.	2015	Nature-based	move the predator, moving preys	Global optimization	follow-up probability,τ
WOA (Mirjalili & Lewis, 2016)	S Mirjalili et al.	2016	Animal-based	Encircling prey, Bubble-net attacking method,	Global optimization	Spiral factor b, Convergence constant a
GSO (Muthiah-Nakarajan & Noel, 2016)	V Muthiah-Nakarajan et al.	2016	swarm-based	galactic motion	global optimization	*Subswarms,* EP_{max} *, c1 , c2 , c3 , c4*
CSA (Askarzadeh, 2016)	A Askarzadeh	2016	Animal-based	the hiding place, follow the crow	*constrained engineering optimization*	*Awareness probability, Flight length*
IPO (Mozaffari et al., 2016)	MH Mozaffari et al.	2016	physics-based	Newton's second law and equations of motion	global optimization	$c_1, c_2, shift_1, shift_2, scale_1, andsacle_2$
ABO (Qi, Zhu, & Zhang, 2017)	X Qi et al.	2017	Nature-based	sunspot flight mode, canopy flight mode, free flight mode	global optimization	$ratio_e$, $step_e$
FFA (Shayanfar & Gharehchopogh, 2018)	H Shayanfar et al.	2018	Nature-based	Multiswarm	*continuous optimization*	*W, Q, K Value*,α, β
QSA (Zhang, 2018)	J Zhang et al.	2018	Human-based	The multi-staff queuing system	*engineering optimization*	*customer*
SSFO (Sang, Pan, & Duan, 2019)	HY Sang et al.	2019	Nature-based	Osphresis foraging, Vision foraging	*global optimization*	PS,P_0, λ_{max}, λ_{min}
AOA (Abualigah, 2020)	L Abualigah et al.	2020	physics-based	Multiplication, Division, Subtraction, and Addition	*global optimization*	α, μ
JS (Chou & Truong, 2021)	JS Chou et al.	2021	swarm-based	active motions and passive motions, time control mechanism	*global optimization*	β and γ
ALSO (Kumar, Singh, & Vidyarthi, 2021)	N Kumar et al.	2021	Animal-based	balanced lumping	*global optimization*	*r1* and *r2*

on Newtonian laws of motion. (Mokhlesi et al., 2013; Sheikhpour, Sabouri, & Zahiri, 2013; Zahiri, 2012). Another physics-based algorithm is the Galactic Swarm Optimization (GSO) algorithm inspired by galactic motion (Muthiah-Nakarajan & Noel, 2016). This algorithm was inspired by the motion of stars, galaxies, and clusters of galaxies under gravity's influence. Another popular algorithm is an Inclined Planes system Optimization (IPO) (Mozaffari, Abdy, & Zahiri, 2016) algorithm, in which search agents work together and move from Newton's second law and equations of motion to better positions in the search space. Due to its good performance, IPO has been used to solve many problems (Mozaffari, Abdy, & Zahiri, 2013; Shahraki & Zahiri, 2017).

Further details about the algorithms reviewed in this section can be found in Table 1.

The algorithm used three common rules in the queuing phenomenon. It is worth mentioning that the researchers in the current research only reviewed a few of the most important and basic metaheuristic algorithms. There are also other metaheuristic optimization algorithms such as: Teaching Learning Based Optimization (TLBO) (Rao, Savsani, & Vakharia, 2011), Cuckoo Search (CS) (Gandomi, Yang, & Alavi, 2013), Simulated Annealing (SA) algorithm (Kirkpatrick, Gelatt, & Vecchi, 1983), Vibrating Particles System (VPS) (Kaveh & Ghazaan, 2017), Gravitational Search Algorithm (GSA) (Rashedi et al., 2009); Biogeography-Based Optimization (BBO) (Simon, 2008), Galaxy-based Search Algorithm (GbSA) (Shah-Hosseini, 2011), Bird Mating Optimizer (BMO) (Askarzadeh, 2014); Big-Bang Big-Crunch (BB-BC) algorithm (Erol & Eksin, 2006), Social Spider Optimization (SSO) (Cuevas et al., 2013), Intelligent Water Drops (IWD) algorithm (Shah-Hosseini, 2009), Colliding Bodies Optimization (CBO) (Kaveh & Mahdavi, 2014), Differential Evolution (DE) (Storn & Price, 1997); Charged System Search (CSS) algorithm (Kaveh & Talatahari, 2010), Water Evaporation Optimization (WEO) algorithm (Kaveh & Bakhshpoori, 2016); Glowworm Swarm Optimization (GSO) (Krishnanand & Ghose, 2009), League Championship Algorithm (LCA) (Kashan, 2014), Dolphin echolocation optimization (DEO) (Kaveh & Farhoudi, 2013), and Water Cycle Algorithm (WCA) (Eskandar et al., 2012).

Considering that scientists are inspired by organisms' movement to solve optimization problems, they formulate and present them under meta-heuristic algorithms. In this paper, we also took inspiration from the behavior of vultures that move en masse to find food and coexistence to introduce a novel algorithm called the AVOA, which will be discussed in detail.

3. Proposed approach based on AVOA

3.1. Africans vultures biological life

Vulture is the name of two groups of hunting birds. New world vultures are native to the Americas, and old-world vultures are native to Europe, Asia, and Africa. There are no vultures in Australia and Antarctica. Most vultures are bald, with no regular feathers. Historically, vultures have been thought to be bald to prevent contamination while feeding on carcasses, but recent research suggests that bare skin plays an essential role in regulating body heat. That is why in cold weather, they dip their heads in the body, and in the heat, they open their necks. Another feature is that, unlike most other birds, they do not make nests. Vultures rarely attack healthy animals but may kill an injured or diseased animal. Numerous vultures have been seen on the battlefields during the wars. Vultures are useful animals to prevent stinging and infecting carcasses, especially in the tropics. Vultures play an essential exosystemic role, and their destruction poses a series of severe health risks to human societies.

The population of vultures is drastically declining, and some African vulture species have been declining to extinction. African countries also need vultures, the most essential and valuable carcasses, given the large rural population and large numbers of colossal animals. There are various vultures in Africa, most of which have the same lifestyle style and find food, often encountering each other and fighting for food (Meteyer et al., 2005; Prinzinger et al., 2002). Some of them are Lappet-faced Vulture Torgos tracheliotos and White-backed Vulture Gyps Africans, and Rüppell's Vulture Gyps rueppelli, as Fig. 1 shows.

Each of the vultures living in Africa has some unique physical characteristics. Therefore, the types of vultures can be divided into three categories (Houston, 1974). The first category includes vultures that are physically abler than all vultures, such as the Lappet-faced Vulture, which have a greater chance of obtaining food than other vultures. The second category includes vultures that are physically weaker than the first type. Some other vultures have a physical advantage: White-backed Vulture Gyps Africans (Houston, 1974; Jackson, Ruxton, & Houston, 2008; Mundy, 1992; Ogada & Buij, 2011). The latter category includes physically weaker vultures than the other two groups: The Hooded Vulture Necrosyrtes monachus. In the natural environment, vultures continually travel long distances to find food (Attwell, 1963; Bamford, Monadjem, & Hardy, 2009; Buckley, 1996; Houston, 1974), one of the most common forms of flight in vultures is rotational flight. Searching for food, vultures move to find one species of vultures that have found food, and it is sometimes possible that several species of vultures move to a single food source, and these vultures come into conflict with each other to obtain food (BosE & Sarrazin, 2007; HOUSTON, 1988; Petrides, 1959). Weak vultures encircle healthy vultures and receive food by tiring the stronger vultures, and the starvation of vultures causes them to become more aggressive (Anderson And Horwitz, 1979; Attwell, 1963; BosE & Sarrazin, 2007; Kendall et al., 2012; Mundy, 1982; Rosewell, Shorrocks, & Edwards, 1990). A new metaheuristic algorithm has inspired this research regarding finding and feeding various vultures in Africa, which will be introduced in more detail in Section 3.2.

3.2. AVOA algorithm

In Section 3.1, the biological principles and how vultures live were discussed. This subsection aims to present a new metaheuristic algorithm called AVOA based on the robust theories and concepts described in Section 3.1. All metaheuristic algorithms in the simulation and formulation stage consider a set of assumptions about the natural environment, then the AVOA algorithm is introduced. In this section, the AVOA algorithm will be implemented step by step, and all the necessary conditions and points will be described in each step of the proposed algorithm according to the basic concepts expressed about vultures. The default AVOA is presented as follows.

- There may be up to N vultures in an environment. It determines the same number of population in the metaheuristic algorithms, and the number depends on the problem the researchers want to apply to the AVOA.
- In a natural environment, numerous vultures can be physically divided into two groups, in which the algorithm first calculates the fitness function of all solutions (initial population) to divide vultures into categories. The best answer is given as the best and first vulture and the second solution as the second-best vulture. Others form a population that moves or replaces one of the two best vultures in each performance.
- The reason for separating groups in this algorithm is that vultures' most crucial natural function can be formulated: group living to find food. Each group of vultures is a different inability to find food and eat.
- The tendency to eat in vultures and looking for food for hours causes them to escape from the hungry trap. At the formulation stage, our anti-hunger compromises, assuming that the worst solution in the population is the weakest and hungriest, the vultures try to keep their distance from the worst and come up with the best solution. In the AVOA, two of the best solutions are considered the strongest and best vultures, and the other vultures try to approach the best.

Fig. 1. A Rüppell's, white-backed, and Lappet-faced Vultures.

Based on the basic concepts of vultures and the four assumptions presented for simulating the artificial vulture's optimization algorithm, the proposed algorithm was further formulated in 4 separate steps. For better understanding, the AVOA flowchart is shown in Fig. 2, and each step of the formulation algorithm is fully introduced.

a. Phase One: Determining the best vulture in any group

After the initial population is formed, the fitness of all solutions is calculated, and the best solution is selected as the best vulture of the first group and the second-best solution as the best vulture of the second group, and the other solutions using Eq. (1) move toward the best solutions for the first and second groups. In each fitness iteration, the entire population is recalculated.

$$R(i) = \begin{cases} BestVulture_1 if p_i = L_1 \\ BestVulture_2 if p_i = L_2 \end{cases} \quad (1)$$

In Eq. (1), the probability of choosing the selected vultures to move the other vultures toward one of the best solutions in each group is calculated, where L_1 and L_2 The parameters to be measured before the search operation, with the values between 0 and 1 and the sum of both parameters is 1. The probability of choosing the best solution is gained using the Roulette wheel to choose each of the best solutions for each group using Eq. (2).

$$p_i = \frac{F_i}{\sum_{i=1}^{n} F_i} \quad (2)$$

If the α-numeric parameter is close to value 1, and the β-numeric parameter is close to value 0, in AVOA, it will cause an increased intensification. Also, if the β-numeric parameter is close to value 1, and the α-numeric parameter is close to value 0, it leads to the increasing diversity in AVOA.

b. Phase TWO: The rate of starvation of vultures

Vultures are often looking for food and have high energy if they are satiated, which makes them go longer distances to search for food, but if they are hungry, they do not have enough energy to fly long and look for food next to the stronger vulture and become aggressive while hungry. For the mathematical modeling of this behavior, Eq. (4) has been used. It has also been used to transfer from the exploration phase to the exploitation phase, which is inspired by the rate at which the vultures are satiated or hungry. The rate of being satiated has a declining trend, and to model, this behavior, Eq. (4) has been used.

$$t = h \times \left(sin^w \left(\frac{\pi}{2} \times \frac{iteration_i}{maxiterations} \right) + cos\left(\frac{\pi}{2} \times \frac{iteration_i}{maxiterations} \right) - 1 \right) \quad (3)$$

$$F = (2 \times rand_1 + 1) \times z \times \left(1 - \frac{iteration_i}{maxiterations} \right) + t \quad (4)$$

In Eqs. (3) and (4), F denotes that the vultures are satiated, $iteration_i$ denotes the current iteration number, *max iterations* denote the total number of iterations, and z is a random number between −1 and 1 that changes each iteration. h is a random number between −2 and 2. $rand_1$ has a random value between 0 and 1. When the z value drops below 0, it means that the vulture is starved, and if it increases to 0, it means the vulture is satiated.

In solving challenging optimization problems, there is no guarantee that the final population will include accurate estimations for the global optimum at the end of the exploration phase. For this reason, it causes premature convergence in the optimal local location. Eq. (3) has been used to increase performance in solving complex optimization problems, which increases the reliability of escape from local optimal points (Jia et al., 2019). The final iterations of the AVOA algorithm perform the exploitation phase and perform exploration operations in some final iterations. This strategy's overall goal is to modify Eq. (3) to change exploration and exploitation phases so that the AVOA algorithm can increase the probability of entering the exploration phase at some point in the optimization operation. In Eq. (3); sin and cos represent the functions of sine and cosine, respectively. w is a parameter with a fixed number set before the optimization operation, which indicates the optimization operation disrupts the exploration and operation phases; as the value of w increases, the probability of entering the exploration phase in the final optimization stages increases, however, by decreasing the parameter w, the probability of entering the exploration phase decreases. The behavior of F, t during the optimization operation, concerning the values of the w parameter, is shown in Figs. 3 and 4.

The rate of vultures being total is decreasing, and it decreases more with each repetition. When the value of $|F|$ is more than 1, vultures search for food in different areas, and the AVOA enters the exploration phase. If the value of $|F|$ is less than 1, AVOA enters the exploitation phase, and vultures search for food in the solutions' neighborhood.

c. Phase Three: Exploration

At this stage, the exploration phase of the AVOA is examined. In the natural environment, vultures have high visual ability and high ability to find food and detect poor dying animals. However, finding food for vultures can be very difficult. Vultures carefully scrutinize their living environment for a long time and travel long distances to search for food (Xue, 2018, 2018). In the AVOA, vultures can examine different random areas, which can be based on two different strategies, and a parameter called P_1 is used to select either strategy. This parameter must be valued before the search operation and should have a value between 0 and 1, determining how each of the two strategies is used.

To select any of the strategies in the $rand_{P1}$ exploration phase, a random number between 0 and 1 generate is generated. If this number is greater than or equal to the P_1 parameter, Eq. (6) is used. But, if $rand_{P1}$ is smaller than the parameter P_1 Eq. (8) is used. In this case, each vulture randomly searches in the environment concerning its satiation. This procedure is shown in Eq. (5).

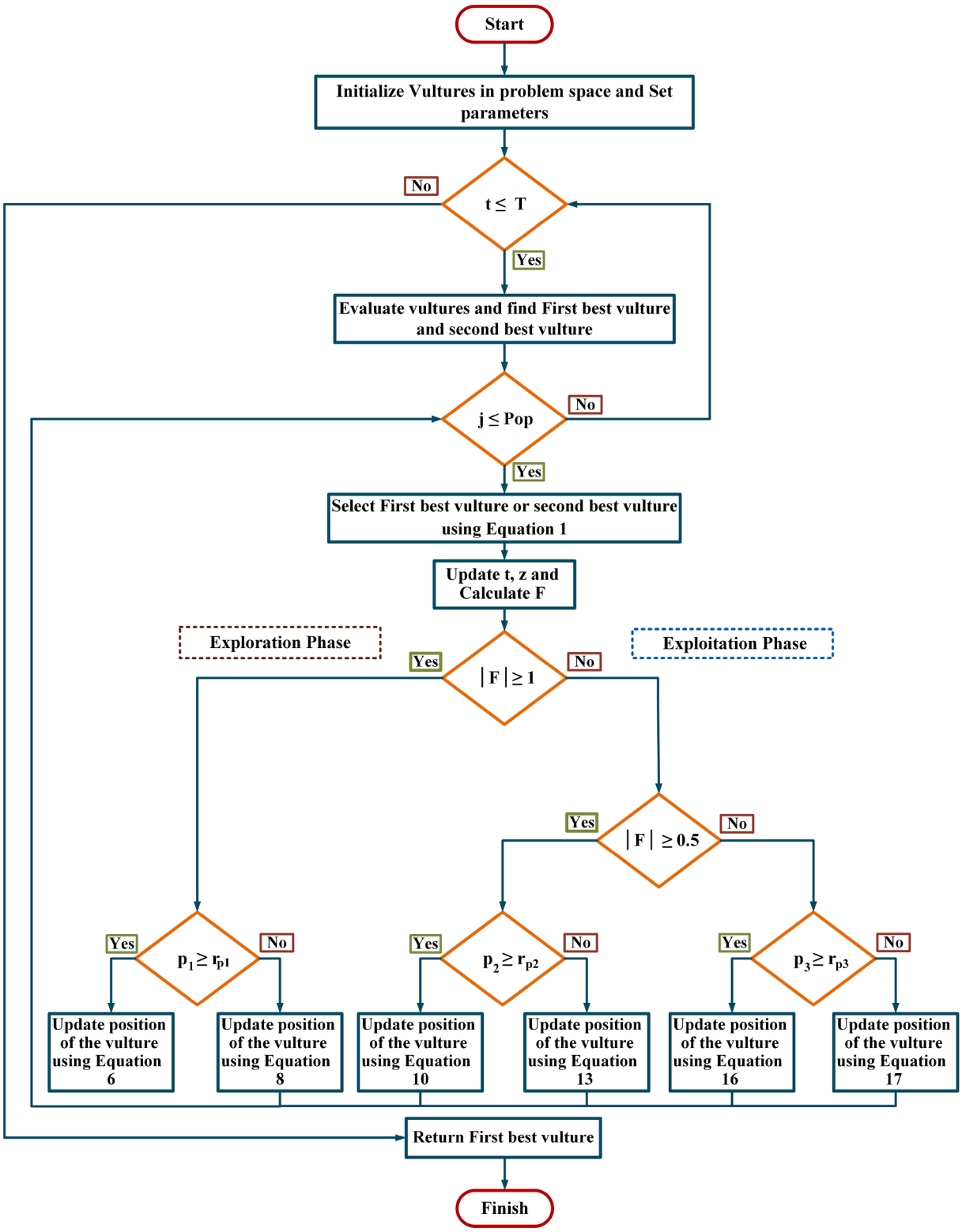

Fig. 2. Flowchart of AVOA.

$$P(i+1) = \begin{cases} Equation(6) if P_1 \geq rand_{P1} \\ Equation(8) if P_1 < rand_{P1} \end{cases} \quad (5)$$

$$P(i+1) = R(i) - D(i) \times F \quad (6)$$

$$D(i) = |X \times R(i) - P(i)| \quad (7)$$

According to Eq. (6), vultures randomly search for food in the surrounding area at a random distance of one of the best cultures of the two groups, where $P(i+1)$ is the vulture position vector in the next iteration, and F is the rate of vulture being satiated which is obtained using Eq. (4) in the current iteration. In Eq. (7), $R(i)$ is one of the best vultures, which is selected by the use of Eq. (1) in the current iteration. Moreover, X is where the vultures move randomly to protect food from other vultures. X is used as a coefficient vector that increases the random

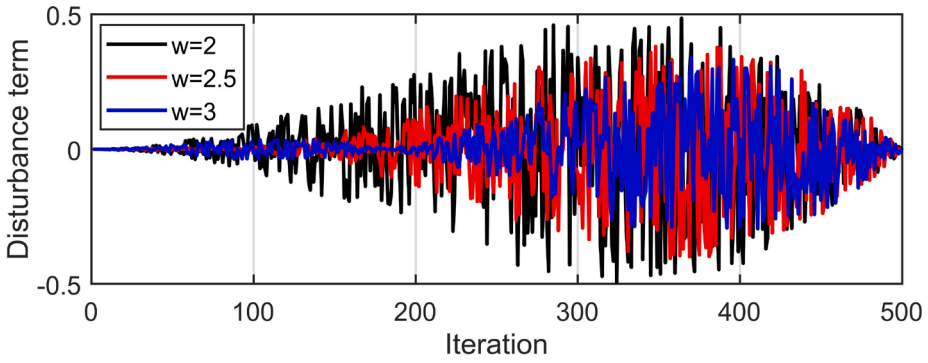

Fig. 3. Variation of the disturbance term t under different values of parameter w.

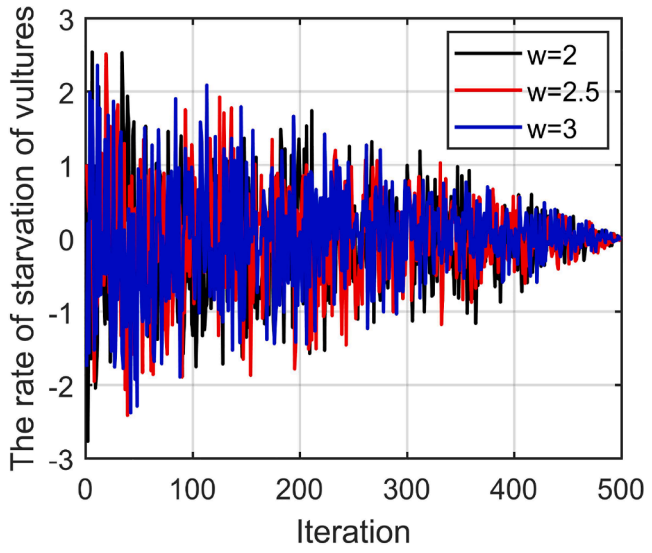

Fig. 4. Variation of the rate of starvation of vultures F under different values of parameter w.

motion, which changes in each iteration, and is obtained using the formula $X = 2 \times rand$, where rand is a random number between 0 and 1. $P(i)$ is the current vector position of the vulture.

$$P(i+1) = R(i) - F + rand_2 \times ((ub - lb) \times rand_3 + lb) \quad (8)$$

In Eq. (8), $R(i)$ is one of the best vultures selected by the use of Eq. (1) in the current iteration. F is the rate of vulture satiation obtained by using Eq. (4) in the current iteration and $rand_2$ has a random value between 0 and 1. lb and ub demonstrate the upper bound and the lower bound of the variables. Using Eq. (8) in the AVOA, a simple model for the random generation of solutions in the range (lb, ub) is produced. $rand_3$ is used to increase the coefficient of random nature. If$rand_3$ takes a number close to 1, it distributes the solutions with similar patterns, which adds a random motion along with the lb. It creates a high random coefficient at the search environment scale to increase diversity and search for different search space areas. In the AVOA, the simplest models are used to model the vulture's movement.

d. Phase Four: Exploitation

At this stage, the efficiency stage in the AVOA is investigated. If the value of $|F|$ is less than 1, the AVOA enters the exploitation phase, which also has two phases with two different strategies being used in each phase. The degree of choosing each strategy in each internal phase is determined by two parameters of P_2 and P_3. Parameter P_2 is used to select the strategies available in the first phase and parameter $P_3$is used to select the strategies available in the second phase. Both parameters must be valued at 0 and 1 before performing the search operation. The vultures' movements to find food, examined in section 3, are formulated and adapted to mathematical problems.

Exploitation: The AVOA enters the first phase in the Exploitation phase when the value $|F|$ is between 1 and 0.5. In the first phase, two different rotating flight and siege-fight strategies are carried out. P_2 is used to determine each strategy's choosing, which must be valued before the searching operation is performed, and the value should be between 0 and 1. At the beginning of this phase, $rand_{P2}$, which is a random number between 0 and 1, is generated. If this number is greater than or equal to the parameter P_2, the Siege-fight strategy is implemented slowly. However, if this random number is smaller than the parameter P_2, rotating flight strategy is carried out. This procedure is shown in Eq. (9).

$$P(i+1) = \begin{cases} Equation(10) if P_2 \geq rand_{P2} \\ Eauation(13) if P_2 < rand_{P2} \end{cases} \quad (9)$$

Competition for Food: When $|F| is \geq 0.5$, the vultures are relatively satiated and have sufficient energy. When many vultures congregate on one food source, it can cause severe conflicts over food acquisition. At such times, vultures that are physically high-powered prefer not to share food with other vultures, as shown in Fig. 5.

On the other hand, the weaker vultures try to tire and get food from the healthy vultures by gathering around healthy vultures and causing small conflicts. Eq. (10) and Eq. (11) are used to model this step.

$$P(i+1) = D(i) \times (F + rand_4) - d(t) \quad (10)$$

$$d(t) = R(i) - P(i) \quad (11)$$

$D(i)$ is calculated using Eq. (7), and F is the satiation rate of vultures, which is calculated using Eq. (4). $rand_4$ is a random number between

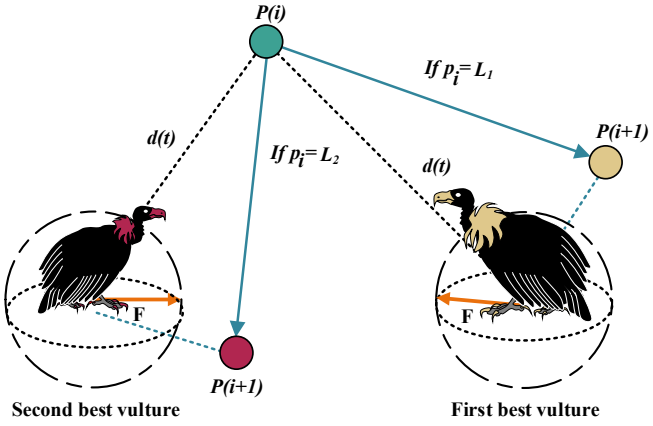

Fig. 5. Example of overall vectors in the case of Competition for Food.

0 and 1, that is used to increase the random coefficient. In Eq. (11), $R(i)$ is one of the best vultures of the two groups selected using Eq. (1) in the current iteration, $P(i)$ is the current vector position of vulture by which the distance between the vulture and one of the best vultures in the two groups is obtained.

Rotating flight of Vultures: Vultures frequently make a rotational flight used to model Spiral Motion Fig. 6.

The spiral model has been used to model rotational flight mathematically. A spiral equation is created between all vultures and one of the two best vultures in this method. The rotational flight is expressed using Eqs. (12) and (13).

$$S_1 = R(i) \times \left(\frac{rand_5 \times P(i)}{2\pi}\right) \times cos(P(i))$$

$$S_2 = R(i) \times \left(\frac{rand_6 \times P(i)}{2\pi}\right) \times sin(P(i)) \quad (12)$$

$$P(i+1) = R(i) - (S_1 + S_2) \quad (13)$$

In Eqs. (12) and (13), R(i) represents the position vector of one of the two best vultures in the current iteration, which is obtained by using Eq. (1). cos and sin represent the functions of sine and cosine, respectively. And,$rand_5$ and $rand_6$ is a random number between 0 and 1. Where S_1 and S_2 are obtained by the use of Eq. (12). Finally, by the use of Eq. (13), the location of the vultures is updated.

e. Exploitation:(Second Phase): In the second phase of exploitation, the two vultures' movements accumulate several types of vultures over the food source, and the siege and aggressive strife to find food are carried out. If $|F|$ number is less than 0.5, this phase of the algorithm is executed. At the beginning of this phase, $rand_{P3}$ is generated, which is a random number between 0 and 1. If $rand_{P3}$ is greater than or equal to the parameter P_3, the strategy is to accumulate several types of vultures over the food source. Otherwise, if the generated value is smaller than the parameter P_3, the aggressive siege-fight strategy is implemented. This procedure is shown in Eq. (14).

$$P(i+1) = \begin{cases} Eq16 if P_3 \geq rand_{P3} \\ Eq17 if P_3 < rand_{P3} \end{cases} \quad (14)$$

The accumulation of several types of vultures over the food source: The movement of all vultures toward the food source is examined. Occasionally, vultures are starved, and there is a great deal of competition for food that may accumulate several species of vultures on one food source. Eqs. (15) and (16) have been used to formulate this movement of vultures.

$$A_1 = BestVulture_1(i) - \frac{BestVulture_1(i) \times P(i)}{BestVulture_1(i) - P(i)^2} \times F$$

$$A_2 = BestVulture_2(i) - \frac{BestVulture_2(i) \times P(i)}{BestVulture_2(i) - P(i)^2} \times F \quad (15)$$

In Eq. (15), $BestVulture_1(i)$ is the best vulture of the first group in the current iteration and $BestVulture_2(i)$ is the best vulture of the second group in the current iteration, and F is the rate of vulture satiation, which is calculated using Eq. (4), and $P(i)$ is the current vector position of a vulture.

$$P(i+1) = \frac{A_1 + A_2}{2} \quad (16)$$

Finally, the aggregation of all vultures is carried out by using Eq. (16), where A_1 and A_2 are obtained by using Eq. (15), and $P(i+1)$ is the vector of the vulture position in the next iteration.

Aggressive Competition for Food: When $|F| < 0.5$, the head vultures become starved and weak and do not have enough energy to deal with the other vultures (see Fig. 7).

On the other hand, other vultures also become aggressive in their quest for food. They move in different directions towards the head

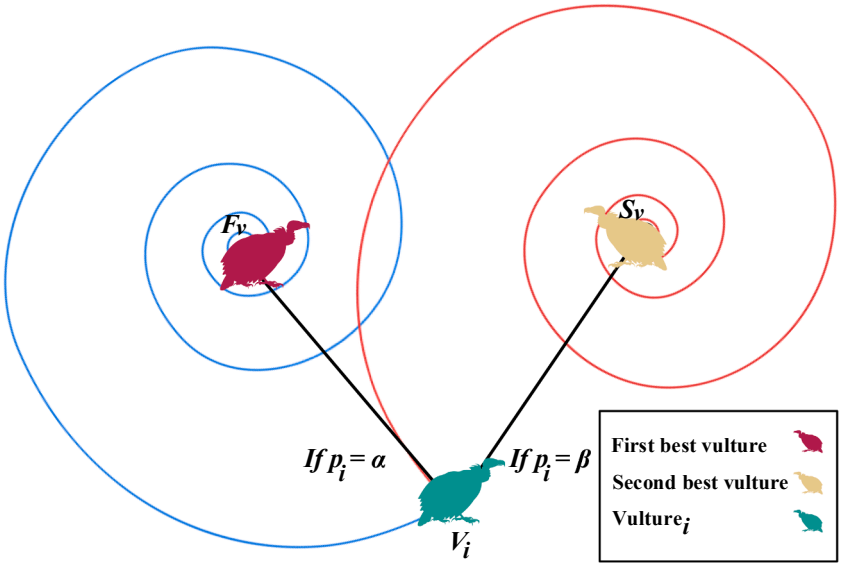

Fig. 6. Example of overall vectors in the case of Rotating flight of vultures.

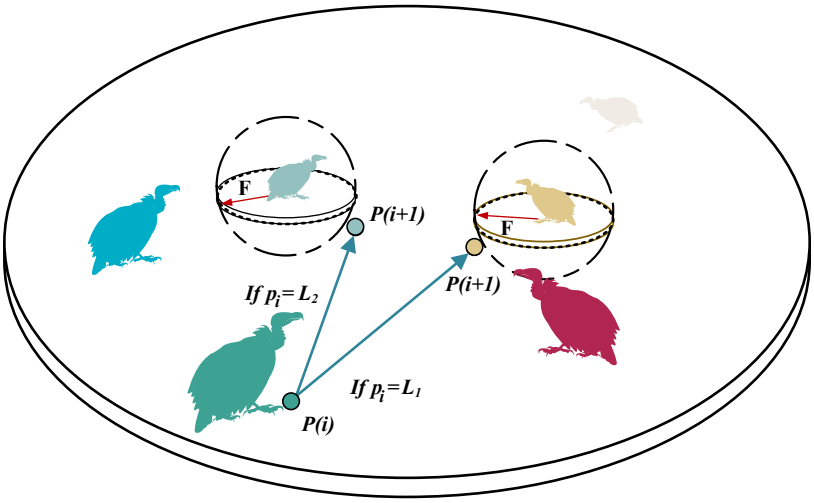

Fig. 7. Example of overall vectors in the case of aggressive Competition for Food.

vulture. Eq. (17) is used to model this motion.

$$P(i+1) = R(i) - |d(t)| \times F \times Levy(d) \tag{17}$$

In Eq. (16), $d(t)$represents the distance of the vulture to one of the best vultures of the two groups, which is calculated by using Eq. (11). Levy flight (LF) (Yang, 2010) patterns have been used to increase the effectiveness of the AVOA in Eq. (17), and LF has been identified and used in the activities of many metaheuristic algorithms (Gautestad & Mysterud, 2006; Shlesinger, 1989; Sims et al., 2008; Viswanathan et al., 2000). The LFs were calculated by using Eq. (18).

$$LF(x) = 0.01 \times \frac{u \times \sigma}{|v|^{\frac{1}{\beta}}}, \sigma = \left(\frac{\Gamma(1+\beta) \times sin(\frac{\pi\beta}{2})}{\Gamma(1+\beta 2) \times \beta \times 2(\frac{\beta-1}{2})} \right)^{\frac{1}{\beta}} \tag{18}$$

In Eq. (18), d represents the problem dimensions, u and v are a random number between 0 and 1, and β is a fixed and default number of 1.5.

f. Pseudocode of AVOA: The pseudo-code of the AVOA is described in Algorithm 1.

Algorithm 1: AVOA

1: Inputs: The population size N and maximum number of iterations T
2: Outputs: The location of Vulture and its fitness value
3: Initialize the random population $P_i (i = 1, 2, ..., N)$
4: **while** (stopping condition is not met) **do**
5: Calculate the fitness values of Vulture
6: Set $P_{BestVulture_1}$ as the location of Vulture (First best location Best Vulture Category 1)
7: Set $P_{BestVulture_2}$ as the location of Vulture (Second best location Best Vulture

(*continued on next column*)

(*continued*)

Algorithm 1: AVOA

Category 2)
8: **for** (each Vulture (P_i)) **do**
9: Select R(i) using Eq. (1)
10: Update the F using Eq. (4)
11: **if** ($|F| \geq 1$) **then**
12: **if** ($P_1 \geq rand_{P1}$) **then**
13: Update the location Vulture using Eq. (6)
14: **else**
15: Update the location Vulture using Eq. (8)
16: **if** ($|F| < 1$) **then**
17: **if** ($|F| \geq 0.5$) **then**
18: **if** ($P_2 \geq rand_{P2}$) **then**
19: Update the location Vulture using Eq. (10)
20: **else**
21: Update the location Vulture using Eq. (13)
22: **else**
23: **if** ($P_3 \geq rand_{P3}$) **then**
24: Update the location Vulture using Eq. (16)
25: **else**
26: Update the location Vulture using Eq. (17)
Return $P_{BestVulture_1}$

g. Computational complexity: The computational complexity of the AVOA algorithm depends on three essential processes: initialization, fitness evaluation, and updating of vultures. Given N vultures, the computational complexity in the initialization process is equal to O(N). Also, the computational complexity in the update mechanism process based on searching for the best location and updating the location vector of all formed vultures is equal to O(T × N) + O(T × N × D). Where T is

Table 2
Details of unimodal benchmark functions.

No	Type	Function	Dimensions	Range	F_{min}
F1	US	$f(x) = \sum_{i=1}^{d} x_i^2$	30,100,500,1000	$[-100, 100]^d$	0
F2	UN	$f(x) = \sum_{i=1}^{d} \|x_i\| + \prod_{i=1}^{d} \|x_i\|$	30,100,500,1000	$[-10, 10]^d$	0
F3	UN	$f(x) = \sum_{i=1}^{d} \left(\sum_{j=1}^{i} x_j \right)^2$	30,100,500,1000	$[-100, 100]^d$	0
F4	US	$f(x) = max_i \{ \|x_i\|, 1 \leq i \leq d \}$	30,100,500,1000	$[-100, 100]^d$	0
F5	UN	$f(x) = \sum_{i=1}^{d-1} \left[100 (x_{i+1} - x_i^2)^2 + (x_i - 1)^2 \right]$	30,100,500,1000	$[-30, 30]^d$	0
F6	US	$f(x) = \sum_{i=1}^{d} (\|x_i + 0.5\|)^2$	30,100,500,1000	$[-100, 100]^d$	0
F7	US	$f(x) = \sum_{i=1}^{d} i x_i^4 + random[0, 1)$	30,100,500,1000	$[-128, 128]^d$	0

Table 3
Details of multi-modal benchmark functions.

No	Type	Function	Dimensions	Range	F_{min}
F8	MS	$f(x) = -\sum_{i=1}^{d}(x_i sin(\sqrt{\lvert x_i \rvert}))$	30,100,500,1000	$[-500,500]^d$	$-418.9829 \times n$
F9	MS	$f(x) = 10d + \sum_{i=1}^{d}[x_i^d - 10cos(2\pi x_i)]$	30,100,500,1000	$[-5.12,5.12]^d$	0
F10	MN	$f(x) = -20exp\left(-0.2\sqrt{\frac{1}{d}\sum_{i=1}^{d}x_i^2}\right) - exp\left(\frac{1}{d}\sum_{i=1}^{d}\cos 2\pi x_i\right) + 20 + e$	30,100,500,1000	$[-32,32]^d$	0
F11	MN	$f(x) = \frac{1}{4000}\sum_{i=1}^{d}x_i^2 - \prod_{i=1}^{d}\cos\left(\frac{x_i}{\sqrt{i}}\right) + 1$	30,100,500,1000	$[-600,600]^d$	0
F12	MN	$f(x) = \frac{\pi}{d}\left\{10\sin(\pi y_1) + \sum_{i=1}^{d-1}(y_i-1)^2[1+10sin^2(\pi y_{i+1})] + (y_d-1)^2\right\} + \sum_{i=1}^{d}U(x_i,10,100,4) y_i = 1 + \frac{x_i+1}{4}$ $U(x_i,a,k,m) = \begin{cases} k(x_i-a)^m x_i > a \\ 0 - a < x_i < a \\ k(-x_i-a)^m x_i < -a \end{cases}$	30,100,500,1000	$[-50,50]^d$	0
F13	MN	$f(x) = 0.1\left\{sin^2(3\pi x_1) + \sum_{i=1}^{d}(x_i-1)^2[1+sin^2(3\pi x_i+1)] + (x_d-1)^2[1+sin^2(2\pi x_d)]\right\} + \sum_{i=1}^{d}U(x_i, 5,100,4)$	30,100,500,1000	$[-50,50]^d$	0

Table 4
Details of fixed-dimension multi-modal benchmark functions.

No	Type	Function	Dimensions	Range	F_{min}
F14	FM	$f(x) = \left[\frac{1}{500} + \sum_{i=1}^{25}\frac{1}{i + \sum_{j=1}^{2}(x_j - a_{j,i})^6}\right]^{-1}$	2	$[-65,65]^d$	1
F15	FM	$f(x) = \sum_{i=1}^{d}\left[a_i - \frac{x_1(b_i^2+b_i x_2)}{b_i^2+b_i x_3+x_4}\right]^2$	4	$[-5,5]^d$	0.00030
F16	FM	$f(x) = 4x_1^2 - 2.1x_1^4 + \frac{1}{3}x_1^6 + x_1x_2 - 4x_2^2 + 4x_2^4$	2	$[-5,5]^d$	−1.0316
F17	FM	$f(x) = \left(x_2 - \frac{5.1}{4\pi^2}x_1^2 + \frac{5}{\pi}x_1 - 6\right)^2 + 10\left(1 - \frac{1}{8\pi}\right)cosx_1 + 10$	2	$[-5,5]^d$	0.398
F18	FM	$f(x) = \left[1+(x_1+x_2+1)^2(19-14x_1+3x_1^2-14x_2+6x_1x_2+3x_2^2)\right] \times \left[30+(2x_1-3x_2)^2 \times (18-32x_1+12x_1^2+48x_2-36x_1x_2+27x_2^2)\right]$	2	$[-2,2]^d$	3
F19	FM	$f(x) = -\sum_{i=1}^{4}a_i exp\left(-\sum_{j=1}^{3}b_{ij}\left(x_j - p_{ij}\right)^2\right)$	3	$[1,3]^d$	−3.86
F20	FM	$f(x) = -\sum_{i=1}^{4}a_i exp\left(-\sum_{j=1}^{6}b_{ij}\left(x_j - p_{ij}\right)^2\right)$	6	$[0,1]^d$	−3.32
F21	FM	$f(x) = -\sum_{i=1}^{5}\left[(X-a_i)(X-a_i)^T + c_i\right]^{-1}$	4	$[0,10]^d$	−10.1532
F22	FM	$f(x) = -\sum_{i=1}^{7}\left[(X-a_i)(X-a_i)^T + c_i\right]^{-1}$	4	$[0,10]^d$	−10.4028
F23	FM	$f(x) = -\sum_{i=1}^{10}\left[(X-a_i)(X-a_i)^T + c_i\right]^{-1}$	4	$[0,10]^d$	−10.5363

the maximum number of iterations, and D is the dimension of the problems. Therefore, according to the given explanation, the computational complexity of the AVOA algorithm is equal to O(N × (T + TD)).

It should be noted that the problem-solving paradigm of AVOA is similar to other metaheuristics. The optimization process starts with a random population of solutions. This population is then iteratively improved until the satisfaction of an end condition. The way the population is improved makes algorithms different, which is also the case in AVOA. The novelty of the proposed algorithm is in its inspiration and the modeling process discussed above.

4. Result and discussion

4.1. Benchmark set and compared algorithms

A set of different benchmark functions have been used to evaluate the performance of the AVOA. This set of benchmark functions consists of three different groups of unimodal (UM), multi-modal (MM), and composition model (CM). UM (F1-F7) benchmark functions, which only have one best global number, can intensify each optimization algorithm's capabilities. If using the MM (F8 – F23) benchmark functions, the optimization algorithms' diversification capabilities are shown. The mathematical formulas and features of the UM and MM benchmark functions are shown in Tables 2–4.

The third set of benchmark functions (F24– F36) used in the CEC 2014 competition (Liang, Qu, & Suganthan, 2014) covers the hybrid composite, rotated and shifted MM cases. These benchmarks have been used in many articles to optimize optimization algorithms' performance using benchmarks because they require a balance between exploration and exploitation in escaping local optimal points in optimization algorithms' ability to solve these problems. Details of the benchmark functions are presented in Table 5 and Fig. 8.

Results and Performance of AVOA with other types of optimization algorithms BBO (Simon, 2008), PSO (Simon, 2008), DE (Simon, 2008), GSA (Rashedi et al., 2009), TLBO (Rao, Savsani, & Vakharia, 2012), SSA (Mirjalili et al., 2017); GWO (Mirjalili et al., 2014); WOA (Mirjalili & Lewis, 2016); MFO (Mirjalili, 2015); FFA (Shayanfar & Gharehchopogh, 2018) and IPO (Mozaffari et al., 2016) have been compared. This comparison is based on the best solution, the worst solution, standard deviation (STD), and average results (AVG). The FFA, MFO, WOA, GWO, SSA, IPO, and TLBO optimization algorithms are selected as powerful and novel optimization algorithms, while BBO, GSA, PSO, and DE algorithms are chosen since they are used a lot in the optimization context. Also, for better evaluation, such as Derrac et al. (Derrac et al., 2011), a

Table 5
Details of hybrid composition functions F24–F36 (S: Scalable, NS: Non-Separable, R: Rotated, MM: Multi-modal, UN: Unimodal, D: Dimension, SH: Shifted, N: Number of functions combined).

ID	(CEC14-ID)	Description	Properties	D	Range
F24	(C1)	Rotated High Conditioned Elliptic Function	UN, NS, R, S	30	$[-100, 100]^D$
F25	(C3)	Rotated Discus Function	UN, NS, R, S	30	$[-100, 100]^D$
F26	(C5)	Shifted and Rotated Ackley's Function	MM, NS, SH, R, S	30	$[-100, 100]^D$
F27	(C10)	Shifted Schwefel's Function	MM, SH, S	30	$[-100, 100]^D$
F28	(C11)	Shifted and Rotated Schwefel's Function	MM, NS, SH, R, S	30	$[-100, 100]^D$
F29	(C18)	Hybrid Function 2 (N = 3)	MM, NS, S	30	$[-100, 100]^D$
F30	(C21)	Hybrid Function 5 (N = 5)	MM, NS, S	30	$[-100, 100]^D$
F31	(C23)	Composition Function 1 (N = 5)	MM, NS, R, S	30	$[-100, 100]^D$
F32	(C24)	Composition Function 2 (N = 3)	MM, NS, R, S	30	$[-100, 100]^D$
F33	(C25)	Composition Function 3 (N = 3)	MM, NS, R, S	30	$[-100, 100]^D$
F34	(C27)	Composition Function 5 (N = 5)	MM, NS, R, S	30	$[-100, 100]^D$
F35	(C28)	Composition Function 6 (N = 5)	MM, NS, R, S	30	$[-100, 100]^D$
F36	(C29)	Composition Function 7 (N = 3)	MM, NS, S	30	$[-100, 100]^D$

Wilcoxon statistical test with a significance level of 5% was performed to detect significant differences concerning the results of AVOA compared to other optimization methods.

4.2. Parameter settings

The AVOA has been tested and executed using the Matlab 9.2 (R2017R) laptop computer running Windows 10 Enterprise 64-bit with an Intel Core i7-4510U 2.6 GHz processor and 8.00 GB RAM, and all tests performed to check the performance of the AVOA were carried out using 30 populations in a maximum of 500 iterations. All results are stored based on the average of 30 independent run results and are compared using the obtained results. The PSO settings, DE and BBO algorithms have been used using the corresponding BBO work's corresponding settings (Simon, 2008) performed by Simon. Whereas algorithms of TLBO (Rao et al., 2012), SSA (Mirjalili et al., 2017); GWO (Mirjalili et al., 2014); WOA (Mirjalili & Lewis, 2016); MFO (Mirjalili, 2015); FFA (Shayanfar & Gharehchopogh, 2018) are used from the settings presented in the original work. Also, Many methods for parameter adjustment have been proposed (Pršić et al., 2017; Stojanovic & Nedic, 2016; Stojanovic et al., 2016). We set AVOA algorithms from an eleven structured design-of-experiment technique, i.e., we have used the face-centered central composite design (CCD) (Balachandran et al., 2012). Based on the face-centered CCD method, each parameter is set according to three levels of different values of the low, medium, and high, the values of which are shown in Table 6.

A total of 3^6 states are generated from the combination of parameters for each level. This paper has tested for this evaluation of the benchmark functions 1–13 with dimensions 30 and different combinations of parameters. Finally, the parameter settings of the optimization algorithms are shown in Table 7.

4.3. Qualitative results of AVOA

Several unimodal and multi-modal standard criteria functions have been used to evaluate the qualitative results of the AVOA, which have been evaluated using four different criteria of the AVOA, including four criteria: search history, convergence behavior, the average fitness of the population and the trajectory of the first Vulture. The search history chart shows the positions visited by artificial vultures. The convergence behavior graph shows how the best vulture of the first group (best solution) varies during the optimization process. The average fitness of the population chart shows how the average population changes throughout the optimization process. The trajectory graph of the first Vulture also shows how the first vulture changes during the optimization process by looking at the search history of diagrams in Figs. 9–15, it can be seen that the AVOA performs a similar pattern in the search operation when the vultures first start exploring different problem areas and then continue to exploit the operation in the nearest solution.

The convergence graphs showing the best vulture's average fitness found in Figs. 9–15 can be seen. By looking at these graphs, it can be concluded that there is a rapidly declining pattern across all graphs. Also, the moment of change from exploration to exploitation phase can be recognized. Moreover, these graphs show the rapid trend in convergence. Also, according to the average fitness of the population criterion, it can be concluded that AVOA is reduced by random movements of vultures and finding better solutions to fitness values. It can also be seen from the diagrams shown in Figs. 9–15 that AVOA can improve all

Table 6
Low, medium, and high levels of parameters.

Parameter	Low	Medium	High
L_1	0.9	0.8	0.7
L_2	0.1	0.2	0.3
w	2	2.5	3
P_1	0.4	0.5	0.6
P_2	0.4	0.5	0.6
P_3	0.4	0.5	0.6

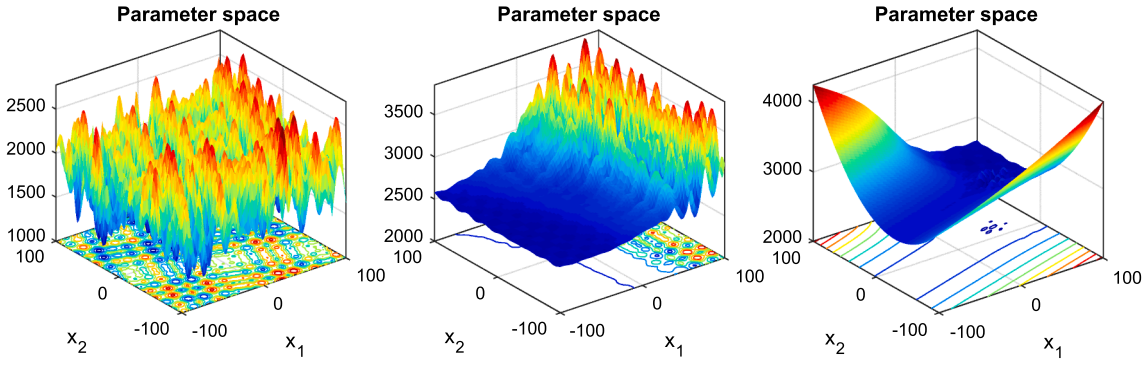

Fig. 8. Parameter space representation of the benchmark functions C11, C24, C25.

Table 7
Parameter settings of optimization algorithms for comparison and evaluation of the AVOA.

Algorithm	Parameter	Value
AVOA	L_1	0.8
	L_2	0.2
	w	2.5
	P_1	0.6
	P_2	0.4
	P_3	0.6
TLBO	Teaching factor T	1, 2
GWO	Convergence constant a	(Karaboga & Basturk, 2007)
DE	Scaling factor	0.5
	Crossover probability	0.5
PSO	Inertia factor	0.3
	c_1	1
	c_2	1
BBO	Habitat modification probability	1
	Immigration probability limits	[0,1]
	Step size	1
	Max emigration (E) and Max immigration (I)	1
	Mutation probability	0.005
MFO	Convergence constant a	[-2–1]
	Spiral factor b	1
FFA	K Value	2
	α	0.6
	β	0.4
	W	1
	Q	0.7
WOA	Convergence constant a	[2,0]
	Spiral factor b	1
SSA	c_1	$2e^{-\left(\frac{4l}{L}\right)^2}$
	c_2	random
	c_3	random
GSA	α	20
	G_0	100
	Power of R	1
	k	[N → 1]
IPO	c_1	0.685
	c_2,	0.653
	$shift_1$	527.392
	$shift_2$	380.811
	$scale_1$	0.423
	$sacle_2$	0.571

vultures at least in half of the repetitions, and it has a decreasing curved pattern on all graphs. It also reduces the range of fitness changes with increasing repetition. Such movements indicate that AVOA focuses more on promising areas during the optimization process. The trajectory chart of the first vulture, which captures the first vulture's behavior to search as representative of other vultures, gives a better understanding of vultures' behavior to search for new and better solutions in the search space. Moreover, using the trajectory diagram shows that the first vulture has a significant and sudden change in the early stages, then a slight change in the late stages. Also, it can be assumed that such activities will cause a P-metaheuristic to converge at one point eventually and to exploit that region.

In Figs. 9–15, the first vulture performed the initial optimization steps with high and sudden movements. This range of changes comprising half of the search space indicates can explore the AVOA. In the later stages of the search and lapse time, the amplitude of the fluctuations and behavioral changes decreased, indicating that the AVOA had shifted from exploration to exploitation phase. Eventually, the first vulture motion was stabilized, indicating that AVOA is in the final stages and tries to exploit promising areas.

4.4. Quantitative results and discussion

In this subsection, the performance of AVOA is compared with other optimization algorithms. For this comparison, the F1-F13 test functions of 30, 100, 500, and 1000 dimensions were additionally evaluated on the F14-F36 MM and CM test functions. The purpose of performing large-scale test functions is to evaluate AVOA in dealing with large-scale issues and AVOA scalability. The scalability assessment also demonstrates AVOA's ability to deliver high-quality solutions that can be found in various dimensions. On the other hand, it reveals AVOA's ability to tackle large-scale issues in retaining its search features. This evaluation is based on the results obtained in 30 independent runs in 500 iterations, and the mean error of STD, AVG, Worst, Best, and STD were used and compared. Figs. 15 and 16 and Tables 8–11 are used to evaluate scalable functions. Also, Table 13 shows the performance of AVOA in test functions F14-F36 against competitors. Finally, Wilcoxon rank-sum statistical test with 5% accuracy was used to investigate the significant differences between the proposed model and other optimization techniques. Tables 14–18 show p-values obtained from Wilcoxon rank-sum statistical test with 5% accuracy. By looking at the results in Tables 8–11 and Figs. 16 and 17, it is evident that AVOA can achieve excellent results in all dimensions. If the dimension increases, it better outperforms other algorithms, and their performance dimensions decrease significantly. Therefore, AVOA is highly capable of maintaining balance in exploration and exploitation against large-scale issues.

As per the results in Table 8, AVOA has achieved significantly better results in F1-F13 test functions than other optimization algorithms. According to Table 14, statistically significant differences can be found in almost all results. By examining Table 9, which is 100 dimensions, AVOA has performed significantly better than other optimization algorithms in the F1-F13 test functions, and this performance is remarkable. Concerning the p-values in Table 15, AVOA has found better solutions in almost all cases. It can also be seen from Table 10 that AVOA will continue to produce better solutions if dimensions are increased to 500 and are better than other optimization algorithms. Given the p-values in Table 16, it can be seen that AVOA performs significantly better than other optimization algorithms. Results are shown in Table 11, which is the dimension of Problem 1000. Similar to that seen in the lower dimensions, AVOA shows significant performance in the F1-F13 test functions. The statistical results visible in Table 17 confirm a significant discrepancy between the results obtained in AVOA and other optimization algorithms in almost all cases. It can also be easily recognized that

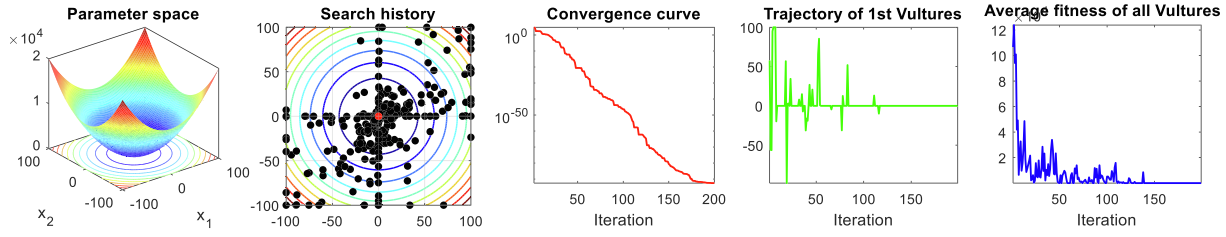

Fig. 9. Qualitative results for the F1 function.

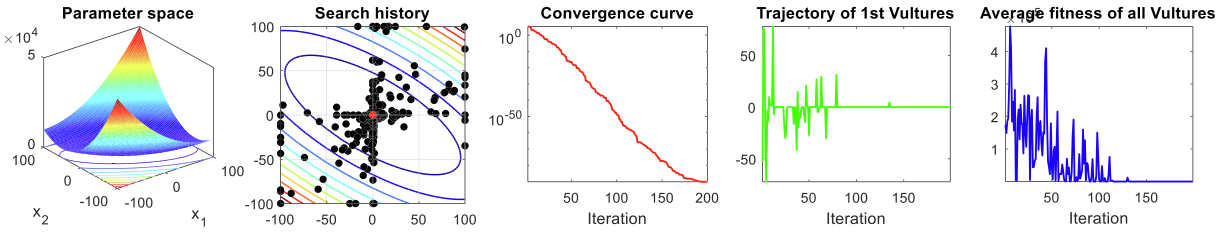

Fig. 10. Qualitative results for the F3 function.

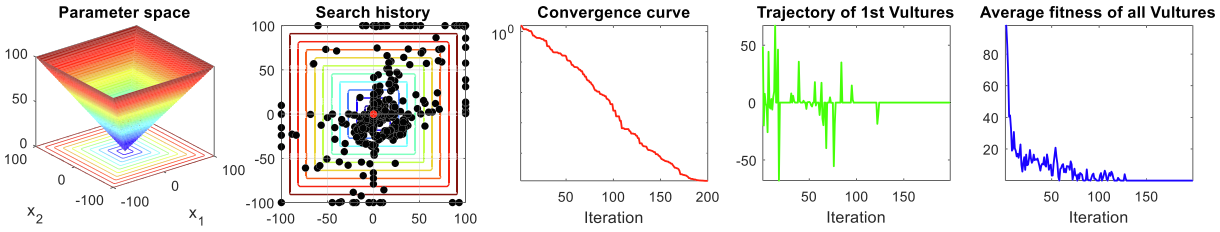

Fig. 11. Qualitative results for the F4 function.

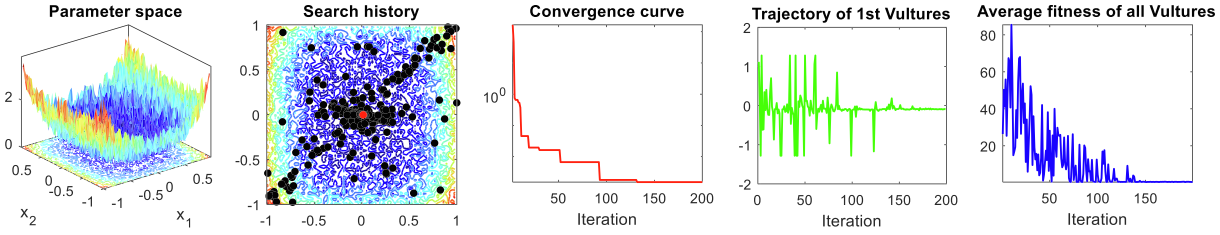

Fig. 12. Qualitative results for the F7 function.

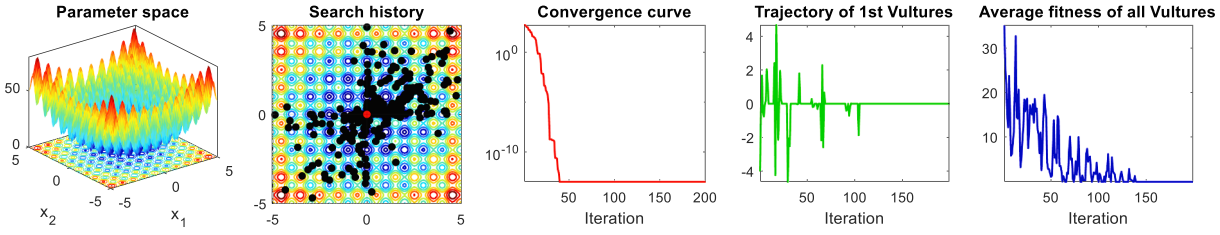

Fig. 13. Qualitative results for the F9 function.

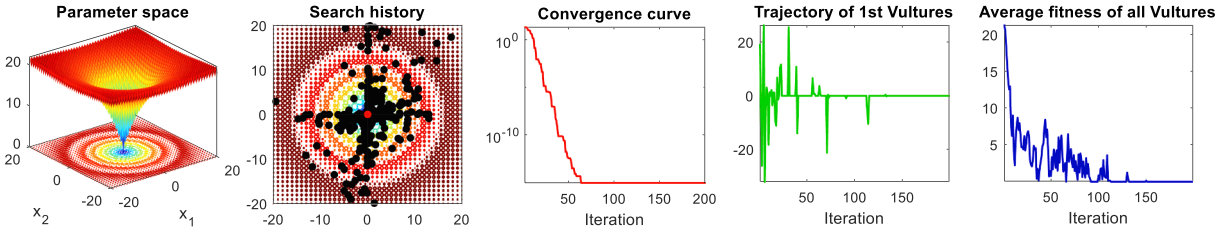

Fig. 14. Qualitative results for the F10 function.

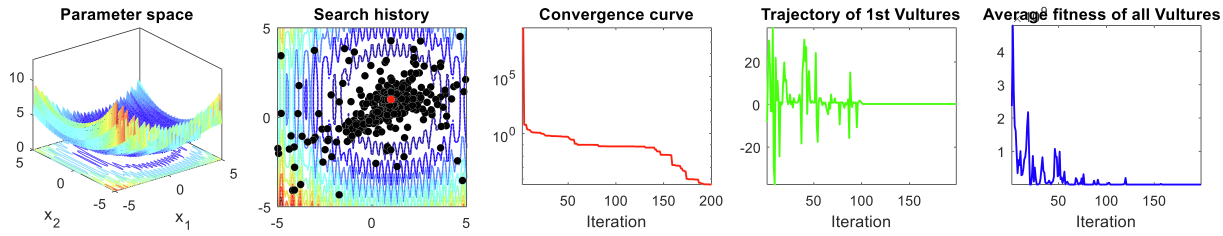

Fig. 15. Qualitative results for the F13 function.

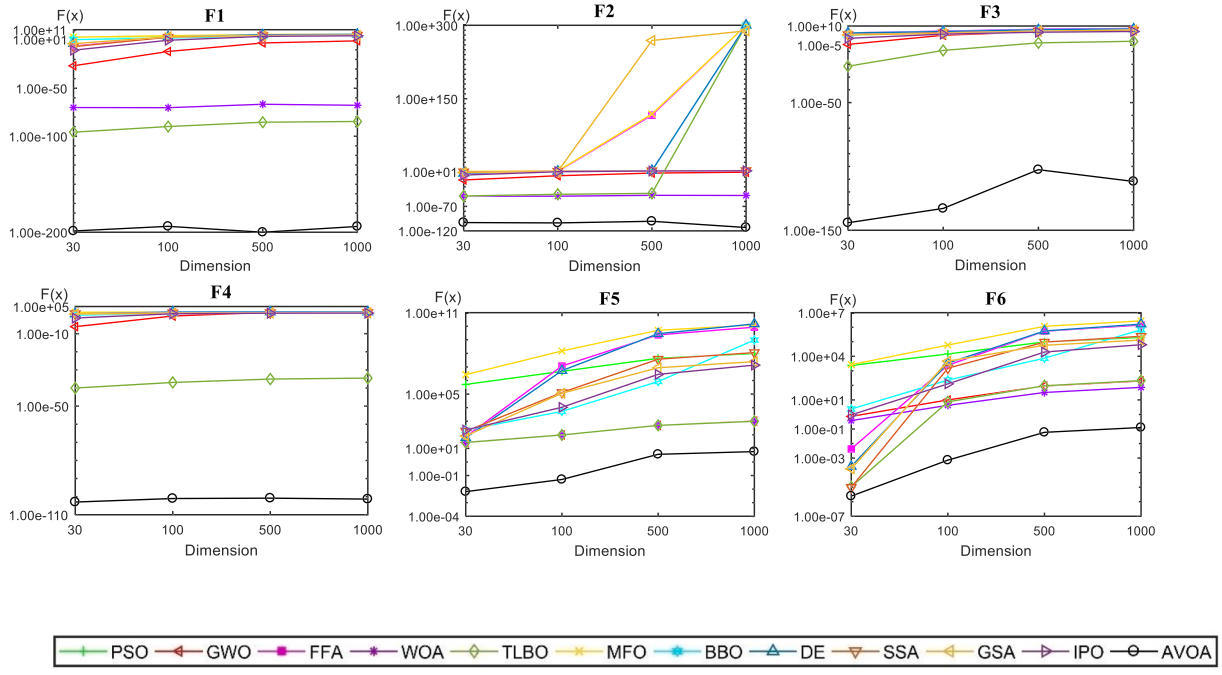

Fig. 16. Results of AVOA scalability evaluation against other optimization algorithms in F1-F6 functions in different dimensions.

AVOA performs better on almost every aspect of the F1-F13 test function in all dimensions. To further evaluate AVOA, the runtime for solving 1000-sided F1-F13 test functions is stored by AVOA and other optimization algorithms (Table 12).

Results shown in Table 12 demonstrate that it can be concluded that AVOA not only has found better solutions than other optimization algorithms in the F1-F13 test functions, it also performs faster than other optimization algorithms in terms of execution time. It even takes less running time to solve large-scale issues, and AVOA has been proved to be fast. According to the average runtime criterion in Table 12, AVOA is faster than all other algorithms in all F1-F13 test functions. These results confirm that the computational complexity of AVOA is less than other algorithms.

The results shown in Table 13 illustrate the superior and highly competitive performance of AVOA in solving F14-F23 fixed dimension MM test cases. The results of the F16-F18 test functions are highly competitive, and almost all optimization algorithms have been able to obtain high-quality results. The AVOA in the F14-F23 test functions has performed better than other optimization algorithms in terms of the results shown in Table 13 and obtain better results. Based on the results in The F24-F36 hybrid CM functions shown in Table 13, AVOA has delivered better and higher quality results and better performance than other optimization algorithms. On the other hand, the p-values shown in Table 18 confirm that AVOA, in most cases, performs significantly better than other optimization algorithms.

According to Fig. 18, which is related to Box plots diagrams, it is clear that the AVOA algorithm performs much better than other optimization algorithms compared to different types of problems. It also shows that AVOA in the component Intensification and diversity systems has excellent performance and excellent convergence ability. According to all the experiments performed, the AVOA algorithm with good results has shown that it can balance the exploration and efficiency phases. Because achieving good results in various issues requires good ability in the exploration and exploitation phases and creates a balance in these two phases.

4.5. *Engineering optimization problem*

In this subsection, the performance of the AVOA algorithm in solving engineering problems has been evaluated. For this purpose, a total of 11 low variable and significant variable engineering problems have been used, of which 7 are common variable engineering problems and the results obtained by AVOA with optimized or modified optimization algorithms are compared. On the other hand, four significant variable engineering problems have been used to examine the performance of AVOA in solving significant variable engineering problems. For this paper, the engineering problems in CEC 2011 Real World Optimization Problems (BosE & Sarrazin, 2007) were used, and the results obtained from the performance of AVOA are compared with the GWO (Mirjalili et al., 2014); MFO (Mirjalili, 2015); FFA (Shayanfar & Gharehchopogh,

Table 8
Results of benchmark functions (F1-F13), with 30 dimensions.

No.		AVOA	PSO	GWO	FFA	WOA	TLBO	MFO	BBO	DE	SSA	GSA	IPO
F1	Best	**5.44e-269**	1.37e+03	6.81e-29	2.27e-07	2.43e-87	1.97e-100	1.01E-01	3.15E+00	7.46e-05	2.75e-08	2.11E-16	1.82E-12
	Worst	**6.05e-198**	4.27e+03	3.14e-26	2.17e-06	2.01e-69	2.26e-95	1.00e+04	6.33E+00	7.89e-04	8.75e-07	8.65E-03	3.88E-10
	Mean	**2.01e-199**	2.37e+03	2.59e-27	7.88e-07	8.04e-71	1.66e-96	1.66e+03	4.47E+00	3.36e-04	2.07e-07	2.88E-04	4.76E-11
	STD	**0.00e+00**	6.17e+02	5.83e-27	5.15e-07	3.72e-70	4.36e-96	3.78e+03	7.54E-01	1.83e-04	2.17e-07	1.58E-03	8.42E-11
F2	Best	**2.87e-136**	1.13e+01	1.29e-17	1.35e-06	5.07e-59	1.57e-50	0.08e+00	3.90e-01	1.54e-03	2.55e-01	5.64E-08	6.77E-08
	Worst	**2.58e-102**	2.77e+01	4.34e-16	8.00e-06	2.16e-48	1.11e-48	7.00e+01	6.00e-01	5.95e-03	8.00e+00	1.19E+00	1.27E-05
	Mean	**8.72e-104**	1.91e+01	9.02e-17	3.82e-06	7.41e-50	1.89e-49	2.92e+01	5.05e-01	3.48e-03	2.39e+00	1.40E-01	8.28E-07
	STD	**4.71e-103**	3.55e+00	8.98e-17	1.54e-06	3.94e-49	2.79e-49	2.03e+01	4.53e-02	1.00e-03	1.72e+00	3.34E-01	2.37E-06
F3	Best	**4.92e-217**	4.07e+03	9.78e-08	2.78e+03	1.02e+04	2.76e-26	3.45e+03	2.51e+02	2.17e+04	4.40e+02	6.57E+02	1.30E+00
	Worst	**2.35e-143**	2.29e+04	7.58e-04	7.39e+03	6.08e+04	2.93e-21	4.48e+04	1.00e+03	5.36e+04	5.37e+03	1.77E+03	4.53E+00
	Mean	**7.83e-145**	9.20e+03	4.02e-05	5.03e+03	4.18e+04	3.35e-22	2.23e+04	4.98e+02	3.64e+04	1.83e+03	1.09E+03	2.41E+00
	STD	**4.29e-144**	4.24e+03	1.46e-04	1.32e+03	1.32e+04	6.76e-22	1.19e+04	1.49e+02	7.01e+03	1.02e+03	3.11E+02	7.86E-01
F4	Best	**2.57e-134**	1.57e+01	6.93e-08	1.33e+01	5.27e+00	1.02e-42	5.39e+01	1.21e+00	6.27e+00	5.22e+00	4.27E+00	2.41E-02
	Worst	**2.84e-102**	2.80e+01	6.17e-06	2.11e+01	8.61e+01	3.41e-40	8.28e+01	2.12e+00	1.75e+01	1.52e+01	1.12E+01	8.47E-02
	Mean	**1.03e-103**	2.14e+01	7.54e-07	1.64e+01	4.94e+01	9.51e-41	6.77e+01	1.56e+00	9.40e+00	1.06e+01	7.43E+00	4.59E-02
	STD	**5.18e-103**	3.51e+00	1.16e-06	2.39e+00	2.79e+01	1.07e-40	8.29e+00	2.00e-01	2.32e+00	2.54e+00	1.95E+00	1.48E-02
F5	Best	**1.96e-05**	1.48e+05	2.61e+01	1.51e+01	2.72e+01	2.66e+01	1.17e+02	4.99e+01	2.75e+01	2.51e+01	2.46E+01	1.34E+02
	Worst	**2.56e-02**	1.62e+06	2.88e+01	1.85e+02	2.84e+01	2.84e+01	7.99e+07	1.64e+03	2.38e+02	1.08e+03	3.27E+02	3.96E+02
	Mean	**6.50e-03**	5.15e+05	2.70e+01	7.31e+01	2.76e+01	2.72e+01	2.69e+06	2.24e+02	6.00e+01	1.85e+02	8.34E+01	2.27E+02
	STD	**7.15e-03**	3.37e+05	7.53e-01	3.94e+01	3.94e-01	4.23e-01	1.45e+07	3.60e+02	6.31e+01	2.46e+02	6.72E+01	7.44E+01
F6	Best	**2.43e-07**	1.19e+03	9.91e-05	1.07e-06	1.00e-01	3.37e-07	2.80e-01	1.37e+00	7.32e-05	8.02e-08	1.16E-16	0.00E+00
	Worst	**6.58e-06**	3.55e+03	1.47e+00	1.24e-01	8.78e-01	5.71e-05	1.95e+04	3.17e+00	5.72e-04	6.62e-05	5.48E-03	4.00E+00
	Mean	**2.43e-06**	2.35e+03	7.34e-01	4.26e-03	3.80e-01	1.06e-05	2.66e+03	2.36e+00	2.65e-04	9.76e-06	1.83E-04	9.33E-01
	STD	**1.89e-06**	5.34e+02	3.06e-01	2.25e-02	1.91e-01	1.28e-05	5.18e+03	4.18e-01	1.47e-04	1.61e-05	1.00E-03	1.17E+00
F7	Best	**4.26e-06**	1.00e-01	6.31e-04	1.94e-02	1.60e-04	4.27e-04	9.10e-02	6.34e-03	3.00e-02	6.10e-02	2.22E-02	9.85E-03
	Worst	**7.61e-04**	8.91e-01	6.15e-03	8.19e-02	1.46e-02	2.66e-03	8.25e+00	2.67e-02	7.44e-02	3.17e-01	1.60E-01	4.36E-02
	Mean	**2.52e-04**	3.77e-01	2.35e-03	5.03e-02	3.24e-03	1.27e-03	1.33e+00	1.62e-02	4.90e-02	1.71e-01	8.69E-02	2.75E-02
	STD	**2.05e-04**	2.10e-01	1.34e-03	1.51e-02	3.45e-03	5.77e-04	2.58e+00	5.71e-03	1.15e-02	7.63e-02	3.90E-02	9.80E-03
F8	Best	**−1.25e+04**	−5.10e+03	−7.31e+03	−9.37e+03	−1.25e+04	−9.54e+03	−1.00e+04	−9.04e+03	−7.59e+03	−9.33e+03	−3.34E+03	−4.12E+03
	Worst	**−1.21e+04**	−2.69e+03	−4.69e+03	−4.88e+03	−7.98e+03	−5.86e+03	−6.47e+03	−7.01e+03	−6.05e+03	−6.14e+03	−1.70E+03	−2.52E+03
	Mean	**−1.25e+04**	−3.82e+03	−5.99e+03	−6.89e+03	−9.69e+03	−7.39e+03	−8.51e+03	−8.10e+03	−6.72e+03	−7.32e+03	−2.47E+03	−3.28E+03
	STD	**1.00e+02**	6.19e+02	6.14e+02	1.14e+03	1.50e+03	9.60e+02	7.76e+02	5.65e+02	3.51e+02	7.84e+02	3.72E+02	3.60E+02
F9	Best	**0.00e+00**	1.08e+02	5.68e-14	3.59e+01	**0.00e+00**	0.00e+00	7.57e+01	2.59e+01	1.29e+02	2.98e+01	1.39E+01	9.25E+00
	Worst	**0.00e+00**	2.11e+02	1.93e+01	1.66e+02	**0.00e+00**	4.52e+01	2.61e+02	8.01e+01	1.74e+02	9.55e+01	4.68E+01	3.17E+01
	Mean	**0.00e+00**	1.48e+02	2.00e+00	7.96e+01	**0.00e+00**	2.08e+01	1.55e+02	5.22e+01	1.57e+02	5.05e+01	2.92E+01	1.68E+01
	STD	**0.00e+00**	2.16e+01	4.07e+00	3.10e+01	**0.00e+00**	9.68e+00	4.15e+01	1.30e+01	1.06e+01	1.58e+01	7.25E+00	4.32E+00
F10	Best	**8.88e-16**	6.71e+00	7.19e-14	9.29e-05	8.84e-16	4.44e-15	5.58e-01	3.80e-01	3.04e-03	1.34e+00	7.68E-09	1.61E+00
	Worst	**8.88e-16**	1.20e+01	1.35e-13	8.73e-04	7.95e-15	7.99e-15	2.00e+01	7.63e-01	7.78e-03	6.28e+00	1.16E+00	3.83E+00
	Mean	**8.88e-16**	1.02e+01	9.70e-14	3.44e-04	4.08e-15	5.98e-15	1.40e+01	5.90e-01	5.19e-03	2.99e+00	6.95E-02	2.30E+00
	STD	**0.00e+00**	1.30e+00	1.55e-14	1.62e-04	2.35e-15	1.79e-15	7.67e+00	9.94e-02	1.32e-03	1.19e+00	2.66E-01	4.82E-01
F11	Best	**0.00e+00**	1.22e+01	0.00e+00	2.77e-06	0.00e+00	0.00e+00	6.32e-01	9.32e-01	3.26e-04	1.59e-03	1.21E+01	1.02E-03
	Worst	**0.00e+00**	3.24e+01	2.93e-02	3.53e-02	1.89e-01	1.20e-04	9.10e+01	1.07e+00	1.29e-01	6.12e-02	4.75E+01	4.30E-02
	Mean	**0.00e+00**	2.11e+01	4.70e-03	6.41e-03	2.21e-02	4.98e-06	8.37e+00	1.01e+00	1.44e-02	1.69e-02	2.88E+01	1.10E-02
	STD	**0.00e+00**	5.28e+00	8.48e-03	7.85e-03	5.38e-02	2.23e-05	2.34e+01	2.46e-02	3.48e-02	1.26e-02	6.76E+00	9.04E-03
F12	Best	**1.72e-08**	9.28e+00	1.26e-02	7.85e-05	5.89e-03	6.03e-10	2.08e+00	2.94e-03	5.02e-05	1.44e+00	1.04E-01	3.05E-02
	Worst	**1.29e-06**	3.58e+03	1.15e-01	1.96e+00	3.17e-01	1.81e-05	5.04e+03	1.38e-02	1.46e-03	1.43e+01	4.34E+00	1.46E+00
	Mean	**3.79e-07**	2.74e+02	5.22e-02	1.32e-01	2.95e-02	1.25e-06	1.80e+02	8.11e-03	3.92e-04	7.24e+00	2.01E+00	3.75E-01
	STD	**3.32e-07**	6.87e+02	2.56e-02	3.72e-01	5.49e-02	3.53e-06	9.18e+02	2.47e-03	4.13e-04	3.26e+00	1.13E+00	3.69E-01
F13	Best	**8.67e-07**	1.36e+04	6.35e-02	1.01e-04	1.44e-01	4.00e-02	4.14e+00	8.53e-02	2.20e-04	2.09e-02	4.00E-02	6.38E-02
	Worst	**8.85e-05**	9.43e+05	1.05e+00	2.89e-01	1.37e+00	1.01e+00	1.91e+03	1.80e-01	7.14e-03	4.88e+01	3.69E+01	2.71E-01
	Mean	**1.10e-05**	1.66e+05	6.10e-01	4.78e-02	5.38e-01	4.38e-01	1.24e+02	1.23e-01	1.60e-03	1.80e+01	1.17E+01	1.21E-01
	STD	**1.56e-05**	2.15e+05	2.63e-01	7.61e-02	3.19e-01	2.69e-01	3.82e+02	2.52e-02	1.59e-03	1.41e+01	8.46E+00	4.09E-02

Table 9
Results of benchmark functions (F1-F13), with 100 dimensions.

No.		AVOA	PSO	GWO	FFA	WOA	TLBO	MFO	BBO	DE	SSA	GSA	IPO
F1	Best	**4.37e-260**	9.85e+03	3.22e-13	1.75e+03	7.24e-84	2.00e-92	3.00e+04	1.66e+02	2.44e+03	7.65e+02	2.74E+03	3.59E-01
	Worst	**2.77e-193**	2.44e+04	8.28e-12	3.29e+03	1.65e-69	1.68e-89	8.90e+04	2.64e+02	5.31e+03	2.73e+03	6.84E+03	2.72E+00
	Mean	**1.35e-194**	1.38e+04	1.89e-12	2.43e+03	5.62e-71	1.30e-90	5.84e+04	2.17e+02	3.50e+03	1.51e+03	4.25E+03	1.01E+00
	STD	**0.00e+00**	3.24e+03	1.69e-12	4.00e+02	3.02e-70	3.09e-90	1.30e+04	2.26e+01	7.32e+02	4.62e+02	8.52E+02	6.69E-01
F2	Best	**1.75e-139**	6.96e+01	1.31e-08	1.72e+01	2.78e-56	2.55e-47	1.95e+02	9.57e+00	3.40e+01	2.94e+01	1.26E+01	4.08E+00
	Worst	**4.65e-103**	1.06e+02	5.88e-08	5.20e+01	1.02e-48	1.48e-45	3.39e+02	1.26e+01	8.40e+01	1.25e+02	3.38E+01	1.01E+01
	Mean	**1.66e-104**	8.92e+01	3.85e-08	2.65e+01	6.24e-50	4.27e-46	2.42e+02	1.01e+01	6.26e+01	5.13e+01	1.84E+01	6.53E+00
	STD	**8.49e-104**	9.79e+00	1.07e-08	7.18e+00	2.02e-49	4.36e-46	2.80e+01	7.06e-01	1.20e+01	1.63e+01	4.78E+00	1.48E+00
F3	Best	**2.06e-208**	2.98e+04	3.91e+01	1.54e+05	6.46e+05	5.39e-14	1.17e+05	3.90e+04	3.04e+05	1.65e+04	8.84E+03	2.90E+03
	Worst	**3.71e-132**	1.86e+05	2.93e+03	2.33e+05	1.71e+06	1.16e-08	3.35e+05	7.08e+04	5.73e+05	1.01e+05	2.64E+04	9.60E+03
	Mean	**1.28e-133**	9.60e+04	6.03e+02	2.14e+05	1.06e+06	7.90e-10	2.34e+05	5.01e+04	4.76e+05	5.10e+04	1.54E+04	4.76E+03
	STD	**6.77e-133**	3.64e+04	6.81e+02	1.56e+04	2.92e+05	2.51e-09	6.22e+04	8.35e+03	6.00e+04	2.45e+04	4.59E+03	1.30E+03
F4	Best	**2.62e-129**	2.41e+01	1.49e-01	8.88e+01	2.74e+01	7.36e-39	8.77e+01	1.54e+01	9.02e+01	2.30e+01	1.63E+01	8.64E+00
	Worst	**2.74e-100**	4.00e+01	2.37e+00	9.76e+01	9.77e+01	4.44e-37	9.74e+01	2.75e+01	9.80e+01	3.75e+01	2.32E+01	1.37E+01
	Mean	**9.17e-102**	3.07e+01	5.79e-01	9.53e+01	8.22e+01	1.17e-37	9.36e+01	2.04e+01	9.49e+01	2.92e+01	1.95E+01	1.06E+01
	STD	**5.00e-101**	3.75e+00	4.84e-01	1.81e+00	1.67e+01	1.09e-37	2.11e+00	2.93e+00	1.85e+00	3.46e+00	1.90E+00	1.30E+00
F5	Best	**4.67e-04**	2.44e+06	9.59e+01	4.28e+06	9.77e+01	9.68e+01	6.30e+07	4.19e+03	2.42e+06	4.71e+04	3.66E+04	5.28E+03
	Worst	**2.88e-01**	7.32e+06	9.81e+01	2.10e+07	9.81e+01	9.84e+01	2.56e+08	7.36e+03	8.88e+06	2.55e+05	2.63E+05	2.59E+04
	Mean	**5.12e-02**	4.75e+06	9.77e+01	1.17e+07	9.79e+01	9.76e+01	1.50e+08	5.31e+03	5.34e+06	1.31e+05	1.15E+05	1.07E+04
	STD	**7.27e-02**	1.34e+06	5.87e-01	3.66e+06	2.15e-01	3.78e-01	5.84e+07	9.20e+02	1.61e+06	5.60e+04	6.87E+04	3.85E+03
F6	Best	**3.29e-06**	1.04e+04	6.88e+00	1.36e+03	2.10e+00	4.72e+00	2.79e+04	1.76e+02	2.38e+03	6.53e+02	2.96E+03	3.40E+01
	Worst	**3.51e-03**	1.89e+04	1.32e+01	3.29e+03	6.92e+00	9.46e+00	1.00e+05	2.99e+02	4.81e+03	2.72e+03	8.75E+03	1.40E+03
	Mean	**7.23e-04**	1.44e+04	1.00e+01	2.41e+03	4.26e+00	7.39e+00	5.91e+04	2.30e+02	3.39e+03	1.52e+03	4.65E+03	1.27E+02
	STD	**1.00e-03**	2.38e+03	1.55e+00	4.63e+02	1.25e+00	1.08e+00	1.45e+04	2.57e+01	6.31e+02	4.43e+02	1.10E+03	2.50E+02
F7	Best	**9.38e-06**	3.15e+00	2.54e-03	9.39e+00	5.81e-05	5.17e-04	5.24e+01	8.27e-02	3.39e+00	1.50e+00	2.15E+00	9.33E-01
	Worst	**4.68e-04**	1.34e+01	1.08e-02	2.06e+01	1.27e-02	3.20e-03	5.24e+02	1.68e-01	1.21e+01	4.72e+00	9.99E+00	3.60E+01
	Mean	**1.83e-04**	7.55e+00	6.72e-03	1.37e+01	3.53e-03	1.77e-03	2.41e+02	1.25e-01	6.56e+00	2.75e+00	4.38E+00	4.49E+00
	STD	**1.38e-04**	2.64e+00	2.26e-03	3.33e+00	3.52e-03	6.45e-04	1.11e+02	2.63e-02	2.14e+00	7.48e-01	1.82E+00	7.89E+00
F8	Best	**−4.15e+04**	−1.06e+04	−2.01e+04	−1.92e+04	−4.18e+04	−2.34e+04	−2.58e+04	−2.55e+04	−1.37e+04	−2.59e+04	−6.02E+03	−1.36E+04
	Worst	**−4.12e+04**	−6.28e+03	−5.85e+03	−8.89e+03	−2.52e+04	−1.05e+04	−1.82e+04	−2.02e+04	−1.09e+04	−1.79e+04	−2.87E+03	−4.91E+03
	Mean	**−4.14e+04**	−7.62e+03	−1.58e+04	−1.36e+04	−3.40e+04	−1.69e+04	−2.17e+04	−2.25e+04	−1.18e+04	−2.14e+04	−4.05E+03	−1.07E+04
	STD	**5.28e+01**	1.13e+03	3.05e+03	3.09e+03	5.69e+03	2.71e+03	1.83e+03	1.03e+03	6.65e+02	1.73e+03	7.99E+02	1.93E+03
F9	Best	**0.00e+00**	6.66e+02	1.38e-10	6.44e+02	**0.00e+00**	**0.00e+00**	7.43e+02	2.55e+02	9.10e+02	1.54e+02	1.37E+02	2.40E+02
	Worst	**0.00e+00**	8.35e+02	2.39e+01	1.08e+03	**0.00e+00**	**0.00e+00**	1.00e+03	3.98e+02	1.02e+03	3.03e+02	2.65E+02	3.43E+02
	Mean	**0.00e+00**	7.36e+02	8.83e+00	8.92e+02	**0.00e+00**	**0.00e+00**	8.64e+02	3.17e+02	9.80e+02	2.35e+02	1.93E+02	2.79E+02
	STD	**0.00e+00**	4.13e+01	6.15e+00	1.19e+02	**0.00e+00**	**0.00e+00**	7.54e+01	3.33e+01	2.85e+01	3.87e+01	3.64E+01	2.58E+01
F10	Best	**8.88e-16**	1.09e+01	7.13e-08	7.59e+00	8.88e-16	4.44e-15	1.94e+01	3.18e+00	7.87e+00	8.38e+00	3.54E+00	4.27E+00
	Worst	**8.88e-16**	1.32e+01	3.21e-07	9.84e+00	7.99e-15	7.99e-15	2.03e+01	3.56e+00	1.00e+01	1.23e+01	6.83E+00	6.45E+00
	Mean	**8.88e-16**	1.19e+01	1.30e-07	8.68e+00	4.08e-15	7.63e-15	1.99e+01	3.42e+00	9.11e+00	1.01e+01	4.96E+00	4.93E+00
	STD	**0.00e+00**	6.76e-01	6.01e-08	5.81e-01	1.94e-15	1.05e-15	1.31e-01	1.19e-01	6.18e-01	1.10e+00	7.62E-01	5.55E-01
F11	Best	**0.00e+00**	9.56e+01	1.93e-13	1.48e+01	**0.00e+00**	**0.00e+00**	3.55e+02	2.65e+00	1.64e+01	6.66e+00	6.10E+02	3.47E-01
	Worst	**0.00e+00**	1.77e+02	3.18e-02	3.22e+01	**0.00e+00**	**0.00e+00**	7.09e+02	3.59e+00	5.61e+01	2.20e+01	7.86E+02	1.09E+00
	Mean	**0.00e+00**	1.23e+02	5.30e-03	2.29e+01	**0.00e+00**	**0.00e+00**	5.33e+02	3.17e+00	3.13e+01	1.34e+01	6.92E+02	8.22E-01
	STD	**0.00e+00**	2.15e+01	1.09e-02	4.15e+00	**0.00e+00**	**0.00e+00**	1.05e+02	2.01e-01	8.05e+00	3.60e+00	4.12E+01	2.48E-01
F12	Best	**4.01e-07**	4.25e+02	1.46e-01	1.09e+07	1.83e-02	7.43e-02	5.11e+07	1.22e+00	3.46e+06	1.20e+01	4.70E+00	5.24E+00
	Worst	**6.36e-05**	6.15e+05	5.08e-01	5.79e+07	1.30e-01	1.62e-01	6.24e+08	1.27e+01	1.94e+07	5.70e+01	1.93E+01	8.15E+00
	Mean	**6.55e-06**	1.21e+05	3.07e-01	2.26e+07	5.34e-02	1.17e-01	2.84e+08	4.05e+00	9.18e+06	3.23e+01	1.17E+01	6.92E+00
	STD	**1.25e-05**	1.30e+05	7.64e-02	1.01e+07	2.89e-02	2.31e-02	1.62e+08	2.41e+00	4.31e+06	9.77e+00	3.91E+00	8.03E-01
F13	Best	**3.39e-05**	7.78e+05	5.76e+00	1.74e+07	1.26e+00	6.62e+00	1.76e+08	9.06e+00	6.15e+06	1.60e+02	1.86E+02	5.39E+00
	Worst	**2.88e-03**	8.58e+06	7.51e+00	8.77e+07	4.62e+00	9.92e+00	1.14e+09	1.34e+01	3.56e+07	5.85e+04	3.02E+04	1.60E+02
	Mean	**7.54e-04**	3.39e+06	6.72e+00	5.33e+07	2.75e+00	8.09e+00	5.71e+08	1.13e+01	1.68e+07	6.04e+03	4.90E+03	3.59E+01
	STD	**7.67e-04**	2.04e+06	3.97e-01	1.87e+07	9.29e-01	9.62e-01	2.90e+08	1.18e+00	7.34e+06	1.19e+04	7.72E+03	4.23E+01

Table 10
Results of benchmark functions (F1-F13), with 500 dimensions.

No.		AVOA	PSO	GWO	FFA	WOA	TLBO	MFO	BBO	DE	SSA	GSA	IPO
F1	Best	**3.18e-249**	7.46e+04	6.20e-04	4.86e+05	1.40e-83	3.47e-88	1.05e+06	6.32e+03	4.89e+05	7.64e+04	5.02E+04	9.28E+03
	Worst	**2.94e-199**	1.19e+05	2.89e-03	5.62e+05	6.09e-66	4.43e-85	1.22e+06	8.16e+03	6.17e+05	1.05e+05	6.22E+04	1.39E+04
	Mean	**1.04e-200**	9.80e+04	1.57e-03	5.25e+05	2.05e-67	4.13e-86	1.12e+06	7.15e+03	5.63e+05	9.33e+04	5.57E+04	1.13E+04
	STD	**0.00e+00**	1.30e+04	5.47e-04	2.02e+04	1.11e-66	9.06e-86	3.11e+04	5.43e+02	2.92e+04	8.25e+03	2.82E+03	1.17E+03
F2	Best	**2.15e-131**	4.49e+02	8.12e-03	1.77e+52	2.13e-55	4.25e-45	5.79e+75	2.05e+02	1.44e+03	4.97e+02	2.80E+02	1.64E+02
	Worst	**1.00e-99**	6.36e+02	1.42e-02	7.09e+117	9.69e-47	3.44e-43	1.77e+120	2.75e+02	1.54e+03	5.75e+02	3.23E+270	1.98E+02
	Mean	**3.38e-101**	5.33e+02	1.09e-02	2.36e+116	3.89e-48	3.95e-44	6.04e+118	2.29e+02	1.50e+03	5.31e+02	1.08E+269	1.81E+02
	STD	**1.84e-100**	4.81e+01	1.58e-03	1.29e+117	1.78e-47	6.78e-44	3.24e+119	1.72e+01	3.50e+01	2.00e+01	1.00e+300	9.43E+00
F3	Best	**7.15e-196**	1.00e+06	2.33e+05	4.74e+06	1.49e+07	6.47e-08	3.31e+06	1.19e+06	8.87e+06	5.20e+05	3.92E+05	1.10E+05
	Worst	**8.95e-102**	5.44e+06	5.27e+05	6.41e+06	5.22e+07	8.04e-03	6.39e+06	2.34e+06	1.32e+07	2.39e+06	3.88E+06	2.20E+05
	Mean	**2.98e-103**	2.29e+06	3.57e+05	5.57e+06	3.04e+07	6.76e-04	4.80e+06	1.55e+06	1.16e+07	1.24e+06	1.17E+06	1.48E+05
	STD	**1.63e-102**	8.31e+05	7.70e+04	4.80e+05	1.00e+07	1.99e-03	9.16e+05	2.25e+05	1.10e+06	6.10e+05	6.80E+05	2.78E+04
F4	Best	**1.87e-136**	3.44e+01	5.69e+01	9.83e+01	1.62e+01	8.57e-37	9.82e+01	4.86e+01	9.88e+01	3.50e+01	2.55E+01	1.84E+01
	Worst	**3.49e-100**	4.77e+01	7.77e+01	9.92e+01	9.87e+01	4.51e-35	9.91e+01	5.75e+01	9.92e+01	4.86e+01	3.27E+01	2.19E+01
	Mean	**1.47e-101**	3.82e+01	6.47e+01	9.89e+01	8.19e+01	8.65e-36	9.85e+01	5.27e+01	9.89e+01	4.03e+01	2.87E+01	2.04E+01
	STD	**6.43e-101**	2.73e+00	5.77e+00	3.01e-01	2.10e+01	9.83e-36	3.71e-01	2.07e+00	1.98e-01	3.30e+00	1.56E+00	9.22E-01
F5	Best	**3.34e-03**	2.16e+07	4.93e+02	1.72e+09	4.91e+02	4.94e+02	4.64e+09	6.08e+05	1.75e+09	2.75e+07	6.49E+06	2.31E+06
	Worst	**1.86e+01**	6.50e+07	4.96e+02	2.95e+09	4.97e+02	4.97e+02	5.45e+09	1.01e+06	6.00e+09	4.72e+07	1.40E+07	3.53E+06
	Mean	**3.66e+00**	4.31e+07	4.94e+02	2.30e+09	4.93e+02	4.95e+02	5.02e+09	8.44e+05	2.82e+09	3.71e+07	8.69E+06	2.85E+06
	STD	**4.12e+00**	1.13e+07	3.30e-01	3.17e+08	3.52e-01	1.13e-01	2.21e+08	9.37e+04	8.04e+08	4.14e+06	1.62E+06	3.81E+05
F6	Best	**2.76e-04**	7.35e+04	8.75e+01	4.72e+05	1.89e+01	9.06e+01	1.05e+06	6.66e+03	4.87e+05	7.57e+04	5.00E+04	1.36E+04
	Worst	**4.78e-01**	1.20e+05	9.44e+01	5.73e+05	4.73e+01	9.82e+01	1.21e+06	8.51e+03	6.23e+05	1.08e+05	6.27E+04	2.71E+04
	Mean	**5.90e-02**	9.65e+04	9.14e+01	5.29e+05	3.24e+01	9.42e+01	1.15e+06	7.35e+03	5.50e+05	9.42e+04	5.70E+04	1.96E+04
	STD	**1.03e-01**	1.42e+04	1.68e+00	2.55e+04	8.30e+00	2.05e+00	3.50e+04	4.77e+02	3.53e+04	6.51e+03	2.75E+03	4.06E+03
F7	Best	**2.71e-06**	1.74e+02	2.62e-02	1.23e+04	1.43e-04	5.14e-04	3.28e+04	3.67e+02	1.16e+04	2.08e+02	7.08E+02	1.77E+03
	Worst	**5.53e-04**	6.70e+02	7.89e-02	1.91e+04	1.40e-02	3.30e-03	4.23e+04	7.03e+02	2.04e+04	3.54e+02	1.44E+03	4.79E+03
	Mean	**2.09e-04**	3.50e+02	5.20e-02	1.59e+04	4.65e-03	1.67e-03	3.87e+04	4.96e+02	1.55e+04	2.75e+02	9.88E+02	2.86E+03
	STD	**1.54e-04**	1.35e+02	1.36e-02	1.49e+03	4.70e-03	6.18e-04	2.31e+03	9.00e+01	2.19e+03	3.96e+01	1.74E+02	7.30E+02
F8	Best	**−2.13e+05**	−2.25e+04	−6.50e+04	−3.92e+04	−2.09e+05	−6.07e+04	−7.14e+04	−7.49e+04	−2.76e+04	−6.80e+04	−1.61E+04	−4.85E+04
	Worst	**−2.10e+05**	−1.34e+04	−4.96e+04	−1.84e+04	−1.26e+05	−2.57e+04	−5.01e+04	−6.62e+04	−2.38e+04	−4.93e+04	−6.32E+03	−9.29E+03
	Mean	**−2.12e+05**	−1.78e+04	−5.80e+04	−2.73e+04	−1.69e+05	−3.96e+04	−6.22e+04	−7.07e+04	−2.55e+04	−6.08e+04	−1.10E+04	−3.06E+04
	STD	**6.16e+02**	2.57e+03	3.75e+03	5.92e+03	3.09e+04	9.39e+03	4.89e+03	2.53e+03	1.12e+03	4.37e+03	2.27E+03	1.44E+04
F9	Best	**0.00e+00**	4.28e+03	2.37e+01	6.50e+03	**0.00e+00**	**0.00e+00**	6.61e+03	5.75e+03	6.51e+03	2.95e+03	2.53E+03	3.17E+03
	Worst	**0.00e+00**	4.86e+03	1.61e+02	7.02e+03	**0.00e+00**	**0.00e+00**	7.27e+03	6.41e+03	7.10e+03	3.34e+03	2.98E+03	3.45E+03
	Mean	**0.00e+00**	4.61e+03	7.88e+01	6.84e+03	**0.00e+00**	**0.00e+00**	6.93e+03	6.05e+03	6.75e+03	3.16e+03	2.73E+03	3.33E+03
	STD	**0.00e+00**	1.58e+02	2.83e+01	1.16e+02	**0.00e+00**	**0.00e+00**	1.65e+02	1.80e+02	1.24e+02	1.04e+02	1.16E+02	7.02E+01
F10	Best	**8.88e-16**	1.21e+01	1.23e-03	1.95e+01	8.88e-16	4.44e-15	2.03e+01	2.02e+01	1.91e+01	1.38e+01	1.01E+01	1.35E+01
	Worst	**8.88e-16**	1.44e+01	3.38e-03	1.98e+01	7.99e-15	7.99e-15	2.05e+01	2.05e+01	2.01e+01	1.46e+01	1.11E+01	1.46E+01
	Mean	**8.88e-16**	1.30e+01	1.90e-03	1.97e+01	4.44e-15	7.87e-15	2.04e+01	2.03e+01	1.95e+01	1.42e+01	1.05E+01	1.41E+01
	STD	**0.00e+00**	6.47e-01	4.40e-04	9.58e-02	2.46e-15	6.48e-16	1.49e-01	8.64e-02	1.45e-01	2.27e-01	2.32E-01	2.56E-01
F11	Best	**0.00e+00**	6.73e+02	1.07e-04	4.18e+03	**0.00e+00**	**0.00e+00**	9.83e+03	2.27e+03	4.02e+03	7.64e+02	8.17E+03	8.63E+01
	Worst	**0.00e+00**	1.28e+03	1.29e-01	5.16e+03	**0.00e+00**	**0.00e+00**	1.06e+04	3.30e+03	5.53e+03	9.47e+02	8.99E+03	1.11E+02
	Mean	**0.00e+00**	9.41e+02	3.35e-02	4.71e+03	**0.00e+00**	**0.00e+00**	1.02e+04	3.02e+03	5.03e+03	8.46e+02	8.61E+03	9.61E+01
	STD	**0.00e+00**	1.74e+02	4.90e-02	2.14e+02	**0.00e+00**	**0.00e+00**	2.86e+02	2.62e+02	3.34e+02	5.56e+01	2.05E+02	5.73E+00
F12	Best	**8.97e-09**	8.55e+05	6.59e-01	4.04e+09	2.45e-02	5.89e-01	1.05e+10	3.84e+08	4.69e+09	2.27e+05	1.99E+02	1.39E+01
	Worst	**4.98e-04**	1.47e+07	8.21e-01	9.90e+09	1.87e-01	7.19e-01	1.24e+10	7.24e+08	1.83e+10	3.69e+06	8.02E+04	2.42E+01
	Mean	**4.19e-05**	4.05e+06	7.43e-01	7.44e+09	8.59e-02	6.52e-01	1.20e+10	4.95e+08	1.13e+10	1.39e+06	1.46E+04	1.92E+01
	STD	**9.45e-05**	3.49e+06	4.36e-02	1.53e+09	4.24e-02	3.33e-02	5.00e+08	8.51e+07	4.24e+09	7.92e+05	1.91E+04	2.40E+00
F13	Best	**3.38e-04**	1.41e+07	4.88e+01	7.74e+09	9.45e+00	4.98e+01	1.94e+10	8.71e+08	7.35e+09	1.85e+07	1.69E+06	6.78E+03
	Worst	**1.99e-01**	1.27e+08	5.40e+01	1.42e+10	2.58e+01	4.99e+01	2.42e+10	1.75e+09	3.43e+10	5.92e+07	7.18E+06	5.47E+04
	Mean	**2.52e-02**	5.34e+07	5.11e+01	1.13e+10	1.80e+01	4.99e+01	2.21e+10	1.35e+09	1.47e+10	3.32e+07	3.89E+06	2.73E+04
	STD	**4.30e-02**	2.83e+07	1.25e+00	1.63e+09	4.12e+00	7.42e-03	9.85e+08	2.47e+08	6.31e+09	8.49e+06	1.33E+06	1.13E+04

Table 11
Results of benchmark functions (F1-F13), with 1000 dimensions.

No.		AVOA	PSO	GWO	FFA	WOA	TLBO	MFO	BBO	DE	SSA	GSA	IPO
F1	Best	**7.50e-278**	1.47e+05	1.41e-01	1.33e+06	9.06e-84	2.06e-87	2.62e+06	6.00e+05	1.49e+06	2.12e+05	1.22E+05	4.10E+04
	Worst	**3.06e-193**	3.04e+05	4.79e-01	1.49e+06	5.41e-67	2.33e-84	2.83e+06	7.30e+05	1.81e+06	2.67e+05	1.48E+05	5.07E+04
	Mean	**1.05e-194**	2.16e+05	2.42e-01	1.43e+06	1.80e-68	2.44e-85	2.73e+06	6.69e+05	1.60e+06	2.37e+05	1.31E+05	4.60E+04
	STD	**0.00e+00**	4.33e+04	7.43e-02	4.49e+04	9.88e-68	4.40e-85	4.83e+04	2.99e+04	8.51e+04	1.30e+04	5.62E+03	2.32E+03
F2	Best	**4.21e-173**	1.00e+300	2.87e-01	1.00e+300	2.13e-56	1.00e+300	1.00e+300	1.00e+300	1.00e+300	1.11e+03	1.17E+263	4.39E+02
	Worst	**2.02e-112**	1.00e+300	2.10e+00	1.00e+300	2.83e-47	1.00e+300	1.00e+300	1.00e+300	1.00e+300	1.25e+03	6.38E+289	4.88E+02
	Mean	**6.75e-114**	1.00e+300	7.17e-01	1.00e+300	1.93e-48	1.00e+300	1.00e+300	1.00e+300	1.00e+300	1.19e+03	3.46E+288	4.60E+02
	STD	**3.69e-113**	1.00e+300	3.96e-01	1.00e+300	5.68e-48	1.00e+300	1.00e+300	1.00e+300	1.00e+300	3.14e+01	1.00e+300	1.04E+01
F3	Best	**2.27e-219**	3.96e+06	1.15e+06	1.83e+07	6.83e+07	4.55e-06	1.31e+07	6.81e+06	3.62e+07	2.37e+06	2.99E+06	3.28E+05
	Worst	**5.26e-111**	1.36e+07	2.65e+06	2.49e+07	2.26e+08	1.59e-01	2.66e+07	1.23e+07	5.94e+07	9.55e+06	1.37E+07	7.63E+05
	Mean	**1.76e-112**	8.18e+06	1.67e+06	2.15e+07	1.32e+08	1.13e-02	1.85e+07	9.66e+06	4.77e+07	5.92e+06	6.53E+06	5.55E+05
	STD	**9.60e-112**	2.44e+06	3.22e+05	1.82e+06	4.84e+07	3.16e-02	3.66e+06	1.60e+06	5.67e+06	1.92e+06	2.56E+06	9.61E+04
F4	Best	**3.10e-143**	3.61e+01	7.28e+01	9.91e+01	9.05e+00	2.61e-36	9.90e+01	8.27e+01	9.88e+01	4.00e+01	3.13E+01	2.24E+01
	Worst	**1.34e-100**	5.58e+01	8.84e+01	9.95e+01	9.96e+01	1.50e-34	9.94e+01	8.99e+01	9.95e+01	5.26e+01	3.72E+01	2.47E+01
	Mean	**4.47e-102**	4.23e+01	7.90e+01	9.92e+01	8.23e+01	2.97e-35	9.92e+01	8.60e+01	9.91e+01	4.48e+01	3.40E+01	2.35E+01
	STD	**2.44e-101**	3.75e+00	3.21e+00	9.52e-02	2.01e+01	2.95e-35	1.42e-01	2.03e+00	1.40e-01	2.82e+00	1.28E+00	7.51E-01
F5	Best	**1.44e-03**	5.25e+07	1.00e+03	6.94e+09	9.92e+02	9.93e+02	1.19e+10	7.96e+08	1.42e+10	9.60e+07	2.09E+07	1.14E+07
	Worst	**5.25e+01**	2.02e+08	1.12e+03	9.62e+09	9.95e+02	9.95e+02	1.31e+10	1.17e+09	1.53e+10	1.53e+08	2.85E+07	1.61E+07
	Mean	**5.80e+00**	9.78e+07	1.02e+03	8.51e+09	9.93e+02	9.94e+02	1.24e+10	9.58e+08	1.48e+10	1.14e+08	2.47E+07	1.36E+07
	STD	**1.11e+01**	3.42e+07	2.12e+01	6.35e+08	7.07e-01	1.31e-01	2.91e+08	8.91e+07	2.77e+08	1.21e+07	1.95E+06	1.09E+06
F6	Best	**2.26e-03**	1.41e+05	1.95e+02	1.28e+06	2.80e+01	2.03e+02	2.57e+06	6.07e+05	1.38e+06	2.15e+05	1.21E+05	4.69E+04
	Worst	**1.05e+00**	2.91e+05	2.06e+02	1.47e+06	1.17e+02	2.18e+02	2.75e+06	7.21e+05	2.27e+06	2.54e+05	1.48E+05	9.84E+04
	Mean	**1.27e-01**	1.99e+05	2.00e+02	1.41e+06	7.29e+01	2.13e+02	2.72e+06	6.66e+05	1.63e+06	2.37e+05	1.31E+05	6.24E+04
	STD	**2.06e-01**	3.44e+04	2.79e+00	5.50e+04	1.91e+01	2.20e+00	4.95e+04	3.34e+04	1.61e+05	1.12e+04	5.65E+03	1.06E+04
F7	Best	**1.41e-05**	8.87e+02	9.98e-02	8.40e+04	1.30e-04	8.77e-04	1.90e+05	1.19e+04	9.92e+04	1.31e+03	5.43E+03	1.83E+04
	Worst	**9.11e-04**	2.64e+03	2.10e-01	1.28e+05	1.87e-02	3.67e-03	2.09e+05	1.56e+04	2.49e+05	2.15e+03	8.26E+03	2.69E+04
	Mean	**2.85e-04**	1.57e+03	1.48e-01	1.10e+05	3.54e-03	2.01e-03	1.97e+05	1.34e+04	2.05e+05	1.69e+03	6.43E+03	2.20E+04
	STD	**2.43e-04**	4.93e+02	3.08e-02	1.27e+04	4.43e-03	6.18e-04	4.50e+03	1.15e+03	5.24e+04	1.74e+02	7.09E+02	2.00E+03
F8	Best	**−4.18e+05**	−3.43e+04	−1.02e+05	−6.79e+04	−4.18e+05	−9.18e+04	−1.79e+05	−8.37e+04	−4.25e+04	−1.01e+05	−2.38E+04	−7.88E+04
	Worst	**−3.95e+05**	−1.98e+04	−1.77e+04	−2.46e+04	−2.21e+05	−2.75e+04	−7.40e+04	−7.22e+04	−3.39e+04	−7.11e+04	−9.51E+03	−1.60E+04
	Mean	**−4.17e+05**	−2.58e+04	−8.58e+04	−3.72e+04	−3.27e+05	−5.87e+04	−8.72e+04	−7.80e+04	−3.64e+04	−8.72e+04	−1.34E+04	−5.47E+04
	STD	**4.69e+03**	3.72e+03	1.88e+04	1.07e+04	6.28e+04	1.38e+04	6.85e+03	2.85e+03	2.00e+03	8.08e+03	2.78E+03	1.89E+04
F9	Best	**0.00e+00**	9.21e+03	1.11e+02	1.38e+04	**0.00e+00**	**0.00e+00**	1.50e+04	1.13e+04	1.38e+04	7.17e+03	6.23E+03	7.62E+03
	Worst	**0.00e+00**	1.00e+04	2.90e+02	1.46e+04	**0.00e+00**	**0.00e+00**	1.58e+04	1.18e+04	1.43e+04	7.93e+03	7.02E+03	8.10E+03
	Mean	**0.00e+00**	9.66e+03	1.90e+02	1.43e+04	**0.00e+00**	**0.00e+00**	1.52e+04	1.17e+04	1.41e+04	7.57e+03	6.69E+03	7.79E+03
	STD	**0.00e+00**	1.87e+02	4.19e+01	1.64e+02	**0.00e+00**	**0.00e+00**	1.92e+02	2.42e+02	2.41e+02	2.07e+02	2.16E+02	1.13E+02
F10	Best	**8.88e-16**	1.24e+01	1.38e-02	1.95e+01	8.88e-16	7.99e-15	2.00e+01	1.96e+01	2.01e+01	1.42e+01	1.10E+01	1.41E+01
	Worst	**8.88e-16**	1.55e+01	2.24e-02	2.03e+01	4.44e-15	1.30e+01	2.06e+01	2.03e+01	2.06e+01	1.49e+01	1.15E+01	1.48E+01
	Mean	**8.88e-16**	1.37e+01	1.83e-02	2.00e+01	3.01e-15	4.29e-01	2.05e+01	2.00e+01	2.03e+01	1.46e+01	1.12E+01	1.45E+01
	STD	**0.00e+00**	8.96e-01	2.17e-03	9.92e-02	1.77e-15	2.34e+00	1.91e-01	8.64e-02	1.10e-01	1.82e-01	1.43E-01	1.51E-01
F11	Best	**0.00e+00**	1.42e+03	8.47e-03	1.12e+04	**0.00e+00**	0.00e+00	2.40e+04	5.15e+03	1.24e+04	1.97e+03	1.98E+04	4.78E+02
	Worst	**0.00e+00**	2.50e+03	2.50e-01	1.38e+04	**0.00e+00**	1.11e-16	2.51e+04	6.47e+03	1.70e+04	2.30e+03	2.13E+04	5.97E+02
	Mean	**0.00e+00**	1.87e+03	5.11e-02	1.28e+04	**0.00e+00**	3.33e-17	2.46e+04	5.86e+03	1.45e+04	2.07e+03	2.05E+04	5.44E+02
	STD	**0.00e+00**	2.73e+02	7.61e-02	5.92e+02	**0.00e+00**	5.17e-17	3.53e+02	3.55e+02	1.02e+03	8.45e+01	3.34E+02	2.69E+01
F12	Best	**2.19e-07**	1.28e+06	9.04e-01	2.38e+10	3.60e-02	8.20e-01	2.79e+10	7.51e+08	3.39e+10	5.05e+06	5.39E+04	2.68E+01
	Worst	**5.89e-04**	3.48e+07	1.88e+00	3.85e+10	3.03e-01	8.94e-01	3.22e+10	1.07e+09	3.79e+10	1.79e+07	5.00E+05	1.90E+02
	Mean	**6.76e-05**	1.09e+07	1.18e+00	3.17e+10	1.05e-01	8.54e-01	3.04e+10	8.87e+08	3.68e+10	1.11e+07	1.88E+05	5.47E+01
	STD	**1.44e-04**	8.13e+06	2.76e-01	4.68e+09	6.06e-02	1.52e-02	1.01e+09	8.29e+07	1.09e+09	3.00e+06	1.19E+05	3.99E+01
F13	Best	**1.93e-03**	3.71e+07	1.06e+02	3.44e+10	1.91e+01	9.98e+01	5.15e+10	2.35e+09	6.49e+10	1.08e+08	9.50E+06	3.58E+05
	Worst	**2.89e-01**	3.20e+08	1.24e+02	4.87e+10	6.70e+01	9.95e+01	5.80e+10	3.42e+09	6.92e+10	2.15e+08	2.66E+07	1.04E+06
	Mean	**5.76e-02**	1.15e+08	1.18e+02	4.44e+10	3.65e+01	9.94e+01	5.55e+10	2.78e+09	6.70e+10	1.46e+08	1.60E+07	6.38E+05
	STD	**8.02e-02**	6.11e+07	5.35e+00	3.17e+09	1.14e+01	1.17e-02	1.44e+09	2.71e+08	1.22e+09	2.20e+07	4.03E+06	1.92E+05

Table 12
Comparison of average running time results (seconds) over 30 runs for larger-scale problems with 1000 variables.

No.		AVOA	PSO	GWO	FFA	WOA	TLBO	MFO	BBO	DE	SSA	GSA	IPO
F1	Best	**9.17E-01**	1.45E+00	2.70E+00	2.77E+00	2.51E+00	1.40E+00	1.85E+00	1.40E+01	1.65E+00	1.56E+00	1.61E+01	6.13E+00
	Worst	**1.08E+00**	2.40E+00	3.16E+00	3.24E+00	2.90E+00	2.39E+00	2.12E+00	1.50E+01	2.08E+00	1.76E+00	1.88E+01	9.62E+00
	Mean	**1.02E+00**	1.64E+00	2.75E+00	2.85E+00	2.74E+00	1.63E+00	1.93E+00	1.42E+01	1.73E+00	1.63E+00	1.64E+01	6.73E+00
	STD	**7.82E-02**	2.19E-01	9.87E-02	1.31E-01	1.08E-01	2.14E-01	6.81E-02	1.48E-01	1.12E-01	4.87E-02	6.90E-01	6.83E-01
F2	Best	**9.92E-01**	1.51E+00	2.79E+00	2.99E+00	2.81E+00	1.50E+00	1.90E+00	1.42E+01	1.69E+00	1.58E+00	6.56E+01	6.00E+00
	Worst	**1.13E+00**	1.86E+00	3.32E+00	4.33E+00	3.18E+00	1.88E+00	2.24E+00	1.87E+01	1.99E+00	1.78E+00	9.04E+01	7.19E+00
	Mean	**1.01E+00**	1.72E+00	2.89E+00	3.27E+00	2.96E+00	1.65E+00	2.00E+00	1.46E+01	1.89E+00	1.62E+00	7.30E+01	6.51E+00
	STD	**4.36E-02**	1.01E-01	1.04E-01	3.16E-01	9.40E-02	8.26E-02	8.58E-02	8.72E-01	8.18E-02	4.77E-02	7.88E+00	2.70E-01
F3	Best	**2.40E+01**	3.02E+01	3.05E+01	5.43E+01	3.06E+01	5.53E+01	2.84E+01	5.85E+01	2.96E+01	2.82E+01	3.94E+01	2.19E+01
	Worst	**2.54E+01**	3.66E+01	3.71E+01	5.95E+01	3.50E+01	6.07E+01	2.98E+01	5.93E+01	3.35E+01	3.00E+01	4.19E+01	3.90E+01
	Mean	**2.41E+01**	3.10E+01	3.10E+01	5.47E+01	3.13E+01	5.60E+01	2.89E+01	5.86E+01	3.01E+01	2.84E+01	3.97E+01	2.95E+01
	STD	**3.34E-01**	1.49E+00	1.45E+00	1.11E+00	9.16E-01	1.03E+00	2.16E-01	3.10E-01	8.12E-01	3.33E-01	6.33E-01	5.66E+00
F4	Best	**8.99E-01**	1.42E+00	2.74E+00	2.63E+00	2.82E+00	1.35E+00	1.82E+00	1.40E+01	1.71E+00	1.54E+00	1.61E+01	6.03E+00
	Worst	**1.07E+00**	2.44E+00	3.25E+00	3.27E+00	3.82E+00	2.13E+00	2.00E+00	1.64E+01	2.23E+00	1.71E+00	1.98E+01	6.64E+00
	Mean	**9.56E-01**	1.69E+00	2.86E+00	2.84E+00	3.04E+00	1.47E+00	1.89E+00	1.43E+01	1.89E+00	1.59E+00	1.64E+01	6.45E+00
	STD	**3.88E-02**	2.00E-01	1.00E-01	1.47E-01	2.05E-01	1.77E-01	5.74E-02	5.73E-01	1.45E-01	4.92E-02	9.44E-01	2.02E-01
F5	Best	**9.97E-01**	1.76E+00	2.80E+00	2.84E+00	2.88E+00	1.54E+00	1.91E+00	1.40E+01	1.64E+00	1.66E+00	1.62E+01	6.32E+00
	Worst	**1.19E+00**	2.09E+00	4.97E+00	3.33E+00	3.71E+00	2.12E+00	2.09E+00	1.56E+01	2.32E+00	1.87E+00	2.14E+01	6.87E+00
	Mean	**1.03E+00**	1.91E+00	3.10E+00	3.03E+00	3.21E+00	1.75E+00	1.97E+00	1.42E+01	1.91E+00	1.74E+00	1.66E+01	6.72E+00
	STD	**4.27E-02**	1.06E-01	4.31E-01	9.62E-02	1.90E-01	1.68E-01	6.04E-02	3.38E-01	1.57E-01	5.85E-02	1.34E+00	9.59E-02
F6	Best	**9.38E-01**	1.45E+00	2.73E+00	2.74E+00	2.94E+00	1.34E+00	1.83E+00	1.41E+01	1.69E+00	1.62E+00	1.61E+01	5.89E+00
	Worst	**1.11E+00**	2.02E+00	3.46E+00	3.17E+00	3.77E+00	1.96E+00	2.00E+00	1.51E+01	2.21E+00	1.90E+00	1.93E+01	6.58E+00
	Mean	**9.74E-01**	1.76E+00	2.88E+00	2.88E+00	3.14E+00	1.52E+00	1.90E+00	1.43E+01	1.91E+00	1.70E+00	1.67E+01	6.36E+00
	STD	**3.80E-02**	1.29E-01	1.82E-01	9.69E-02	1.58E-01	1.60E-01	5.20E-02	1.33E-01	1.34E-01	6.84E-02	1.03E+00	1.45E-01
F7	Best	**2.94E+00**	3.97E+00	5.20E+00	7.25E+00	5.08E+00	6.17E+00	4.21E+00	1.51E+01	4.06E+00	3.97E+00	1.82E+01	7.24E+00
	Worst	**3.41E+00**	4.54E+00	5.52E+00	7.75E+00	6.75E+00	6.56E+00	4.51E+00	1.65E+01	4.37E+00	4.27E+00	2.60E+01	1.03E+01
	Mean	**3.05E+00**	4.07E+00	5.27E+00	7.37E+00	5.37E+00	6.24E+00	4.25E+00	1.55E+01	4.12E+00	4.02E+00	2.01E+01	7.86E+00
	STD	**1.11E-01**	1.88E-01	8.60E-02	1.25E-01	3.59E-01	8.83E-02	6.89E-02	3.20E-01	8.51E-02	6.51E-02	3.27E+00	6.37E-01
F8	Best	**1.26E+00**	2.45E+00	3.17E+00	3.89E+00	3.33E+00	2.51E+00	2.28E+00	1.50E+01	2.60E+00	2.19E+00	2.38E+01	6.12E+00
	Worst	**1.77E+00**	3.51E+00	3.74E+00	4.71E+00	3.92E+00	3.19E+00	2.77E+00	1.59E+01	3.64E+00	2.54E+00	2.88E+01	6.94E+00
	Mean	**1.35E+00**	2.71E+00	3.23E+00	4.25E+00	3.59E+00	2.78E+00	2.41E+00	1.52E+01	2.82E+00	2.32E+00	2.45E+01	6.62E+00
	STD	**1.19E-01**	1.84E-01	1.08E-01	1.68E-01	1.38E-01	1.72E-01	1.13E-01	2.54E-01	2.25E-01	7.37E-02	1.34E+00	1.57E-01
F9	Best	**1.02E+00**	2.26E+00	2.93E+00	3.72E+00	3.05E+00	1.88E+00	2.18E+00	1.45E+01	2.53E+00	2.03E+00	1.63E+01	6.25E+00
	Worst	**1.26E+00**	3.00E+00	3.23E+00	4.51E+00	3.68E+00	2.58E+00	2.67E+00	1.55E+01	2.89E+00	2.31E+00	2.38E+01	9.95E+00
	Mean	**1.07E+00**	2.48E+00	3.00E+00	4.02E+00	3.29E+00	2.17E+00	2.28E+00	1.50E+01	2.62E+00	2.13E+00	1.91E+01	6.87E+00
	STD	**4.70E-02**	1.56E-01	7.73E-02	2.07E-01	1.41E-01	1.78E-01	9.77E-02	1.69E-01	6.92E-02	7.15E-02	3.54E+00	6.97E-01
F10	Best	**1.07E+00**	2.10E+00	2.98E+00	3.75E+00	3.05E+00	1.96E+00	2.26E+00	1.46E+01	2.58E+00	2.08E+00	1.64E+01	4.77E+00
	Worst	**1.54E+00**	2.77E+00	3.27E+00	4.86E+00	3.69E+00	2.61E+00	2.52E+00	1.56E+01	3.12E+00	2.35E+00	1.95E+01	5.42E+00
	Mean	**1.16E+00**	2.34E+00	3.01E+00	4.00E+00	3.31E+00	2.24E+00	2.32E+00	1.50E+01	2.74E+00	2.18E+00	1.66E+01	4.95E+00
	STD	**9.40E-02**	1.90E-01	8.05E-02	2.43E-01	1.32E-01	1.88E-01	5.85E-02	2.08E-01	1.34E-01	7.08E-02	7.95E-01	1.09E-01
F11	Best	**1.23E+00**	2.27E+00	3.10E+00	4.16E+00	3.27E+00	2.24E+00	2.38E+00	1.46E+01	2.81E+00	2.25E+00	1.66E+01	6.52E+00
	Worst	**1.56E+00**	3.50E+00	3.70E+00	5.20E+00	4.40E+00	2.91E+00	2.69E+00	1.55E+01	3.26E+00	2.53E+00	1.73E+01	1.03E+01
	Mean	**1.29E+00**	2.60E+00	3.21E+00	4.42E+00	3.51E+00	2.48E+00	2.49E+00	1.50E+01	2.92E+00	2.35E+00	1.67E+01	7.19E+00
	STD	**8.44E-02**	2.20E-01	1.45E-01	2.19E-01	2.00E-01	1.76E-01	7.97E-02	2.29E-01	1.14E-01	6.92E-02	1.69E-01	6.23E-01
F12	Best	**3.62E+00**	5.27E+00	6.16E+00	9.41E+00	6.24E+00	8.40E+00	5.24E+00	1.53E+01	5.66E+00	5.00E+00	1.89E+01	8.98E+00
	Worst	**4.41E+00**	6.35E+00	6.68E+00	1.02E+01	6.66E+00	9.02E+00	5.63E+00	2.12E+01	6.17E+00	5.47E+00	2.23E+01	9.70E+00
	Mean	**3.76E+00**	5.44E+00	6.29E+00	9.80E+00	6.39E+00	8.54E+00	5.31E+00	1.58E+01	5.79E+00	5.09E+00	1.94E+01	9.45E+00
	STD	**1.83E-01**	2.55E-01	1.35E-01	1.49E-01	9.46E-02	1.24E-01	8.54E-02	1.01E+00	1.20E-01	9.87E-02	9.67E-01	1.19E-01
F13	Best	**3.62E+00**	5.33E+00	6.09E+00	9.33E+00	6.18E+00	7.96E+00	5.18E+00	1.54E+01	5.51E+00	5.09E+00	1.90E+01	9.90E+00
	Worst	**4.42E+00**	6.37E+00	6.73E+00	1.00E+01	6.83E+00	8.49E+00	5.67E+00	1.65E+01	6.40E+00	5.50E+00	1.93E+01	1.07E+01
	Mean	**3.77E+00**	5.48E+00	6.20E+00	9.68E+00	6.41E+00	8.15E+00	5.27E+00	1.58E+01	5.82E+00	5.19E+00	1.91E+01	1.01E+01
	STD	**1.96E-01**	2.54E-01	1.24E-01	1.66E-01	1.27E-01	1.22E-01	1.04E-01	2.07E-01	2.07E-01	9.25E-02	7.58E-02	1.33E-01

Table 13
Results of benchmark functions (F14-F36).

No.		AVOA	PSO	GWO	FFA	WOA	TLBO	MFO	BBO	DE	SSA	GSA	IPO
F14	Best	9.98E-01	9.98E-01	9.98E-01	9.98E-01	9.98E-01	**9.98E-01**	9.98E-01	9.98E-01	9.98E-01	9.98E-01	9.98E-01	9.98E-01
	Worst	2.98E+00	1.60E+01	1.27E+01	7.83E+00	1.08E+01	**9.98E-01**	1.27E+01	7.87E+00	5.93E+00	4.95E+00	1.25E+01	6.90E+00
	Mean	1.26E+00	5.95E+00	4.06E+00	1.91E+00	2.57E+00	**9.98E-01**	2.87E+00	3.27E+00	1.39E+00	1.39E+00	5.41E+00	2.61E+00
	STD	5.79E-01	3.76E+00	4.18E+00	2.07E+00	2.54E+00	**4.12E-17**	2.55E+00	2.12E+00	1.26E+00	8.85E-01	3.35E+00	1.82E+00
F15	Best	**3.08E-04**	4.20E-04	3.07E-04	3.34E-04	3.08E-04	3.07E-04	7.12E-04	3.93E-04	3.08E-04	3.08E-04	1.17E-03	3.07E-04
	Worst	**7.57E-04**	5.67E-02	2.04E-02	8.75E-04	2.13E-03	2.04E-02	2.01E-02	2.04E-02	2.01E-02	6.33E-02	1.29E-02	7.14E-04
	Mean	**4.65E-04**	1.07E-02	4.39E-03	5.90E-04	6.55E-04	1.09E-03	1.93E-03	4.79E-03	1.14E-03	4.28E-03	4.35E-03	4.30E-04
	STD	**1.48E-04**	1.80E-02	8.13E-03	1.19E-04	4.22E-04	3.65E-03	3.75E-03	7.92E-03	3.64E-03	1.22E-02	2.74E-03	1.36E-04
F16	Best	**−1.03e+00**	−1.03e+00	−1.03e+00	**−1.03e+00**	−1.03e+00	**−1.03e+00**	**−1.03e+00**	−1.03e+00	**−1.03e+00**	−1.03e+00	−1.03E+00	−1.03E+00
	Worst	**−1.03e+00**	−1.03e+00	−1.03e+00	**−1.03e+00**	−1.03e+00	**−1.03e+00**	**−1.03e+00**	−1.03e+00	**−1.03e+00**	−1.03e+00	−1.03E+00	−1.03E+00
	Mean	**−1.03e+00**	−1.03e+00	−1.03e+00	**−1.03e+00**	−1.03e+00	**−1.03e+00**	**−1.03e+00**	−1.03e+00	**−1.03e+00**	−1.03e+00	−1.03E+00	−1.03E+00
	STD	**6.78e-16**	6.59e-06	1.56e-08	**6.78e-16**	2.02e-09	**6.78e-16**	**6.78e-16**	4.43e-12	**6.78e-16**	4.09e-14	4.88E-16	5.61E-16
F17	Best	**3.98e-01**	3.98e-01	3.98e-01	3.98e-01	3.98e-01	**3.98e-01**	**3.98e-01**	3.98e-01	**3.98e-01**	3.98e-01	**3.98E-01**	3.98E-01
	Worst	**3.98e-01**	8.86e-01	3.98e-01	3.98e-01	3.98e-01	**3.98e-01**	**3.98e-01**	8.92e-01	**3.98e-01**	3.98e-01	**3.98E-01**	3.98E-01
	Mean	**3.98e-01**	4.62e-01	3.98e-01	3.98e-01	3.98e-01	**3.98e-01**	**3.98e-01**	4.77e-01	**3.98e-01**	3.98e-01	**3.98E-01**	3.98E-01
	STD	**1.69e-16**	1.15e-01	1.47e-06	3.95e-12	6.06e-06	**1.69e-16**	**1.69e-16**	1.39e-01	**1.69e-16**	2.29e-05	**1.69e-16**	2.87E-13
F18	Best	**3.00e+00**	3.00e+00	3.00e+00	**3.00e+00**	3.00e+00	**3.00e+00**	**3.00e+00**	3.00e+00	**3.00e+00**	3.00e+00	3.00E+00	3.00E+00
	Worst	**3.00e+00**	8.40e+01	3.00e+00	**3.00e+00**	3.00e+00	**3.00e+00**	**3.00e+00**	8.43e+01	**3.00e+00**	3.00e+00	3.00E+00	3.00E+00
	Mean	**3.00e+00**	1.06e+01	3.00e+00	**3.00e+00**	3.00e+00	**3.00e+00**	**3.00e+00**	7.51e+00	**3.00e+00**	3.00e+00	3.00E+00	3.00E+00
	STD	**0.00e+00**	1.72e+01	3.93e-05	**0.00e+00**	2.29e-04	**0.00e+00**	**0.00e+00**	1.60e+01	**0.00e+00**	2.74e-12	4.20E-15	2.78E-15
F19	Best	−3.86e+00	−3.86e+00	−3.86e+00	−3.86e+00	−3.86e+00	−3.86e+00	−3.86e+00	−3.86e+00	−3.86e+00	−3.86e+00	−3.86E+00	**−3.86E+00**
	Worst	−3.86e+00	−3.32e+00	−3.85e+00	−3.86e+00	−3.79e+00	−3.86e+00	−3.86e+00	−3.86e+00	−3.86e+00	−3.86e+00	−3.86E+00	**−3.86E+00**
	Mean	−3.86e+00	−3.80e+00	−3.86e+00	−3.86e+00	−3.85e+00	−3.86e+00	−3.86e+00	−3.86e+00	−3.86e+00	−3.86e+00	−3.86E+00	**−3.86E+00**
	STD	9.16e-10	1.05e-01	2.45e-03	3.48e-08	1.60e-02	2.63e-15	1.44e-03	3.42e-15	2.71e-15	5.26e-10	2.31E-15	**2.25E-15**
F20	Best	−3.3219	−3.2912	−3.3220	−3.3220	−3.3211	−3.3220	−3.3220	−3.3220	−3.3220	−3.3220	**−3.32E+00**	−3.32E+00
	Worst	−3.2031	−1.2950	−3.0904	−3.2019	−3.0661	−3.2031	−3.1376	−3.2031	−3.2031	−3.1461	**−3.32E+00**	−3.20E+00
	Mean	−3.3141	−2.7683	−3.2690	−3.2989	−3.1946	−3.2902	−3.2163	−3.2784	−3.2943	−3.2286	**−3.32E+00**	−3.31E+00
	STD	3.02e-02	4.31e-01	7.55e-02	4.43e-02	9.04e-02	5.34e-02	5.20e-02	5.83e-02	5.11e-02	6.33e-02	**1.61E-15**	3.03E-02
F21	Best	**−10.1532**	−10.1282	−10.1531	−10.1532	−10.1518	−10.1532	−10.1532	−10.1532	−10.1532	−10.1532	−1.02E+01	−1.02E+01
	Worst	**−10.1532**	−0.6874	−2.6827	−4.8135	−2.6296	−2.6829	−2.6305	−2.6305	−2.6829	−2.6305	−2.63E+00	−2.63E+00
	Mean	**−10.1532**	−3.7801	−8.1541	−9.0241	−7.6578	−9.2584	−5.5612	−5.0679	−9.3989	−6.3027	−7.03E+00	−8.07E+00
	STD	**1.08e-10**	2.86e+00	2.95e+00	1.96e+00	2.90e+00	2.02e+00	3.41e+00	3.24e+00	1.99e+00	3.53e+00	3.68E+00	3.29E+00
F22	Best	**−10.4028**	−10.4015	−10.4027	−10.4028	−10.4025	−10.4028	−10.4028	−10.4028	−10.4028	−10.4028	−1.04E+01	−1.04E+01
	Worst	**−10.4028**	−1.6032	−10.3976	−3.6759	−2.7635	−3.6146	−2.7519	−2.7519	−2.7519	−2.7519	−2.77E+00	−2.75E+00
	Mean	**−10.4028**	−5.0383	−10.4009	−9.6782	−7.7905	−8.6988	−9.0478	−5.9625	−9.8480	−8.8874	−9.79E+00	−9.89E+00
	STD	**9.14e-11**	2.92e+00	1.32e-03	2.05e+00	3.09e+00	2.67e+00	2.78e+00	3.47e+00	1.85e+00	2.85e+00	1.90E+00	1.94E+00
F23	Best	**−10.5363**	−10.5331	−10.5360	−10.5364	−10.5292	−10.5363	−10.5363	−10.5363	−10.5363	−10.5363	−1.05E+01	−1.05E+01
	Worst	**−10.5363**	−1.6341	−2.4217	−2.8711	−0.7894	−3.8354	−2.4273	−1.8595	−2.8711	−2.4273	−2.43E+00	−2.42E+00
	Mean	**−10.5363**	−4.8850	−10.2640	−9.8138	−6.8061	−9.8663	−8.6808	−5.2796	−10.2809	−8.5273	−9.49E+00	−7.81E+00
	STD	**4.34e-11**	3.20e+00	1.48e+00	2.14e+00	3.34e+00	2.04e+00	3.16e+00	3.55e+00	1.40e+00	3.42e+00	2.72E+00	3.49E+00
F24	Best	**8.74e+06**	4.94e+08	3.04e+07	1.57e+07	6.63e+07	2.16e+07	1.13e+07	1.13e+07	6.45e+07	2.37e+07	1.62E+07	2.22E+07
	Worst	**6.88e+07**	1.70e+09	3.38e+08	1.05e+08	4.87e+08	2.35e+08	7.53e+08	7.53e+08	3.42e+08	1.28e+08	2.55E+08	3.30E+08
	Mean	**2.95e+07**	1.02e+09	1.15e+08	5.16e+07	2.16e+08	8.64e+07	1.35e+08	1.35e+08	1.75e+08	6.63e+07	1.17E+08	1.03E+08
	STD	**1.49e+07**	2.97e+08	6.65e+07	2.36e+07	1.04e+08	4.60e+07	1.52e+08	1.52e+08	6.06e+07	2.58e+07	6.37E+07	8.02E+07
F25	Best	**1.70e+04**	6.61e+04	3.45e+04	8.54e+03	6.17e+04	2.23e+04	4.33e+03	8.96e+03	1.14e+04	4.47e+04	3.29E+04	3.14E+04
	Worst	**5.84e+04**	1.58e+05	8.87e+04	9.70e+04	3.16e+05	6.25e+04	1.76e+05	9.23e+04	1.33e+05	2.50e+05	9.25E+04	7.50E+04
	Mean	**3.21e+04**	1.09e+05	5.91e+04	5.45e+04	1.16e+05	4.34e+04	9.06e+04	4.61e+04	4.55e+04	1.17e+05	5.79E+04	5.36E+04
	STD	**1.01e+04**	2.74e+04	1.54e+04	2.25e+04	6.53e+04	1.03e+04	4.77e+04	2.02e+04	2.30e+04	4.19e+04	1.48E+04	1.25E+04
F26	Best	**5.20e+02**	5.21e+02	5.21e+02	5.21e+02	5.21e+02	5.21e+02	5.20e+02	5.20e+02	5.21e+02	5.20e+02	5.21E+02	5.21E+02
	Worst	**5.20e+02**	5.21e+02	5.21e+02	5.21e+02	5.21e+02	5.21e+02	5.21e+02	5.21e+02	5.21e+02	5.21e+02	5.21E+02	5.21E+02
	Mean	**5.20e+02**	5.21e+02	5.21e+02	5.21e+02	5.21e+02	5.21e+02	5.21e+02	5.21e+02	5.21e+02	5.21e+02	5.21E+02	5.21E+02
	STD	**8.43e-02**	8.07e-02	4.37e-02	5.51e-02	9.79e-02	5.77e-02	1.58e-01	8.28e-02	5.72e-02	1.51e-01	4.93E-02	5.70E-02
F27	Best	**2.53e+03**	5.59e+03	2.60e+03	2.26e+03	6.06e+03	1.89e+03	2.51e+03	3.02e+03	4.58e+03	3.04e+03	2.83E+03	2.52E+03
	Worst	**5.16e+03**	8.09e+03	7.90e+03	7.56e+03	8.85e+03	7.81e+03	6.03e+03	6.31e+03	5.94e+03	6.80e+03	8.46E+03	5.33E+03

(*continued on next page*)

Table 13 (*continued*)

No.		AVOA	PSO	GWO	FFA	WOA	TLBO	MFO	BBO	DE	SSA	GSA	IPO
	Mean	**3.40e+03**	6.85e+03	4.03e+03	5.37e+03	7.52e+03	4.75e+03	4.52e+03	4.47e+03	5.27e+03	4.92e+03	3.85E+03	3.72E+03
	STD	**6.48e+02**	6.02e+02	1.15e+03	1.26e+03	6.75e+02	1.66e+03	8.76e+02	7.44e+02	3.52e+02	7.47e+02	1.01E+03	6.68E+02
F28	Best	**4.02e+03**	5.72e+03	4.55e+03	7.28e+03	5.95e+03	7.01e+03	4.31e+03	4.79e+03	7.66e+03	3.75e+03	3.57E+03	3.30E+03
	Worst	**6.74e+03**	8.99e+03	9.76e+03	8.87e+03	9.00e+03	9.33e+03	7.18e+03	7.29e+03	9.34e+03	6.77e+03	9.57E+03	9.05E+03
	Mean	**5.14e+03**	7.63e+03	5.91e+03	8.40e+03	7.23e+03	8.25e+03	5.52e+03	5.89e+03	8.64e+03	5.28e+03	5.22E+03	5.64E+03
	STD	**6.10e+02**	8.58e+02	1.56e+03	3.79e+02	7.27e+02	3.99e+02	7.09e+02	6.57e+02	3.43e+02	7.50e+02	1.50E+03	1.49E+03
F29	Best	**2.09e+03**	5.47e+08	1.54e+04	2.54e+03	5.83e+05	2.26e+03	2.41e+03	2.84e+03	7.84e+03	2.56e+03	2.55E+04	1.72E+04
	Worst	**1.32e+04**	4.72e+09	1.72e+08	7.81e+06	1.33e+08	6.36e+06	3.93e+08	2.99e+04	2.46e+06	1.04e+05	1.24E+08	9.10E+07
	Mean	**4.64e+03**	2.39e+09	2.09e+07	4.18e+05	1.11e+07	3.08e+05	2.66e+07	1.19e+04	3.35e+05	1.43e+04	2.12E+07	2.12E+07
	STD	**2.94e+03**	1.16e+09	3.89e+07	1.42e+06	2.64e+07	1.17e+06	9.97e+07	7.04e+03	5.54e+05	1.93e+04	3.92E+07	3.12E+07
F30	Best	**4.34e+04**	4.83e+05	3.80e+04	7.07e+04	1.48e+06	1.21e+05	6.63e+04	3.70e+04	1.89e+05	1.11e+05	5.84E+04	8.15E+04
	Worst	**1.93e+06**	1.14e+08	1.10e+07	2.27e+06	3.92e+07	4.69e+06	4.40e+06	2.08e+06	4.42e+06	5.50e+06	1.05E+07	9.55E+06
	Mean	**5.03e+05**	2.52e+07	1.56e+06	7.99e+05	1.40e+07	9.54e+05	1.31e+06	8.45e+05	1.24e+06	9.60e+05	1.99E+06	1.25E+06
	STD	**4.40e+05**	2.36e+07	2.23e+06	5.70e+05	1.03e+07	9.32e+05	1.21e+06	6.16e+05	7.95e+05	1.02e+06	3.07E+06	2.19E+06
F31	Best	**2.50e+03**	2.75e+03	2.60e+03	2.62e+03	2.62e+03	2.62e+03	2.62e+03	2.62e+03	2.62e+03	2.63e+03	2.63E+03	2.63E+03
	Worst	**2.50e+03**	3.33e+03	2.66e+03	2.62e+03	2.78e+03	2.62e+03	2.79e+03	2.62e+03	2.62e+03	2.67e+03	2.69E+03	2.69E+03
	Mean	**2.50e+03**	3.02e+03	2.62e+03	2.62e+03	2.70e+03	2.62e+03	2.67e+03	2.62e+03	2.62e+03	2.65e+03	2.65E+03	2.65E+03
	STD	**0.00e+00**	1.45e+02	1.62e+01	2.67e-01	3.61e+01	5.28e-01	4.21e+01	7.99e-02	5.91e-02	1.28e+01	1.51E+01	1.54E+01
F32	Best	**2.60e+03**	2.66e+03	2.60e+03	2.63e+03	2.60e+03	2.60e+03	2.63e+03	2.63e+03	2.63e+03	2.63e+03	2.60E+03	2.60E+03
	Worst	**2.60e+03**	2.70e+03	2.63e+03	2.64e+03	2.62e+03	2.63e+03	2.77e+03	2.65e+03	2.64e+03	2.66e+03	2.60E+03	2.60E+03
	Mean	**2.60e+03**	2.68e+03	2.62e+03	2.63e+03	2.61e+03	2.61e+03	2.67e+03	2.64e+03	2.63e+03	2.65e+03	2.60E+03	2.60E+03
	STD	**7.24e-06**	9.81e+00	5.41e+00	4.18e+00	6.84e+00	8.01e+00	3.04e+01	7.15e+00	2.98e+00	6.90e+00	4.73E-02	3.69E-02
F33	Best	**2.70e+03**	2.72e+03	2.70e+03	2.71e+03	2.70e+03	2.70e+03	2.71e+03	2.71e+03	2.73e+03	2.71e+03	2.70E+03	2.70E+03
	Worst	**2.70e+03**	2.76e+03	2.72e+03	2.73e+03	2.77e+03	2.72e+03	2.75e+03	2.74e+03	2.76e+03	2.73e+03	2.72E+03	2.72E+03
	Mean	**2.70e+03**	2.74e+03	2.71e+03	2.72e+03	2.72e+03	2.71e+03	2.72e+03	2.72e+03	2.74e+03	2.72e+03	2.71E+03	2.71E+03
	STD	**0.00e+00**	9.80e+00	5.21e+00	4.79e+00	2.36e+01	6.92e+00	9.28e+00	7.62e+00	6.86e+00	4.73e+00	7.46E+00	6.82E+00
F34	Best	**2.90e+03**	3.56e+03	3.12e+03	3.13e+03	3.17e+03	3.08e+03	3.08e+03	3.07e+03	3.26e+03	3.10e+03	3.14E+03	3.15E+03
	Worst	**2.90e+03**	4.77e+03	4.00e+03	3.41e+03	4.23e+03	3.79e+03	3.90e+03	3.72e+03	3.76e+03	3.88e+03	3.66E+03	3.54E+03
	Mean	**2.90e+03**	4.23e+03	3.41e+03	3.22e+03	3.94e+03	3.40e+03	3.58e+03	3.37e+03	3.56e+03	3.58e+03	3.45E+03	3.42E+03
	STD	**0.00e+00**	3.27e+02	1.74e+02	6.94e+01	3.22e+02	2.23e+02	2.52e+02	1.94e+02	1.34e+02	1.92e+02	1.19E+02	9.28E+01
F35	Best	**3.00e+03**	8.69e+03	3.69e+03	3.61e+03	4.74e+03	3.73e+03	3.74e+03	4.00e+03	3.57e+03	3.69e+03	3.76E+03	3.68E+03
	Worst	**3.00e+03**	1.15e+04	5.67e+03	4.01e+03	7.31e+03	4.73e+03	4.49e+03	6.62e+03	3.84e+03	5.28e+03	5.03E+03	4.79E+03
	Mean	**3.00e+03**	1.01e+04	4.35e+03	3.73e+03	5.67e+03	4.07e+03	3.91e+03	5.38e+03	3.72e+03	4.22e+03	4.23E+03	4.14E+03
	STD	**0.00e+00**	7.48e+02	4.93e+02	8.23e+01	6.88e+02	2.40e+02	1.52e+02	7.96e+02	6.30e+01	4.51e+02	3.70E+02	3.34E+02
F36	Best	**3.10e+03**	2.69e+08	1.64e+04	4.05e+03	1.37e+05	4.11e+03	7.89e+03	4.30e+03	5.45e+03	1.44e+04	9.75E+03	1.06E+04
	Worst	**2.30e+04**	1.21e+09	1.84e+07	1.82e+04	9.27e+07	2.21e+07	8.63e+06	8.89e+06	8.70e+06	2.79e+07	1.41E+07	1.66E+07
	Mean	**5.23e+03**	6.99e+08	3.81e+06	6.99e+03	2.32e+07	4.63e+06	2.14e+06	3.02e+05	7.40e+05	4.03e+06	1.88E+06	1.09E+06
	STD	**5.13e+03**	2.04e+08	4.95e+06	3.61e+03	1.75e+07	6.95e+06	3.00e+06	1.63e+06	2.31e+06	8.37e+06	3.60E+06	3.01E+06

Table 14
p-values of the Wilcoxon rank-sum test with 5% significance for F1–F13 with 30 dimensions (p-values $\geq$ 0.05 are shown in boldface).

No.	PSO	GWO	FFA	WOA	TLBO	MFO	BBO	DE	SSA	GSA	IPO
F1	3.0199e-11	3.0199e-11	3.0199e-11	3.0199e-11	3.0199e-11	3.0199e-11	3.0199e-11	3.0199e-11	3.0199e-11	3.0199e-11	3.0199e-11
F2	3.0199e-11	3.0199e-11	3.0199e-11	3.0199e-11	3.0199e-11	3.0199e-11	3.0199e-11	3.0199e-11	3.0199e-11	3.0199e-11	3.0199e-11
F3	3.0199e-11	3.0199e-11	3.0199e-11	3.0199e-11	3.0199e-11	3.0199e-11	3.0199e-11	3.0199e-11	3.0199e-11	3.0199e-11	3.0199e-11
F4	3.0199e-11	3.0199e-11	3.0199e-11	3.0199e-11	3.0199e-11	3.0199e-11	3.0199e-11	3.0199e-11	3.0199e-11	3.0199e-11	3.0199e-11
F5	3.0199e-11	3.0199e-11	3.0199e-11	3.0199e-11	3.0199e-11	3.0199e-11	3.0199e-11	3.0199e-11	3.0199e-11	3.0199e-11	3.0199e-11
F6	3.0199e-11	3.0199e-11	6.0104e-08	3.0199e-11	3.9881e-04	3.0199e-11	3.0199e-11	3.0199e-11	**1.2967e-01**	3.0199e-11	3.0199e-11
F7	3.0199e-11	1.0702e-09	3.0199e-11	6.0104e-08	6.5183e-09	3.0199e-11	3.0199e-11	3.0199e-11	3.0199e-11	3.0199e-11	3.0199e-11
F8	3.0199e-11	3.0199e-11	3.0199e-11	4.9752e-11	3.0199e-11	3.0199e-11	3.0199e-11	3.0199e-11	3.0199e-11	3.0199e-11	3.0199e-11
F9	1.2118e-12	4.4282e-12	1.2118e-12	NaN	1.6572e-11	1.2118e-12	1.2118e-12	1.2118e-12	1.2118e-12	1.2118e-12	1.2118e-12
F10	1.2118e-12	1.1101e-12	1.2118e-12	1.0055e-08	4.1697e-13	1.2118e-12	1.2118e-12	1.2118e-12	1.2118e-12	1.2118e-12	1.2118e-12
F11	1.2118e-12	2.1577e-02	1.2118e-12	2.1577e-02	**1.6080e-01**	1.2118e-12	1.2118e-12	1.2118e-12	1.2118e-12	1.2118e-12	1.2118e-12
F12	3.0199e-11	3.0199e-11	3.0199e-11	3.0199e-11	4.3584e-02	3.0199e-11	3.0199e-11	3.0199e-11	3.0199e-11	3.0199e-11	3.0199e-11
F13	3.0199e-11	3.0199e-11	3.0199e-11	3.0199e-11	2.6015e-08	3.0199e-11	3.0199e-11	3.0199e-11	3.0199e-11	3.0199e-11	3.0199e-11

Table 15
p-values of the Wilcoxon rank-sum test with 5% significance for F1–F13 with 100 dimensions (p-values $\geq$ 0.05 are shown in boldface).

No.	PSO	GWO	FFA	WOA	TLBO	MFO	BBO	DE	SSA	GSA	IPO
F1	3.0199e-11	3.0199e-11	3.0199e-11	3.0199e-11	3.0199e-11	3.0199e-11	3.0199e-11	3.0199e-11	3.0199e-11	3.0199e-11	3.0199e-11
F2	3.0199e-11	3.0199e-11	3.0199e-11	3.0199e-11	3.0199e-11	3.0199e-11	3.0199e-11	3.0199e-11	3.0199e-11	3.0199e-11	3.0199e-11
F3	3.0199e-11	3.0199e-11	3.0199e-11	3.0199e-11	3.0199e-11	3.0199e-11	3.0199e-11	3.0199e-11	3.0199e-11	3.0199e-11	3.0199e-11
F4	3.0199e-11	3.0199e-11	3.0199e-11	3.0199e-11	3.0199e-11	3.0199e-11	3.0199e-11	3.0199e-11	3.0199e-11	3.0199e-11	3.0199e-11
F5	3.0199e-11	3.0199e-11	3.0199e-11	3.0199e-11	3.0199e-11	3.0199e-11	3.0199e-11	3.0199e-11	3.0199e-11	3.0199e-11	3.0199e-11
F6	3.0199e-11	3.0199e-11	3.0199e-11	3.0199e-11	3.0199e-11	3.0199e-11	3.0199e-11	3.0199e-11	3.0199e-11	3.0199e-11	3.0199e-11
F7	3.0199e-11	3.0199e-11	3.0199e-11	3.1967e-09	1.4643e-10	3.0199e-11	3.0199e-11	3.0199e-11	3.0199e-11	3.0199e-11	3.0199e-11
F8	3.0199e-11	3.0199e-11	3.0199e-11	7.3803e-10	3.0199e-11	3.0199e-11	3.0199e-11	3.0199e-11	3.0199e-11	3.0199e-11	3.0199e-11
F9	1.2118e-12	1.2118e-12	1.2118e-12	NaN	NaN	1.2118e-12	1.2118e-12	1.2118e-12	1.2118e-12	1.2118e-12	1.2118e-12
F10	1.2118e-12	1.2118e-12	1.2118e-12	3.5728e-10	4.1574e-14	1.2118e-12	1.2118e-12	1.2118e-12	1.2118e-12	1.2118e-12	1.2118e-12
F11	1.2118e-12	1.2118e-12	1.2118e-12	NaN	NaN	1.2118e-12	1.2118e-12	1.2118e-12	1.2118e-12	1.2118e-12	1.2118e-12
F12	3.0199e-11	3.0199e-11	3.0199e-11	3.0199e-11	3.0199e-11	3.0199e-11	3.0199e-11	3.0199e-11	3.0199e-11	3.0199e-11	3.0199e-11
F13	3.0199e-11	3.0199e-11	3.0199e-11	3.0199e-11	3.0199e-11	3.0199e-11	3.0199e-11	3.0199e-11	3.0199e-11	3.0199e-11	3.0199e-11

Table 16
p-values of the Wilcoxon rank-sum test with 5% significance for F1–F13 with 500 dimensions (p-values $\geq$ 0.05 are shown in boldface).

No.	PSO	GWO	FFA	WOA	TLBO	MFO	BBO	DE	SSA	GSA	IPO
F1	3.0199e-11	3.0199e-11	3.0199e-11	3.0199e-11	3.0199e-11	3.0199e-11	3.0199e-11	3.0199e-11	3.0199e-11	3.0199e-11	3.0199e-11
F2	3.0199e-11	3.0199e-11	3.0199e-11	3.0199e-11	3.0199e-11	3.0199e-11	3.0199e-11	3.0199e-11	3.0199e-11	3.0199e-11	3.0199e-11
F3	3.0199e-11	3.0199e-11	3.0199e-11	3.0199e-11	3.0199e-11	3.0199e-11	3.0199e-11	3.0199e-11	3.0199e-11	3.0199e-11	3.0199e-11
F4	3.0199e-11	3.0199e-11	3.0199e-11	3.0199e-11	3.0199e-11	3.0199e-11	3.0199e-11	3.0199e-11	3.0199e-11	3.0199e-11	3.0199e-11
F5	3.0199e-11	3.0199e-11	3.0199e-11	3.0199e-11	3.0199e-11	3.0199e-11	3.0199e-11	3.0199e-11	3.0199e-11	3.0199e-11	3.0199e-11
F6	3.0199e-11	3.0199e-11	3.0199e-11	3.0199e-11	3.0199e-11	3.0199e-11	3.0199e-11	3.0199e-11	3.0199e-11	3.0199e-11	3.0199e-11
F7	3.0199e-11	3.0199e-11	3.0199e-11	9.2603e-09	3.0199e-11	3.0199e-11	3.0199e-11	3.0199e-11	3.0199e-11	3.0199e-11	3.0199e-11
F8	3.0199e-11	3.0199e-11	3.0199e-11	1.5581e-08	3.0199e-11	3.0199e-11	3.0199e-11	3.0199e-11	3.0199e-11	3.0199e-11	3.0199e-11
F9	1.2118e-12	1.2118e-12	1.2118e-12	NaN	NaN	1.2118e-12	1.2118e-12	1.2118e-12	1.2118e-12	1.2118e-12	1.2118e-12
F10	1.2118e-12	1.2118e-12	1.2118e-12	9.1593e-09	6.1151e-14	1.2118e-12	1.2118e-12	1.2118e-12	1.2118e-12	1.2118e-12	1.2118e-12
F11	1.2118e-12	1.2118e-12	1.2118e-12	NaN	NaN	1.2118e-12	1.2118e-12	1.2118e-12	1.2118e-12	1.2118e-12	1.2118e-12
F12	3.0199e-11	3.0199e-11	3.0199e-11	3.0199e-11	3.0199e-11	3.0199e-11	3.0199e-11	3.0199e-11	3.0199e-11	3.0199e-11	3.0199e-11
F13	3.0199e-11	3.0199e-11	3.0199e-11	3.0199e-11	3.0199e-11	3.0199e-11	3.0199e-11	3.0199e-11	3.0199e-11	3.0199e-11	3.0199e-11

Table 17
p-values of the Wilcoxon rank-sum test with 5% significance for F1–F13 with 1000 dimensions (p-values $\geq$ 0.05 are shown in boldface).

No.	PSO	GWO	FFA	WOA	TLBO	MFO	BBO	DE	SSA	GSA	IPO
F1	3.0199e-11	3.0199e-11	3.0199e-11	3.0199e-11	3.0199e-11	3.0199e-11	3.0199e-11	3.0199e-11	3.0199e-11	3.0199e-11	3.0199e-11
F2	1.2118e-12	3.0199e-11	1.2118e-12	3.0199e-11	1.2118e-12	1.2118e-12	1.2118e-12	1.2118e-12	3.0199e-11	3.0199e-11	3.0199e-11
F3	3.0199e-11	3.0199e-11	3.0199e-11	3.0199e-11	3.0199e-11	3.0199e-11	3.0199e-11	3.0199e-11	3.0199e-11	3.0199e-11	3.0199e-11
F4	3.0199e-11	3.0199e-11	3.0199e-11	3.0199e-11	3.0199e-11	3.0199e-11	3.0199e-11	3.0199e-11	3.0199e-11	3.0199e-11	3.0199e-11
F5	3.0199e-11	3.0199e-11	3.0199e-11	3.0199e-11	3.0199e-11	3.0199e-11	3.0199e-11	3.0199e-11	3.0199e-11	3.0199e-11	3.0199e-11
F6	3.0199e-11	3.0199e-11	3.0199e-11	3.0199e-11	3.0199e-11	3.0199e-11	3.0199e-11	3.0199e-11	3.0199e-11	3.0199e-11	3.0199e-11
F7	3.0199e-11	3.0199e-11	3.0199e-11	3.8249e-09	4.9752e-11	3.0199e-11	3.0199e-11	3.0199e-11	3.0199e-11	3.0199e-11	3.0199e-11
F8	3.0199e-11	3.0199e-11	3.0199e-11	7.3803e-10	3.0199e-11	3.0199e-11	3.0199e-11	3.0199e-11	3.0199e-11	3.0199e-11	3.0199e-11
F9	1.2118e-12	1.2118e-12	1.2118e-12	NaN	NaN	1.2118e-12	1.2118e-12	1.2118e-12	1.2118e-12	1.2118e-12	1.2118e-12
F10	1.2118e-12	1.2118e-12	1.2118e-12	2.7420e-09	2.7085e-14	1.2118e-12	1.2118e-12	1.2118e-12	1.2118e-12	1.2118e-12	1.2118e-12
F11	1.2118e-12	1.2118e-12	1.2118e-12	NaN	1.6853e-14	1.2118e-12	1.2118e-12	1.2118e-12	1.2118e-12	1.2118e-12	1.2118e-12
F12	3.0199e-11	3.0199e-11	3.0199e-11	3.0199e-11	3.0199e-11	3.0199e-11	3.0199e-11	3.0199e-11	3.0199e-11	3.0199e-11	3.0199e-11
F13	3.0199e-11	3.0199e-11	3.0199e-11	3.0199e-11	3.0199e-11	3.0199e-11	3.0199e-11	3.0199e-11	3.0199e-11	3.0199e-11	3.0199e-11

Table 18
p-values of the Wilcoxon rank-sum test with 5% significance for F14–F36 problems (p-values ≥ 0.05 are shown in boldface).

No.	PSO	GWO	FFA	WOA	TLBO	MFO	BBO	DE	SSA	GSA	IPO
F14	3.2628e-10	1.4744e-09	1.6166e-04	1.7023e-11	8.7458e-12	1.2074E-03	3.2333e-09	9.8943e-10	2.8391E-03	3.2167e-10	1.4457e-05
F15	1.3289e-10	**2.1702e-01**	1.4733e-07	4.4592e-04	7.9573e-03	3.1776e-09	5.9673e-09	2.2358e-02	2.0338e-09	4.5043e-11	1.7023e-11
F16	6.2538e-10	1.2118e-12	NAN	1.2118e-12	NAN	NAN	4.5031e-12	NAN	1.2118e-12	5.9598e-13	1.4342e-06
F17	1.7857e-10	6.4743e-12	**3.7854e-01**	6.4743e-12	**1.6073e-01**	NAN	6.4743e-12	NAN	6.4743e-12	1.1000E-02	**6.0830E-01**
F18	5.2114e-12	5.2114e-12	NAN	5.2114e-12	NAN	NAN	5.2114e-12	NAN	5.2114e-12	NAN	4.1900E-02
F19	3.0199e-11	3.0199e-11	4.5587e-11	3.0199e-11	1.1570e-11	4.5587e-11	1.8602e-06	1.9779e-05	**2.5494e-01**	3.9346e-11	4.1986e-10
F20	6.5749e-11	1.1553e-09	5.1257e-07	1.7463e-10	3.3177e-03	1.9276e-03	1.6708e-04	1.1210e-04	3.9658e-04	9.9414e-12	1.3150e-04
F21	3.0199e-11	3.0199e-11	8.2895e-06	3.0199e-11	3.3628e-04	6.4112e-05	3.0059e-04	7.0839e-08	7.7387e-06	2.6400E-02	7.3000E-03
F22	3.0199e-11	3.0199e-11	1.1658e-05	3.0199e-11	4.7783e-07	4.3780e-05	2.5045e-02	3.4261e-08	4.7138e-04	4.5715e-09	8.4387e-09
F23	3.0199e-11	3.0199e-11	3.1541e-05	3.0199e-11	7.5807e-08	1.5959e-03	7.9373e-03	7.7540e-11	7.6588e-05	7.5070e-08	3.0059e-04
F24	3.0199e-11	8.0965e-10	1.4868e-04	3.0199e-11	1.0105e-08	7.5991e-07	7.6008e-07	3.3384e-11	5.5342e-08	1.0105e-08	4.1127e-07
F25	3.0199e-11	1.1043e-08	3.5873e-05	3.0199e-11	1.0407e-04	1.0188e-05	2.3827e-03	4.0330e-03	4.0794e-11	1.0105e-08	5.5329e-08
F26	3.0199e-11	3.0199e-11	3.0199e-11	3.0199e-11	3.0199e-11	4.0772e-11	3.3384e-11	3.0199e-11	3.3426e-11	3.0199e-11	3.0199e-11
F27	3.0199e-11	1.8391e-02	1.1607e-07	3.0199e-11	8.1200e-04	2.1540e-06	1.0277e-06	9.9186e-11	7.7670e-09	1.5959e-03	**5.0100E-02**
F28	6.6955e-11	4.2054e-02	3.0199e-11	8.9869e-11	3.0199e-11	2.6077e-02	5.6139e-05	3.0199e-11	**3.3315e-01**	**2.9050E-01**	3.3900E-02
F29	3.0199e-11	3.0199e-11	1.5981e-07	3.0199e-11	1.4087e-04	4.1127e-07	1.1077e-06	4.9752e-11	2.6041e-05	3.0199e-11	3.0199e-11
F30	9.9186e-11	4.6427e-03	1.8413e-02	3.3440e-11	1.2212e-02	2.2658e-03	2.7086e-02	4.7445e-06	1.4977e-02	2.7400E-02	4.8800E-02
F31	1.2118e-12	1.2118e-12	1.2118e-12	1.2118e-12	1.2118e-12	1.2118e-12	1.2118e-12	1.2118e-12	1.2118e-12	1.2118e-12	1.2118e-12
F32	9.4001e-12	9.4001e-12	9.4001e-12	9.4001e-12	9.4001e-12	9.4001e-12	9.4001e-12	9.4001e-12	9.4001e-12	9.4001e-12	9.4001e-12
F33	1.2118e-12	1.2118e-12	1.2118e-12	6.1994e-10	1.2118e-12	1.2118e-12	1.2118e-12	1.2118e-12	1.2118e-12	1.2118e-12	1.2118e-12
F34	1.2118e-12	1.2118e-12	1.2118e-12	1.2118e-12	1.2118e-12	1.2118e-12	1.2118e-12	1.2118e-12	1.2118e-12	1.2118e-12	1.2118e-12
F35	1.2118e-12	1.2118e-12	1.2118e-12	1.2118e-12	1.2118e-12	1.2118e-12	1.2118e-12	1.2118e-12	1.2118e-12	1.2118e-12	1.2118e-12
F36	5.2190e-12	8.0270e-12	2.0345e-06	5.2190e-12	5.7099e-09	8.9256e-12	2.9561e-06	5.2890e-08	1.5174e-11	1.2296e-11	1.6891e-11

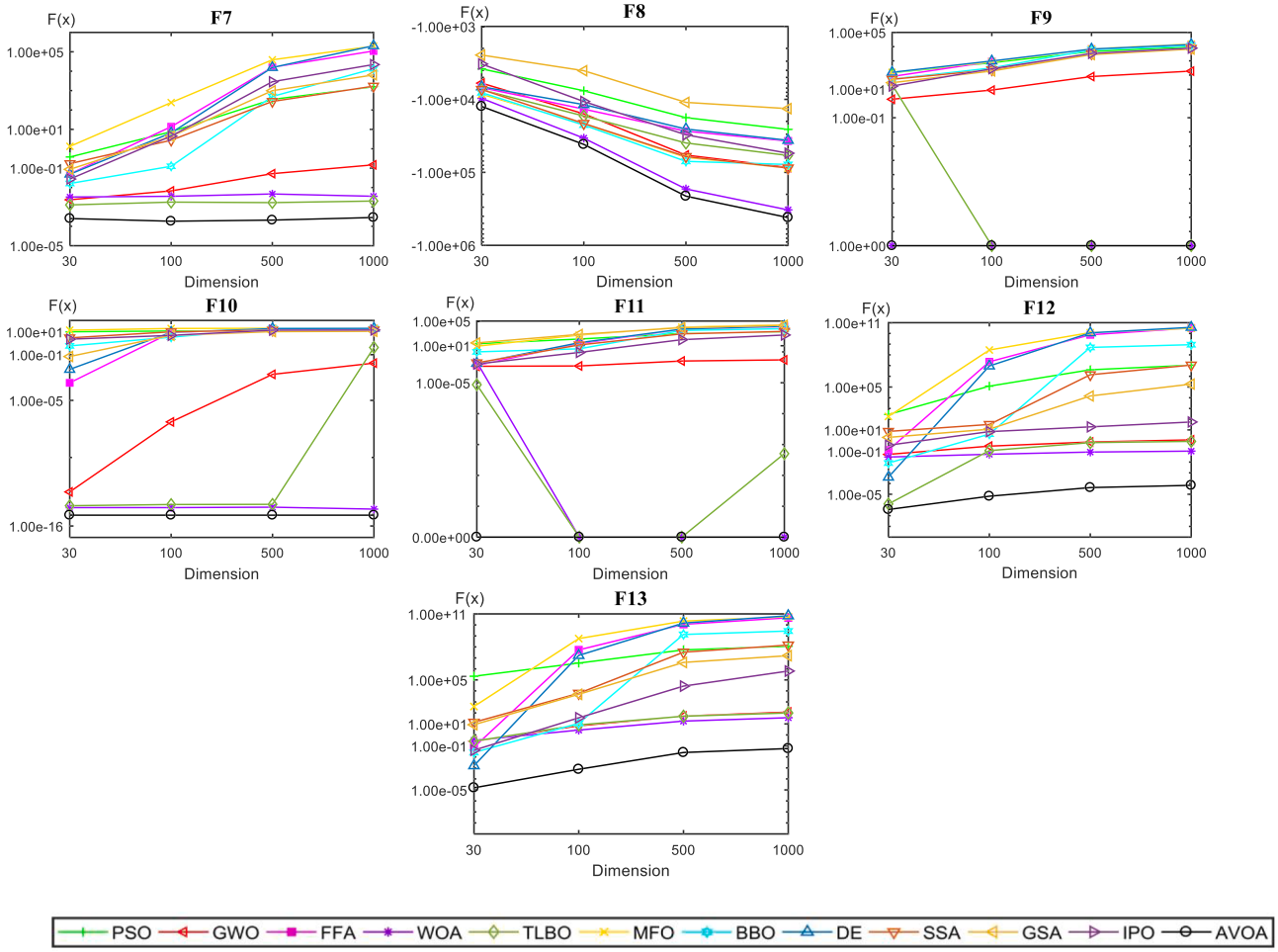

Fig. 17. Results of AVOA scalability evaluation against other optimization algorithms in F7-F13 functions in different dimensions.

2018), TSA (Kaur et al., 2020), EO (Faramarzi et al., 2020)optimization algorithms. This evaluation is based on 30 independent runs using 30 populations and a maximum of 500 iterations, and finally, the best solution obtained in each optimization algorithm is used for comparison.

4.5.1. *The three-bar truss design problem*

As shown in Fig. 19, this engineering problem illustrates the truss's form and the forces applied to the structure. According to Fig. 16, this problem has two design parameters($x_1 x_2$). The purpose of this problem

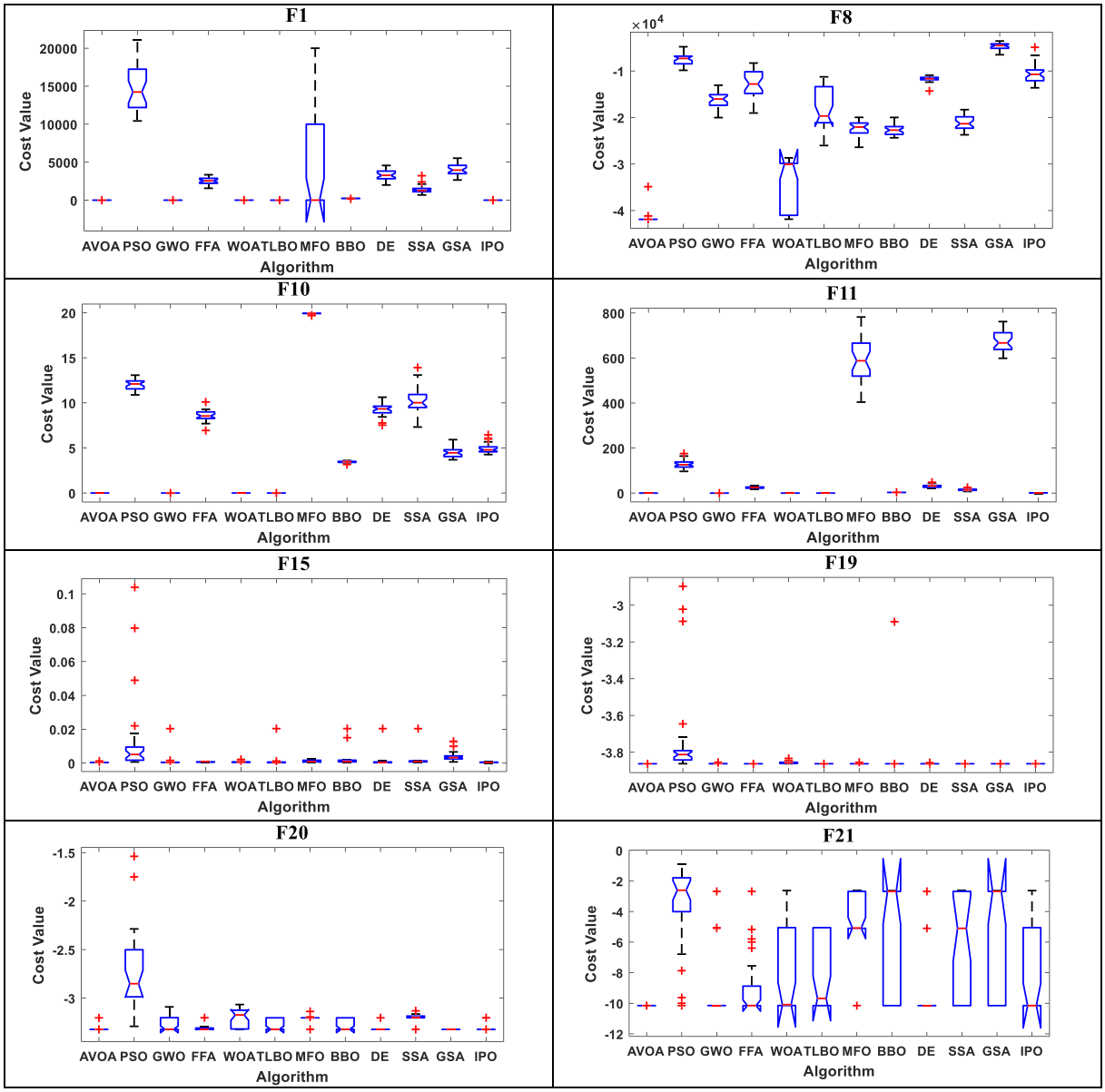

Fig. 18. Box plots of the obtained results from AVOA and other optimization algorithms.

is to minimize the total weight of the structure. It also has various constraints, such as deflection, buckling, and stress.

It was done using 30 vultures in 500 iterations and 30 independent performances. Since this issue has limitations, there is a need to integrate restraint control techniques into AVOA. Because of the simplicity of the barrier penalty (Coello, 2000) approach, this approach has been used in AVOA. It is mathematically stated as follows:

$$Consider\,\vec{X} = [x_1 x_2] = [A_1 A_2],$$

$$Minimise f(\vec{X}) = \left(2\sqrt{2}X_1 + X_2\right) \times L,$$

$$Subject to g_1(\vec{X}) = \frac{\sqrt{2}x_1 + x_2}{\sqrt{2}x_1^2 + 2x_1 x_2} P - \sigma \leq 0,$$

$$g_2(\vec{X}) = \frac{x_2}{\sqrt{2}x_1^2 + 2x_1 x_2} P - \sigma \leq 0,$$

$$g_3(\vec{X}) = \frac{1}{\sqrt{2}x_2 + x_1} P - \sigma \leq 0,$$

$$Variable range 0 \leq x_1, x_2 \leq 1,$$

$$where L = 100cm, P = 2KN/cm^2, \sigma = 2KN/cm^2$$

Results obtained by AVOA have been compared with other optimization methods, including GOA (Saremi, Mirjalili, & Lewis, 2017), MBA (Sadollah et al., 2013), SSA (Mirjalili et al., 2017), PSO-DE (Liu, Cai, & Wang, 2010), DEDS (Zhang, Luo, & Wang, 2008), MFO (Mirjalili, 2015), MVO (Mirjalili, Mirjalili, & Hatamlou, 2016), Ray and Sain (Ray & Saini, 2001), CS (Gandomi et al., 2013), TSA (Tsai, 2005) and the results of these comparisons are shown in Table 17. By looking at Table 19, it can be seen that AVOA has obtained close and competitive results with SSA, PSO-DE, and DEDS optimization algorithms, and AVOA has been able to perform better than other optimization algorithms. In addition, the results show that AVOA has a good ability to solve problems in confined

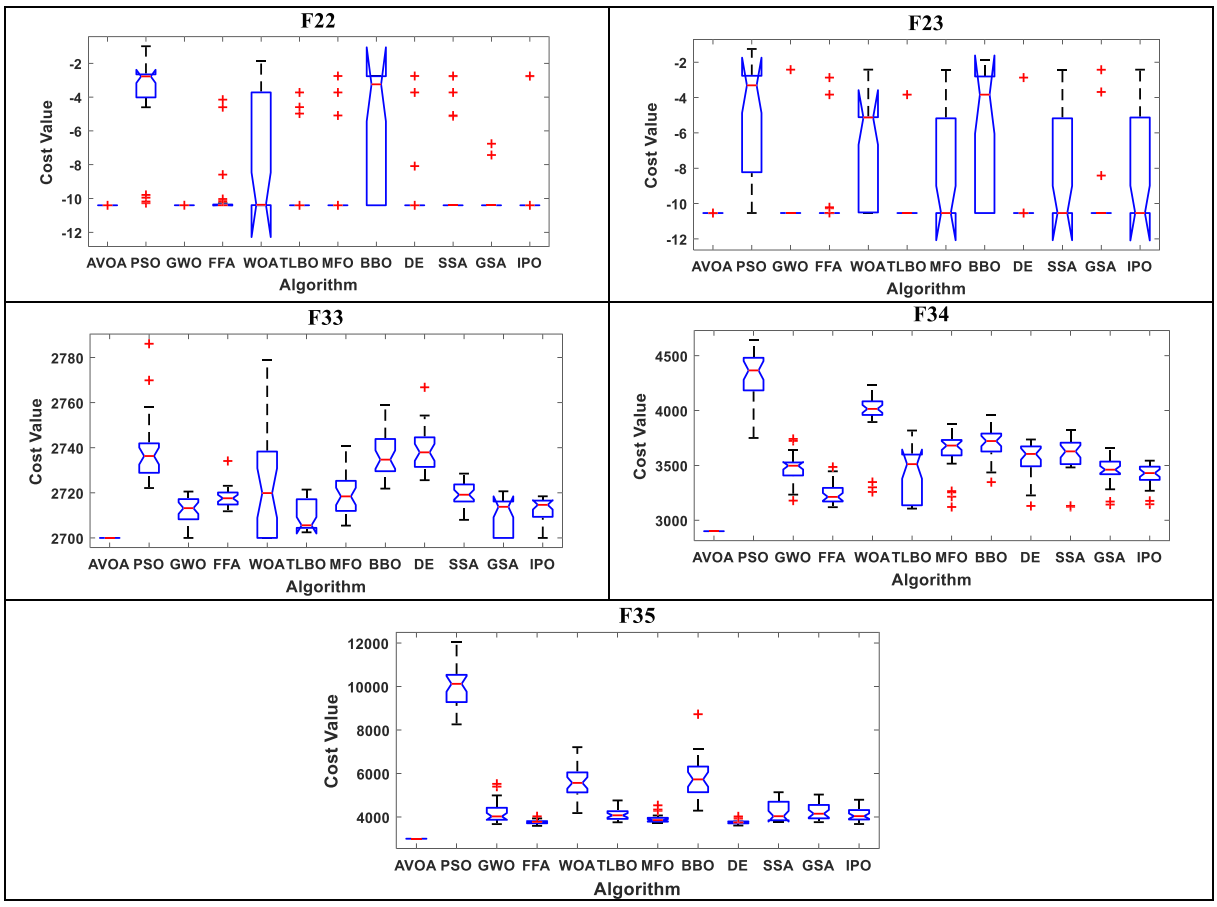

Fig. 18. (*continued*).

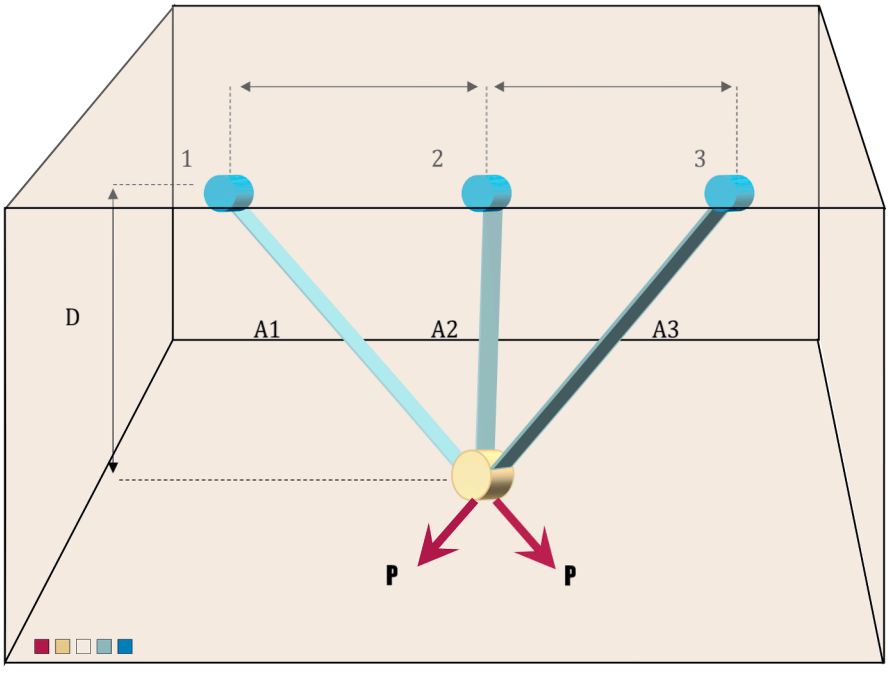

Fig. 19. Three-bar truss design problem.

Table 19
Comparison of results for the three-bar truss design problem.

Algorithm	Optimal values for variables		Optimal weight
	x_1	x_2	
AVOA	0.788680394972034	0.408233412073586	263.895843396802
GOA (Saremi et al., 2017)	0.788897555578973	0.407619570115153	263.895881496069
MBA (Sadollah, 2013)	0.7885650	0.4085597	263.8958522
SSA (Mirjalili, 2017)	0.788665414	0.408275784444547	263.8958434
PSO-DE (Liu et al., 2010)	0.7886751	0.4082482	263.8958433
DEDS (Zhang et al., 2008)	0.78867513	0.40824828	263.8958434
MFO (Mirjalili, 2015)	0.788244771	0.409466905784741	263.8959797
MVO (Mirjalili et al., 2016)	0.78860276	0.408453070000000	263.8958499
Ray and Sain (Ray & Saini, 2001)	0.795	0.395	264.3
CS (Gandomi et al., 2013)	0.78867	0.40902	263.9716
Tsa (Tsai, 2005)	0.788	0.408	263.68

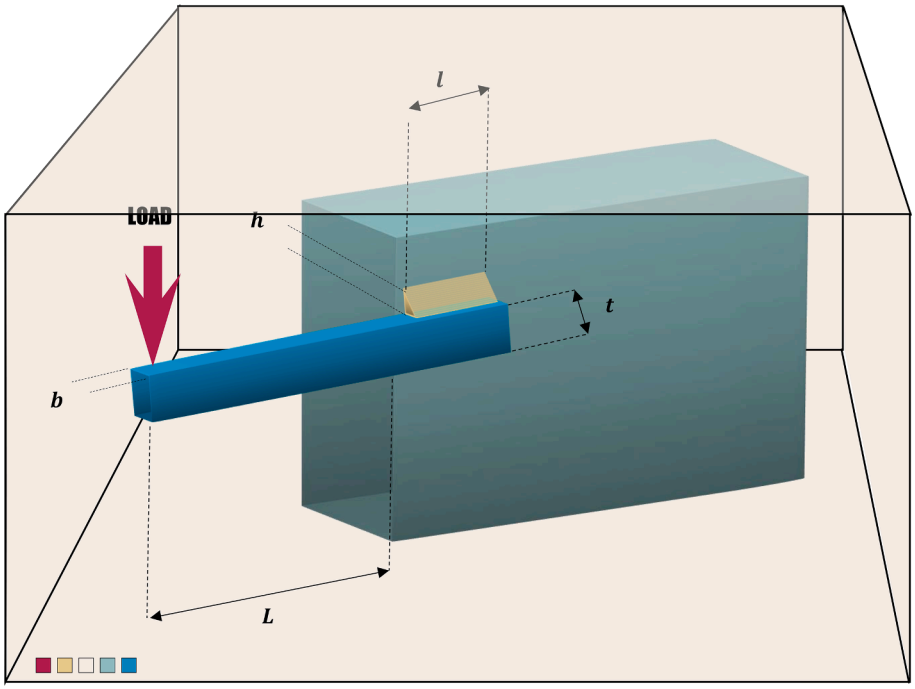

Fig. 20. Welded beam design problem.

space.

4.5.2. The welded beam design problem

The main objective in this problem, shown in Fig. 20, is to minimize the Welded beam's cost and obtain the best construction cost concerning the design constraints. Variables in this problem are height (t), the thickness of the weld (h), the thickness of the bar (b), and length (l).

Mathematically, this issue has been stated as follows:

$$Consider\ \vec{z} = [z_1, z_2, z_3, z_4] = [h, l, t, b],$$

$$Minimisef(\vec{z}) = 1.10471 z_1^2 z_2 + 0.04811 z_3 z_4 (14.0 + z_2),$$

$$Subjecttog_1(\vec{z}) = \tau(\vec{z}) - \tau_{max} \le 0,$$

$$g_2(\vec{z}) = \sigma(\vec{z}) - \sigma_{max} \le 0,$$

$$g_3(\vec{z}) = \delta(\vec{z}) - \delta_{max} \le 0,$$

$$g_4(\vec{z}) = z_1 - z_4 \le 0,$$

$$g_5(\vec{z}) = P - P_c(\vec{z}) \le 0,$$

$$g_6(\vec{z}) = 0.125 - z_1 \le 0,$$

$$g_6(\vec{z}) = 1.10471 z_1^2 + 0.04811 z_3 z_4 (14.0 + z_2) - 5.0 \le 0,$$

$$Variablerange 0.05 \le z_1 \le 2.00, 0.25 \le z_2 \le 1.30, 2.00 \le z_3 \le 15.0$$

Where:

$$\tau(\vec{z}) = \sqrt{\tau'^2 2\tau' \tau'' \frac{z_2}{2R} + \tau''^2}, \tau' = \frac{P}{\sqrt{2} z_1 z_2}, \tau'' \frac{MR}{J}, M = P\left(L + \frac{z_2}{2}\right),$$

$$R = \sqrt{\frac{z_2^2}{4} + \left(\frac{z_1 + z_3}{2}\right)^2}, J = 2\left\{\sqrt{2} z_1 z_2 \left[\frac{z_2^2}{12} + \left(\frac{z_1 + z_3}{2}\right)^2\right]\right\}, \sigma(\vec{z}) = \frac{6PL}{z_4 z_3^2}$$

$$\delta(\vec{z}) = \frac{4PL^3}{E z_3^3 z_4}, P_c(\vec{z}) = \frac{4.013E\sqrt{\frac{z_3^2 z_4^6}{36}}}{L^2}\left(1 - \frac{z_3}{2L}\sqrt{\frac{E}{4G}}\right),$$

$$P = 6000lb, L = 14in, E = 30 \times 10^6 psi, G = 12 \times 10^6 psi,$$

Optimized results of AVOA with optimization algorithms GA1 (Deb, 1991), HS (Lee & Geem, 2004), GSA (Mirjalili & Lewis, 2016), GA2

(Coello, 2000), DAVID (Ragsdell & Phillips, 1976), APPROX (Ragsdell & Phillips, 1976), SIMPLEX (Ragsdell & Phillips, 1976), RANDOM (Ragsdell & Phillips, 1976), CDE (Huang, Wang, & He, 2007), ESs (Mezura-Montes & Coello, 2005) are compared and are presented in Table 20. AVOA has obtained the best design guarantees with the least amount of fitness over other optimization algorithms.

4.5.3. Multi-plate disc clutch brake

This engineering problem's main objective is to optimize the multiple disc clutch brake's total weight concerning several variables, including actuating force, inner and outer radius, number of friction surfaces, and discs' thickness. It also has eight limitations. This engineering problem is expressed mathematically below:

$$f(x) = \Pi\left(r_o^2 - r_i^2\right)t(Z+1)\rho$$

subjectto :

$$g_1(x) = r_o - r_i - \Delta r \geq 0,$$

$$g_2(x) = l_{max} - (Z+1)(t+\delta) \geq 0,$$

$$g_3(x) = P_{max} - Prz \geq 0,$$

$$g_4(x) = P_{max}v_{srmax} - P_{rz}\nu_{sr} \geq 0,$$

$$g_5(x) = v_{srmax} - v_{sr} \geq 0,$$

$$g_6 = T_{max} - T \geq 0,$$

$$g_7(x) = M_h - sM_s \geq 0,$$

$$g_8(x) = T \geq 0,$$

where,

$$M_h = \frac{2}{3}\mu FZ\frac{r_o^3 - r_i^2}{r_o^2 - r_i^3}, P_{rz} = \frac{F}{\Pi(r_o^2 - r_i^2)},$$

$$v_{rz} = \frac{2\Pi n\left(r_o^3 - r_i^3\right)}{90\left(r_o^2 - r_i^2\right)}, T = \frac{I_z\Pi n}{30(M_h + M_f)}$$

$$\Delta r = 20mm, I_z = 55kgmm^2, P_{max} = 1MPa, F_{max} = 1000N,$$

$$T_{max} = 15s, \mu = 0.5, s = 1.5, M_s = 40Nm,$$

$$M_f = 3Nm, n = 250rpm,$$

$$v_{srmax} = 10m/s, l_{max} = 30mm, r_{imin} = 60,$$

$$r_{imax} = 80, r_{omin} = 90,$$

$$r_{omax} = 110, t_{min} = 1.5, t_{max} = 3, F_{min} = 600,$$

$$F_{max} = 1000, Z_{min} = 2, Z_{max} = 9,$$

The optimal results obtained by AVOA are compared with the results of algorithms TLBO (Rao et al., 2011), HHO (Heidari et al., 2019), WCA (Eskandar et al., 2012), PVS (Savsani & Savsani, 2016); and these results are shown in Table 21. A review of Table 21 shows that AVOA performs better than TLBO, WCA, and PVS algorithms while achieving close and competitive results compared to HHO algorithms.

4.5.4. Pressure vessel design problem

This problem is shown in Fig. 21. The primary purpose of this problem is to minimize the cost of construction. It has four constraints and four parameters, which are (z_1 - z_4): T_s (z_1, the thickness of the shell), T_h (z_2, the thickness of the head), r (z_3, inner radius), L (z_4, length of the section without the head).

The mathematical formula of this problem is as follows:

$$Consider\ \vec{z} = [z_1 z_2 z_3 z_4] = [T_s T_h RL],$$

$$Minimisef(\vec{z}) = 0.6224z_1z_3z_4 + 1.7781z_2z_3^2 + 3.1661z_1^2z_4 + 19.84z_1^2z_3,$$

$$Subjecttog_1(\vec{z}) = -z_1 + 0.0193z_3 \leq 0,$$

$$g_2(\vec{z}) = -z_3 + 0.00954z_3 \leq 0,$$

$$g_3(\vec{z}) = -\Pi z_3^2 z_4 - \frac{4}{3}\Pi z_3^3 + 1,296,000 \leq 0,$$

$$g_4(\vec{z}) = z_4 - 240 \leq 0,$$

The design space for this case is limited to $0 \leq z_1, z_2 \leq 99$, $0 \leq z_3, z_4 \leq 200$.

Results obtained in solving this problem using AVOA have been compared with other optimization algorithms WOA (Mirjalili & Lewis, 2016), BA (Gandomi et al., 2013), MDDE (Mezura-Montes et al., 2007), CPSO (He & Wang, 2007), CSS (Kaveh & Talatahari, 2010), BIANCA (Montemurro, Vincenti, & Vannucci, 2013), HPSO (He & Wang, 2007), G-QPSO (dos Santos Coelho, 2010), WEO (Kaveh & Bakhshpoori, 2016), IACO (Rosenbrock, 1960), MFO (Mirjalili, 2015), GA3 (Coello & Montes, 2002), GWO (Mirjalili et al., 2014), ESs (Mezura-Montes & Coello, 2005), GA (Deb, 1991), DELC (Wang & Li, 2010), Branch-bound (Sandgren) (Mirjalili & Lewis, 2016), Lagrangian multiplier (Kannan) (Mirjalili & Lewis, 2016). The optimal results obtained by using AVOA in other optimization algorithms are shown in Table 22. Also, by examining these results, it can be concluded that AVOA performs better than other algorithms in dealing with this problem, and the results obtained from AVOA are much better than other methods.

Table 20
Comparison of results for the welded beam design problem.

Algorithm	H	l	t	b	Optimal cost
AVOA	0.205730	3.470474	9.036621	0.205730	1.724852
GA1 (Deb, 1991)	0.248900	6.173000	8.178900	0.253300	2.433116
HS (Lee & Geem, 2004)	0.2442	6.2231	8.2915	0.2443	2.3807
GSA (Mirjalili & Lewis, 2016)	0.182129	3.856979	10	0.202376	1.879952
GA2 (Coello, 2000)	0.208800	3.420500	8.997500	0.210000	1.748310
DAVID (Ragsdell & Phillips, 1976)	0.2434	6.2552	8.2915	0.2444	2.3841
APPROX (Ragsdell & Phillips, 1976)	0.2444	6.2189	8.2915	0.2444	2.3815
SIMPLEX (Ragsdell & Phillips, 1976)	0.2792	5.6256	7.7512	0.2796	2.5307
RANDOM (Ragsdell & Phillips, 1976)	0.4575	4.7313	5.0853	0.66	4.1185
CDE (Huang et al., 2007)	0.203137	3.542998	9.033498	0.206179	1.733462
ESs (Mezura-Montes & Coello, 2005)	0.199742	3.61206	9.0375	0.206082	1.7373

Table 21
Comparison of results for multi-plate disc clutch brake.

Algorithm	TLBO (Rao et al., 2011)	HHO (Heidari, 2019)	WCA (Eskandar, 2012)	PVS (Savsani & Savsani, 2016)	AVOA
r_i	70	69.9999999992493	70	70	69.99999999994678
r_0	90	90	90	90	90
t	1	1	1	1	1
F	810	1000	910	980	1000
Z	3	2.312781994	3	3	2.312781982
Optimal cost	0.313656	0.259768993	0.313656	0.31366	0.259768992

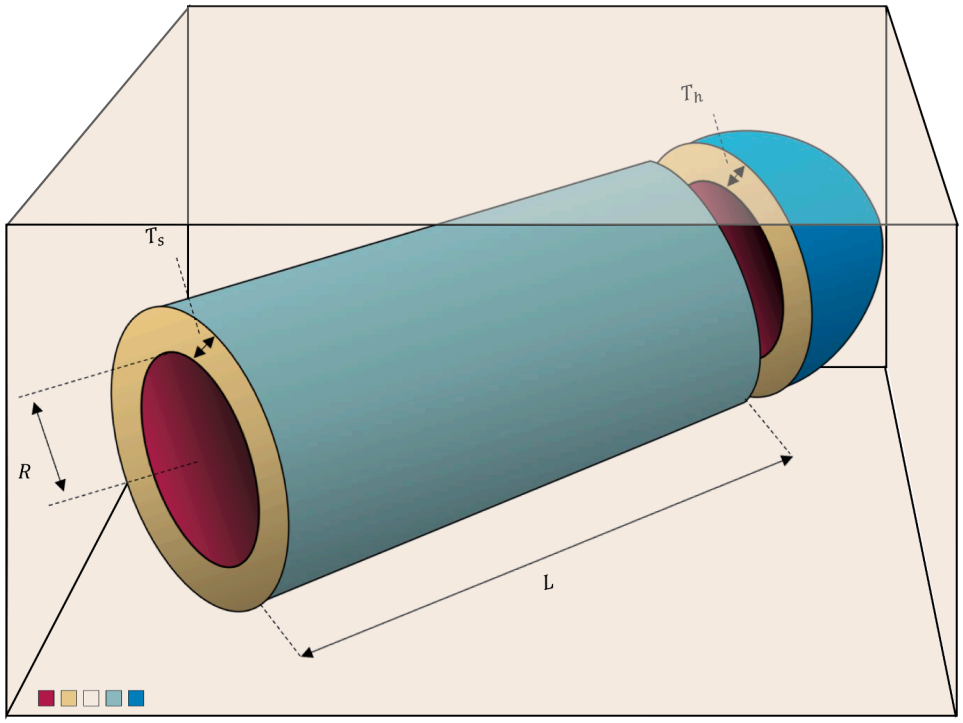

Fig. 21. Pressure vessel design problem.

4.5.5. Tension/compression spring design

This problem, shown in Fig. 22, is the primary purpose of minimizing a spring's weight. The variables used to design the problem are mean coil diameter (D), wire diameter (d), and several active coils (N).

When solving this problem, the minimum deflection, shear stress, and surge frequency constraints must be applied during the weight optimization process. It can be said mathematically as follows:

$$Consider\ \vec{z} = [z_1 z_2 z_3] = [dDN],$$

$$Minimisef(\vec{z}) = (z_3 + 2) z_2 z_1^2,$$

$$Subjecttog_1(\vec{z}) = 1 - \frac{z_2^3 z_3}{71785 z_1^4} \leq 0,$$

$$g_2(\vec{z}) = \frac{4z_2^2 - z_1 z_2}{12566(z_2 z_1^3 - z_1^4)} + \frac{1}{5108 z_1^2} \leq 0,$$

$$g_3(\vec{z}) = 1 - \frac{140.45 z_1}{z_2^2 z_3} \leq 0,$$

$$g_4(\vec{z}) = \frac{z_1 + z_2}{1.5} - 1 \leq 0,$$

To investigate, the results obtained by AVOA have been compared with several optimization algorithms that have solved this problem including Belegundu (Belegundu & Arora, 1985), GWO (Mirjalili et al., 2014), HEAA (Wang et al., 2009), CPSO (He & Wang, 2007), SFS (Salimi, 2015), Arora (Arora, 2004), MFO (Mirjalili, 2015), WOA (Mirjalili & Lewis, 2016), BA (Gandomi et al., 2013), GA2 (Deb, 1991), GSA (Rashedi et al., 2009), ESs (Mezura-Montes & Coello, 2005), Rank-iMDDE (Gong, Cai, & Liang, 2014), WCA (Eskandar et al., 2012), WEO (Kaveh & Bakhshpoori, 2016), GA3 (Coello & Montes, 2002), TEO (Kaveh & Dadras, 2017), DELC (Wang & Li, 2010), DEDS (Zhang et al., 2008), SSA (Mirjalili et al., 2017). The results of this comparison are also shown in Table 23, which shows that AVOA can produce good quality solutions and has been able to design well. On the other hand, the results are very close and competitive compared to the TEO and SFS optimization algorithms.

By examining and evaluating the proposed algorithm in various benchmarks and engineering problems, it can be seen that it performs better than other comparative algorithms and can be presented as a robust new metaheuristic algorithm.

4.5.6. Rolling element bearing design problem

This engineering problem is shown in Fig. 23 has ten variables and

Table 22
Comparison of results for pressure vessel design problem.

Algorithms	$T_s(x_1)$	$T_h(x_2)$	$R(x_3)$	$L(x_4)$	Optimal cost
AVOA	0.778954	0.3850374	40.360312	199.434299	5886.676593
WOA (Mirjalili & Lewis, 2016)	0.812500	0.437500	42.0982699	176.638998	6059.7410
BA (Gandomi, 2013)	0.812500	0.437500	42.098445	176.636595	6059.7143
MDDE (Mezura-Montes, 2007)	0.812500	0.437500	42.098446	176.636047	6059.701660
CPSO (He & Wang, 2007)	0.812500	0.437500	42.091266	176.746500	6061.0777
CSS (Kaveh & Talatahari, 2010)	0.812500	0.437500	42.103624	176.572656	6059.0888
BIANCA (Montemurro et al., 2013)	0.812500	0.437500	42.096800	176.658000	6059.9384
HPSO (He & Wang, 2007)	0.812500	0.437500	42.0984	176.6366	6059.7143
G-QPSO (dos Santos Coelho, 2010)	0.812500	0.437500	42.0984	176.6372	6059.7208
WEO (Kaveh & Bakhshpoori, 2016)	0.812500	0.437500	42.098444	176.636622	6059.71
IACO (Rosenbrock, 1960)	0.812500	0.437500	42.098353	176.637751	6059.7258
MFO (Mirjalili, 2015)	0.8125	0.4375	42.098445	176.636596	6059.7143
GA3 (Coello & Montes, 2002)	0.812500	0.437500	42.0974	176.6540	6059.9463
GWO (Mirjalili et al., 2014)	0.8125	0.4345	42.089181	176.758731	6051.5639
ESs (Mezura-Montes & Coello, 2005)	0.812500	0.437500	42.098087	176.640518	6059.7456
GA (Deb, 1991)	0.812500	0.437500	42.097398	176.654050	6059.9463
DELC (Wang & Li, 2010)	0.812500	0.437500	42.0984456	176.6365958	6059.7143
Branch-bound (Sandgren) (Mirjalili & Lewis, 2016)	1.125000	0.625000	47.700000	117.701000	8129.1036
Lagrangian multiplier (Kannan) (Mirjalili & Lewis, 2016)	1.125000	0.625000	58.291000	43.6900000	7198 0.0428

nine constraints.

That aim to maximize the load-carrying capacity is mathematically stated below:

$$Maximize C_d = f_c Z^{2/3} D_b^{1.8} if D \le 25.4mm$$

$$C_d = 3.647 f_c Z^{2/3} D_b^{1.4} if D > 25.4mm$$

Subjectto

$$g_1(\vec{z}) = \frac{\varphi_0}{2sin^{-1}(D_b/D_m)} - Z + 1 \le 0,$$

$$g_2(\vec{z}) = 2D_b - K_{Dmin}(D-d) > 0,$$

$$g_3(\vec{z}) = K_{Dmax}(D-d) - 2D_b \ge 0,$$

$$g_4(\vec{z}) = \zeta B_w - D_b \le 0,$$

$$g_5(\vec{z}) = D_m - 0.5(D+d) \ge 0,$$

$$g_6(\vec{z}) = (0.5+e)(D+d) - D_m \ge 0,$$

$$g_7(\vec{z}) = 0.5(D - D_m - D_b) - \epsilon D_b \ge 0,$$

$$g_8(\vec{z}) = f_i \ge 0.515,$$

$$g_9(\vec{z}) = f_o \ge 0.515,$$

where

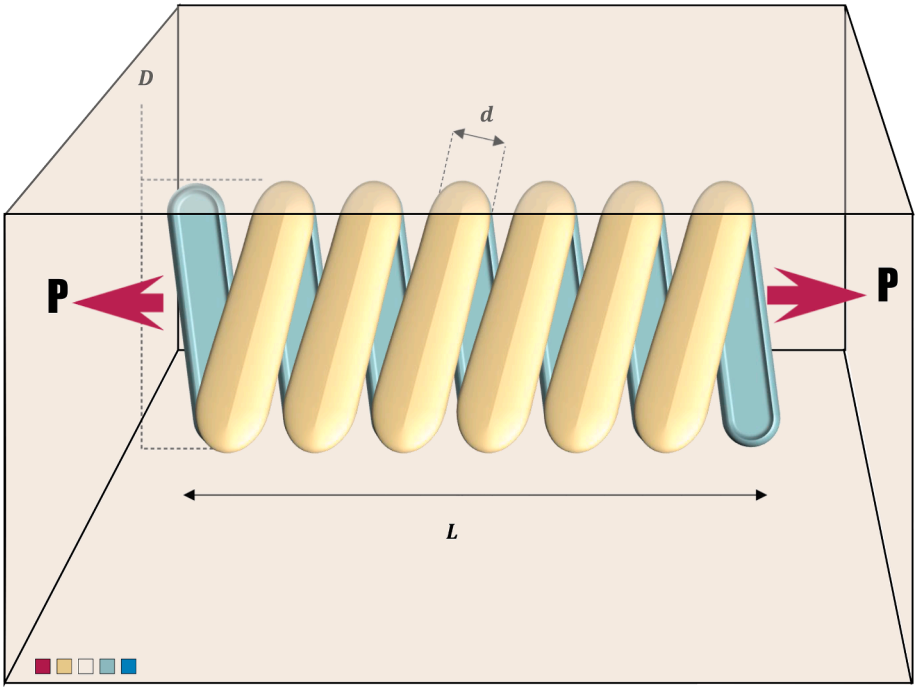

Fig. 22. Pressure vessel design problem.

Table 23
Comparison of results for tension/compression spring problem.

Algorithms	D	D	N	Optimal cost
AVOA	0.051669833	0.356255347	11.316126	0.012665240
Belegundu (Belegundu & Arora, 1985)	0.05	0.315900	14.250000	0.012833
GWO (Mirjalili et al., 2014)	0.05169	0.356737	11.28885	0.012666
HEAA (Wang, 2009)	0.051689	0.356729	11.288293	0.012665
CPSO (He & Wang, 2007)	0.051728	0.357644	11.244543	0.012674
SFS (Salimi, 2015)	0.051689061	0.356717736	11.288966	0.012665233
Arora (Arora, 2004)	0.053396	0.399180	9.185400	0.012730
MFO (Mirjalili, 2015)	0.051994457	0.36410932	10.868422	0.0126669
WOA (Mirjalili & Lewis, 2016)	0 0.051207	0 0.345215	12.004032	0.0126763
BA (Gandomi, 2013)	0.05169	0.35673	11.2885	0.012665
GA2 (Deb, 1991)	0.051480	0.351661	11.632201	0.012704
GSA (Rashedi et al., 2009)	0.050276	0.323680	13.525410	0.012702
ESs (Mezura-Montes & Coello, 2005)	0.051643	0.355360	11.397926	0.012698
Rank-iMDDE (Gong et al., 2014)	0.051689	0.35671718	11.288999	0.012665
WCA (Eskandar, 2012)	0.05168	0.356522	11.30041	0.012665
WEO (Kaveh & Bakhshpoori, 2016)	0.051685	0.356630	11.294103	0.012665
GA3 (Coello & Montes, 2002)	0.051989	0.363965	10.890522	0.012681
TEO (Kaveh & Dadras, 2017)	0.051775	0.3587919	11.16839	0.012665
DELC (Wang & Li, 2010)	0.051689	0.356717	11.288965	0.012665
DEDS (Zhang et al., 2008)	0.051689	0.356717	11.288965	0.012665
SSA (Mirjalili, 2017)	0.051207	0.345215	12.004032	0.0126763

$$f_c = 37.91\left[1+\left\{1.04\left(\frac{1-\gamma}{1+\gamma}\right)^{1.72}\left(\frac{f_i(2f_o-1)}{f_o(2f_i-1)}\right)^{0.41}\right\}^{10/3}\right]^{-0.3}$$

$$\times\left[\frac{\gamma^{0.3}(1-\gamma)^{1.39}}{(1+\gamma)^{1/3}}\right]\left[\frac{2f_i}{2f_i-1}\right]^{0.41}$$

$$x = [\{(D-d)/2-3(T/4)\}^2+\{D/2-T/4-D_b\}^2-\{d/2+T/4\}^2]$$

$$y = 2\{(D-d)/2-3(T/4)\}\{D/2-T/4-D_b\}$$

$$\varphi_o = 2\Pi - cos^{-1}\left(\frac{x}{y}\right)$$

$$\gamma = \frac{D_b}{D_m}, f_i = \frac{r_i}{D_b}, f_o = \frac{r_o}{D_b}, T = D-d-2D_b$$

$$D = 160, d = 90,$$

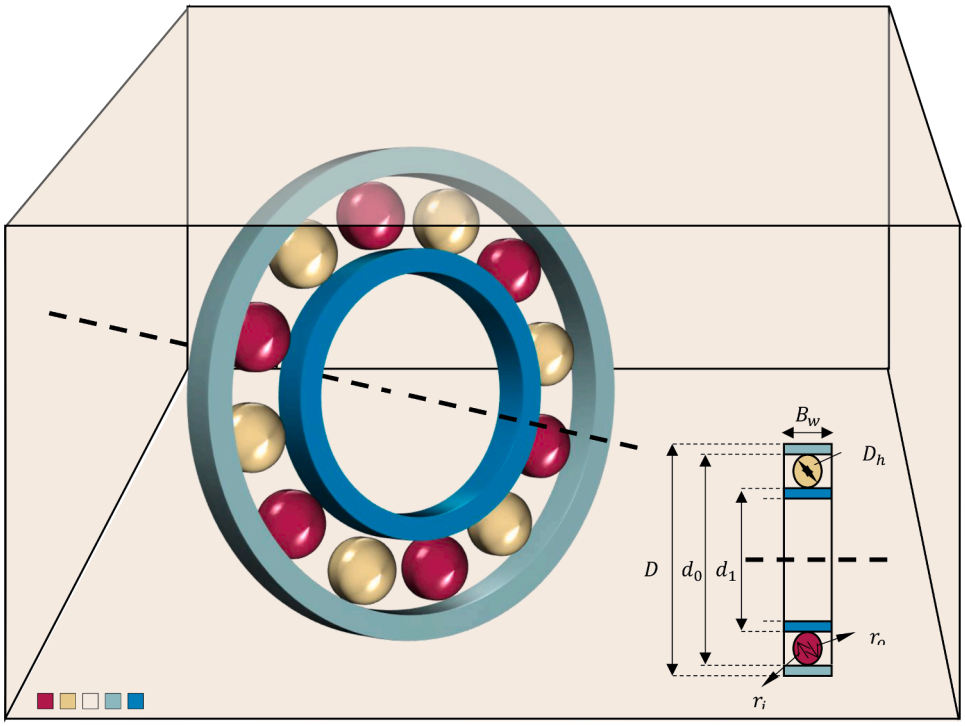

Fig. 23. Rolling element bearing design problem.

Table 24
Comparison of results for rolling element bearing design problem.

Algorithms	PVS (Savsani & Savsani, 2016)	TLBO (Rao et al., 2011)	GA4 (Gupta et al., 2007)	AVOA
D_m	125.719060	125.7191	125.717100	125.722717
D_b	21.425590	21.42559	21.423000	21.423294
Z	11.000000	11.000000	11.000000	11.001162
f_i	0.515000	0.515000	0.515000	0.515000
f_o	0.515000	0.515000	0.515000	0.515000
K_{Dmin}	0.400430	0.424266	0.415900	0.404428
K_{Dmax}	0.680160	0.633948	0.651000	0.618679
$\in$	0.300000	0.300000	0.300043	0.300000
e	0.079990	0.068858	0.022300	0.0691299
ξ	0.700000	0.799498	0.751000	0.602470
Maximum cost	81859.741210	81859.74	81843.30	85539.15785

$$B_w = 30, r_i = r_o = 11.0330.5(D+d) \le D_m \le 0.6(D+d),$$

$$0.15(D-d) \le D_b \le 0.45(D-d), 4 \le Z \le 50, 0.515 \le f_i and f_o \le 0.6,$$

$$0.4 \le K_{Dmin} \le 0.5,$$

$$0.6 \le K_{Dmax} \le 0.7, 0.3 \le e \le 0.4, 0.02 \le e \le 0.1,$$

$$0.6 \le \zeta \le 0.85$$

The results obtained by AVOA are compared with the optimization algorithms of PVS (Savsani & Savsani, 2016), TLBO (Rao et al., 2011), GA4 (Gupta, Tiwari, & Nair, 2007). By examining the results shown in Table 24, it is found that AVOA has achieved much better results than the other algorithms.

4.5.7. Cassini 2: Spacecraft trajectory optimization problem

One of the correct issues to evaluate optimization algorithms' performance is Multiple Gravity Assist (MGA), which is mathematically one of the optimization problems with a nonlinear limit and finite-dimensional. In other words, when a spaceship wants to travel from Earth to another planet, it uses MGA to find the best possible route. The spacecraft also has limitations on moving to other planets. Moreover, these limitations are necessary and essential to find the right path. These constraints can be achieved using the MGS with a Deep space maneuver (MGA-1DSM) problem. Therefore, using this problem, large-scale optimization problems can be solved.

Further details of these issues are described in (Cassioli et al., 2012; Izzo, 2010; Schlueter, 2012; Vinkó and Izzo, 2008). The Cassini 2 problem's primary goal is to find the best possible path to reach the planet Saturn using the Earth-to-Venus and Venus-to-Earth paths, and finally Jupiter to Saturn using deep space maneuvers. According to this path, different patterns can be determined for this path, making solving this problem very complex with 22 limitations. Given the results of evaluating the performance of AVOA and other optimization algorithms selected for comparison illustrated in Table 25, it can be concluded that AVOA was able to find a more suitable solution than other optimization algorithms.

4.5.8. Messenger: Spacecraft trajectory optimization problem

The Messenger problem is a path optimization problem to reach Mercury that has been implemented using the MGA-1DSM problem. Due to the path and order of movement between the planets in this issue, it is more complex and has 26 constraints. The results of the AVOA and other optimization algorithms in solving Messenger: Spacecraft Trajectory Optimization Problems are shown in Table 26. Although we can use the AVOA algorithm to find a better solution than other optimization algorithms, the solution obtained differs from the EO and MFO algorithms, which indicates a competitive performance between these algorithms.

4.5.9. Lennard-Jones potential problem

The Lennard-Jones Potential problem is a potential energy optimization problem to minimize molecular potential energy concerning the pure Lennard-Jones (LJ) cluster (Hoare, 1979; Moloi & Ali, 2005). It is a multi-modal optimization problem (Hoare, 1979), which has 30 limitations and dimensions—Lennard-Jones pair potential for N atoms, given by the Cartesian coordinates.

$$\vec{p}_i = \left\{ \vec{x}_i, \vec{y}_i, \vec{z}_i \right\}, i = 1, \cdots, N$$

Which is given as follows:

$$V_N(p) = \sum_{i=1}^{N-1} \sum_{j=i+1}^{N} \left(r_{ij}^{-12} - 2.r_{ij}^{-6} \right),$$

where $r_{ij} = \|\vec{p}_i - \vec{p}_i\|_2$ with gradient

Table 25
Comparison of results for Cassini 2: Spacecraft Trajectory Optimization Problem.

Algorithms	MFO	GWO	TSA	FFA	EO	AVOA
Tt0	−1000	−998.930192	−1000	−300.816357	−813.306116	−865.668410
Vinf	3	3.881950	3.009250	3.018228	3.001390	3
u	0.812645	0.450559	0.140415	0.751572	0.122989	9.30e-07
v	0.456991	0.640499	0.979454	0.269100	1	0.885853
T1	322.388770	400	355.506412	263.368511	169.030432	256.997348
T2	391.488895	499.263439	444.987107	405.510937	444.076628	408.106189
T3	128.419029	169.069537	66.458152	243.188731	63.635266	63.337310
T4	595.313284	589.957913	567.802773	1598.771390	551.870975	569.159515
T5	2200	1769.756577	2163.624558	2199.955887	2100.254840	2001.824430
eta1	0.346752	0.343112	0.419605	0.206914	0.010072	0.207577
eta2	0.010000	0.406296	0.172066	0.116102	0.090152	0.010542
eta3	0.010788	0.298430	0.728345	0.020155	0.349834	0.026929
eta4	0.010000	0.131444	0.139238	0.022256	0.024913	0.010000
eta5	0.899990	0.048243	0.019171	0.396211	0.383785	0.023093
r_p1	6	2.132062	1.365580	2.592061	1.412377	2.694092
r_p2	1.802242	1.503928	6	2.264369	2.976653	3.058354
r_p3	1.150000	6.127783	2.667007	1.150071	1.150688	1.150000
r_p4	89.926894	185.730246	167.113219	177.149202	96.088895	105.245047
b_incl1	3.141593	−1.212044	−1.126902	−1.550885	−1.387017	−1.488603
b_incl2	0.997268	2.313293	−0.574262	0.972126	−2.662249	−2.296031
b_incl3	−1.635556	0.140330	1.859224	−1.550300	−1.460296	−1.480176
b_incl4	−1.520395	−1.768837	−1.205054	1.368765	−1.409105	−1.521308
Minimum cost	18.079373	20.980714	24.605896	20.960024	16.362097	15.171915

Table 26
Comparison of results for Messenger: Spacecraft Trajectory Optimization Problem.

Algorithms	MFO	GWO	TSA	FFA	EO	AVOA
t0	1902.364811	1901.455464	2088.721463	2068.934257	2032.698792	2216.615442
Vinf	4.050000	3.560149	3.045955	3.795900	4.040619	3.565780
u	0.840586	0.787216	0.434033	0.666900	0.693936	0.000474
v	0.605011	0.413798	0.513188	0.518845	0.574787	0.322470
T1	373.946861	287.114058	323.715345	218.731733	236.788965	451.805792
T2	209.957837	144.096170	251.767337	441.251119	443.431416	487.499561
T3	291.642882	118.263227	245.838202	431.969647	444.476059	233.388722
T4	167.880898	177.597717	170.857340	349.208404	352.259713	350.919286
T5	175.943804	177.658369	181.647343	356.985053	351.721264	352.393831
T6	179.891410	175.878978	352.181483	347.700740	349.680269	263.028751
eta1	0.455639	0.198760	0.543330	0.290636	0.301618	0.349104
eta2	0.776265	0.015098	0.165663	0.132284	0.056577	0.426777
eta3	0.551376	0.232544	0.468173	0.369651	0.500410	0.060200
eta4	0.010000	0.179472	0.237455	0.090221	0.013905	0.010000
eta5	0.203178	0.200541	0.117333	0.379904	0.179869	0.262564
eta6	0.422833	0.020700	0.539783	0.154061	0.214756	0.010000
r_p1	1.100000	2.589951	5.469795	1.413043	1.137458	3.104201
r_p2	1.324203	2.955345	1.888253	6	5.477875	1.100000
r_p3	1.050000	4.640633	1.166690	2.506175	1.050002	3.918683
r_p4	6	1.625374	1.819400	4.237258	4.109871	4.806820
r_p5	4.945862	1.793623	1.184916	3.896266	4.703857	1.051619
b_incl1	1.628774	−0.775932	2.956381	−1.314154	−1.490212	−2.437367
b_incl2	−3.141593	2.989541	0.635766	−1.697342	−1.537325	1.854809
b_incl3	1.505063	−0.128824	0.303471	−2.038993	−3.140204	0.112028
b_incl4	−0.216599	−0.227998	−0.330576	−0.880073	−3.139964	3.141417
b_incl5	3.141593	−0.018299	0.394435	1.422127	2.676317	3.121624
Minimum cost	16.860205	20.554325	21.091370	17.713020	16.721914	16.361947

Table 27
Comparison of results for the Lennard-Jones potential problem.

Algorithms	MFO	GWO	TSA	FFA	EO	AVOA
x(1)	1.416504	0.255820	0.622205	0.884433	0.105175	0.345030
x(2)	3.686410	0.730303	1.748767	0.255559	0.625135	1.503041
x(3)	1.082861	0.768470	1.04e-09	1.642994	1.366766	0.992429
x(4)	1.534301	0.016643	−0.953055	0.001638	0.860202	0.282883
x(5)	3.353444	0.549480	0.001554	0.539284	0.582864	0.576242
x(6)	2.011316	−0.829992	−0.661348	3.162107	0.736038	1.302393
x(7)	−3.903341	−0.083182	−0.505123	0.445842	0.076537	−0.159941
x(8)	3.767257	−0.089971	−0.865548	−0.324140	−0.025796	0.249484
x(9)	−2.277135	1.151557	−0.696309	0.936118	0.616760	0.480557
x(10)	1.967110	−0.014371	−0.571184	1.504310	−0.809343	0.815476
x(11)	4.499556	0.083321	−0.270891	−0.608356	−0.322937	−0.020983
x(12)	0.914657	0.020983	−1.526452	1.320995	0.348924	0.758585
x(13)	−4.058396	−0.723934	−0.377515	1.543428	−0.040158	0.612487
x(14)	4.750000	0.403426	−1.128572	0.524843	0.955222	0.835508
x(15)	−2.234039	0.594605	0.297083	0.849062	0.437474	0.338649
x(16)	−4.494627	−0.424965	−2.436684	5	−0.222609	−0.577658
x(17)	4.210410	−0.684620	−4.030792	1.158178	0.349338	0.114326
x(18)	−2.954524	0.450541	−3.284560	−1.122023	−0.301677	1.379445
x(19)	2.291952	0.691200	−0.971542	5.218708	−0.003685	−0.537930
x(20)	3.813372	0.762388	0.431816	0.223484	1.325947	1.029761
x(21)	1.561473	−0.112457	0.291978	−0.543159	−0.491236	0.993735
x(22)	2.276717	−0.250852	3.601123	0.693535	0.692661	−0.370835
x(23)	3.599797	1.068155	−1.754918	−0.754984	0.690366	0.917145
x(24)	0.589606	0.012284	2.553447	1.826601	−0.220094	1.956546
x(25)	2.009555	−0.594314	−0.314324	−0.123462	−0.024031	1.187308
x(26)	2.902706	−0.489230	−0.233014	0.027109	−0.600723	0.895239
x(27)	1.255854	−0.517767	0.018549	1.608426	−0.198832	1.129722
x(28)	−4.799733	−0.877085	0.103935	−4.182153	0.885739	−0.253036
x(29)	4.117652	0.440859	0.005652	4.157162	−0.206309	1.200065
x(30)	−2.007703	−0.387264	−0.848757	0.560424	0.131492	0.080763
Minimum cost	−18.299281	−26.102613	−13.051830	−10.590915	−24.862582	−26.329419

Table 28
Comparison of results for static economic load dispatch problem.

Algorithms	MFO	GWO	TSA	FFA	EO	AVOA
x(1)	83.322980	70.647612	106.112515	36	98.513927	113.999884
x(2)	56.028647	92.598648	36	84.109163	109.480900	61.893597
x(3)	120	63.317598	85.573427	64.767848	77.810178	119.999970
x(4)	170.574485	187.548600	181.860672	165.753369	119.473179	189.690572
x(5)	73.886984	90.526601	49.526256	90.828669	69.711918	96.999762
x(6)	140	138.791589	124.976887	109.624652	131.045960	139.984893
x(7)	300	264.352608	196.648893	267.370431	289.542097	298.316079
x(8)	270.279248	135.027006	293.811133	300	296.927086	299.414186
x(9)	300	289.211584	300	300	285.509831	299.972862
x(10)	130	205.956740	156.482179	260.909367	270.259727	299.999811
x(11)	94	277.215679	345.806588	175.492684	253.169118	96.132319
x(12)	360.752785	185.763529	250.198898	370.348366	367.285889	374.998757
x(13)	453.025792	427.540409	500	468.389704	495.969412	125
x(14)	500	500	500	394.883939	405.524046	125.000069
x(15)	500	274.935565	270.639905	433.783720	401.282719	499.999757
x(16)	431.829894	496.713990	500	439.203795	490.975756	499.999281
x(17)	435.666133	465.132741	429.336272	500	500	220.000470
x(18)	226.228549	380.009025	404.604102	361.699908	474.044038	499.996902
x(19)	544.422824	537.701111	527.175411	417.785969	393.774413	547.918248
x(20)	550	520.962314	550	550	451.475995	549.994988
x(21)	331.600053	524.370866	525.511008	499.256713	540.496859	548.010593
x(22)	502.654350	475.089509	550	550	544.763777	549.999676
x(23)	330.411419	550	528.064968	423.025459	549.999928	549.998770
x(24)	498.400464	479.873102	522.153972	529.480201	258.018982	549.982092
x(25)	550	522.923588	494.119033	526.736880	467.616496	549.999925
x(26)	550	536.090164	550	447.333347	532.145930	550
x(27)	10	67.162320	51.608200	20.819159	18.686359	11.800953
x(28)	61.233484	35.785534	65.690509	18.912207	47.433319	10.103418
x(29)	18.469576	64.280653	27.408085	32.432086	12.832593	10.289573
x(30)	47	83.044875	76.469023	83.797541	81.111668	96.994419
x(31)	190	129.444241	180.175126	85.714828	184.313107	190
x(32)	190	109.556000	63.623107	158.086112	73.622696	190
x(33)	190	174.075604	104.801645	144.360778	182.978154	60.000911
x(34)	163.821842	133.119895	151.442180	196.005766	115.183720	90.112454
x(35)	174.507508	168.502412	177.678703	140.966065	93.234351	91.281689
x(36)	200	167.293714	122.546861	194.939693	167.126151	197.061124
x(37)	110	101.521717	30.682474	90.625616	35.398474	109.842470
x(38)	110	54.160220	35.337986	43.228063	35.942734	25.256500
x(39)	48.131426	50.332608	88.058766	54.181994	65.560500	109.971652
x(40)	483.751672	469.423327	345.883893	469.155794	511.757927	549.980875
Minimum cost	1.32e+05	1.34e+05	1.35e+05	1.32e+05	1.32e+05	1.29e+05

Table 29
Results and statistical analysis on Plant (A, B).

Same order IIR system modeling for Plant (A)					
MSE	PSO (Mohammadi et al., 2019)	GSA (Mohammadi et al., 2019)	IPO (Mohammadi et al., 2019)	GA (Mohammadi et al., 2019)	AVOA
Min	4.5298e−05	3.944e−05	4.7799e−05	7.8604e−05	**3.8547e−05**
Mean	7.7398e−05	0.00011143	9.5737e−05	0.0014774	**6.9734e−05**
Max	0.00012485	0.00046248	0.00022601	0.0095933	**0.0001027**
STD	1.7107e−05	6.9407e−05	3.4047e−05	0.0018016	**1.2428e−05**
Reduced-order IIR system modeling for Plant (A)					
Min	0.0027955	0.0029346	0.0029402	0.00405	**0.0024712**
Mean	0.0037106	0.0037366	0.0036725	0.0049063	**0.0029857**
Max	0.0050009	0.0045917	0.0044194	0.0057504	**0.0042511**
STD	0.00046478	0.00035947	0.00038962	0.00052748	**0.0003078**
Exact order IIR system modeling for Plant (B)					
Min	5.1985e−05	4.8656e−05	4.8542e−05	8.8033e−05	**4.7543e−05**
Mean	8.0999e−05	7.7387e−05	6.5836e−05	8.8033e−05	**6.2785e−05**
Max	9.8948e−05	9.8739e−05	8.1884e−05	8.8033e−05	**8.0289e−05**
STD	1.6851e−05	1.8004e−05	1.1977e−05	0	**1.0649e−05**
Reduced-order IIR system modeling for Plant (B)					
Min	6.0534e−05	4.7195e−05	5.8187e−05	9.0526e−05	**4.6457e−05**
Mean	8.2009e−05	8.1244e−05	8.2263e−05	0.00015238	**8.0185e−05**
Max	0.00010584	0.00024126	0.00012361	0.00028314	**0.00019694**
STD	1.7583e−05	4.3547e−05	**1.5695e−05**	6.7789e−05	2.6792e−05

$$\nabla_j V_N(p) = -12\sum_{i=1,i\neq j}^{N}\left(r_{ij}^{-14} - r_{ij}^{-8}\right)\left(\overrightarrow{p}_j - \overrightarrow{p}_i\right), j = 1,\cdots,N$$

The first variable due to the second atom i.e. $x_1 \in [0,4]$, t, then the second and third variables are such that $x_2 \in [0,4]$ a and $x_3 \in [0,\pi]$. The coordinates x_i for any other atom is taken to be bound in the range:

$$\left[-4 - \frac{1}{4}\left\lfloor\frac{i-4}{3}\right\rfloor, 4 + \frac{1}{4}\left\lfloor\frac{i-4}{3}\right\rfloor\right]$$

Table 27 illustrates the evaluation of AVOA and other optimization algorithms in solving the Lennard-Jones Potential Problem.

Given the results shown in Table 27, it can be concluded that AVOA has been able to find a much better solution than the MFO, TSA, and FFA algorithms, but there is a close and competitive performance between AVOA and GWO.

4.5.10. Static economic load dispatch (ELD) problem (instance 4)

The static ELD problem is used to minimize production units' fuel costs in a specific period, usually one working hour. In this case, the generator's operating limitations are due to the ramp rate limitations and some functional areas' prohibition. This problem includes 40 restrictions. Two models are used for this problem: smooth cost functions and non-smooth cost function, which are as follows.

Objective Function: The objective function related to production cost can be considered as follows:

$$\text{Minimize}: F = \sum_{i=1}^{N_G} f_i(P_i)$$

The cost function can be described for a unit with a valve point loading effect as follows:

$$f_i(P_i) = a_i P_i^2 + b_i P_i + c_i + \left|e_i sin\left(f_i\left(P_i^{min} - P_i\right)\right)\right|$$

There are several limitations to this, including power balance constraints to consider the energy balance and ramp rate limits and prohibited operating zones.

Power Balance Constraints or Demand Constraints: These constraints are based on balancing the total system output and the total system load (P_D) and losses(P_L).

$$\sum_{i=1}^{N_G} P_i = P_D + P_L$$

Where, P_L is obtained using B- coefficients, given by:

$$P_L = \sum_{i=1}^{N_G}\sum_{j=1}^{N_G} P_i B_{ij} P_j + \sum_{i=1}^{N_G} B_{0i} P_i + B_{00}$$

Generator Constraints: The upper and lower bound of each generating unit using a pair of inequality constraints are as follows:

$$P_i^{min} \le P_i \le P_i^{max}$$

Ramp Rate Limits: The existence of limitations in units is due to ramp rate constraints, which are as follows.

If power generation increases, $P_i - P_i^{t-1} \le UR_i$

If power generation decreases,$P_i^{t-1} - P_i \le DR_i$

Limitations related to generator performance are as follows:

$$\max\left(P_i^{min}, UR_i - P_i\right) \le P_i \le min\left(P_i^{max}, P_i^{t-1} - DR_i\right)$$

Prohibited Operating Zones: Prohibition of work activity in some areas to save is described below:

$$P_i \le \widehat{P}^{pz} and P_i \le \widehat{P}^{pz}$$

The results obtained from AVOA and other optimization algorithms in solving the Static Economic Load Dispatch Problem are shown in Table 28.

The results indicate that the EO, FFA, and MFO algorithms are performed very closely. However, the performance of TSA and GWO algorithms is much worse than other optimization algorithms. However, AVOA has presented a much better solution than the matching optimization algorithms.

4.5.11. IIR digital filtering systems modeling problem

For modeling systems based on IIR digital filter, the model IIR is repeatedly adjusted to minimize the error between the unknown system and the model IIR. Filter models include two types of challenging IIR plants. The input–output relation of the IIR system is given by:

$$y(n) = -\sum_{k=1}^{n} b_k y(n-k) + \sum_{k=0}^{m} a_k u(n-k)$$

The adaptive IIR digital filtering system transfer function is as follows:

$$H(z) = \frac{\sum_{i=0}^{M} b_i z^{-i}}{1 + \sum_{i=1}^{N} a_i z^{-i}}$$

In solving this problem, the main goal is to find the IIR filter coefficient vector [a_i, b_i] so that the adaptive IIR filtering system's estimated result is close to and similar to the system's actual result. fitness function J_v given by the following: $MinJ_v for v \in V$, $v = [b_0, b_1, \cdots, b_M, a_1, a_2, \cdots, a_N]$ that represents with filter coefficients vector. See (Mohammadi & Zahiri, 2017; Mohammadi, Zahiri, & Razavi, 2019; Oualla, 2021) for more information. The results obtained from the IIR digital filtering systems modeling problem obtained from PSO (Mohammadi et al., 2019), GSA (Mohammadi et al., 2019), IPO (Mohammadi et al., 2019), GA (Mohammadi et al., 2019), and AVOA algorithms are shown in Table 29.

Table 29 shows the results obtained from the solution of the IIR digital filtering systems modeling problem. According to the results shown, the AVOA algorithm has performed better than the compared algorithms and has also been able to have better and higher quality solutions than the compared algorithms.

Given the assessment obtained from the AVOA to solve the engineering problems and the results obtained from other optimization algorithms that have been compared with other optimization algorithms, AVOA has presented a high performance in solving engineering problems in small and large dimensions well as high complexity.

5. Conclusion and future works

In this paper, a new metaheuristic algorithm was proposed, inspired by lifestyle and food search and competition for food by various vultures in the African continent, and is a population-based algorithm. Because of the optimal use of the two best solutions in the algorithm, as a representative of the two vulture's more powerful groups than the other vultures, a balance between diversity and resonance is created, which increases the performance of the proposed model. The proposed algorithm was broken down into four distinct stages, and each step was presented and formulated in theory to solve the continuous optimization problems. The proposed metaheuristic algorithm performs the search space using several different and varied mechanisms in the exploitation and exploration stages that focus more on exploration in the early stages of the optimization operation than on exploitation in the later stages of the optimization operation. This algorithm has low computational complexity and is more flexible than other metaheuristic algorithms and is also the point of distinction and strength of the proposed algorithm in balancing the resonance and variability of the proposed algorithm. It has been able to achieve its main features against large-scale issues.

On the other hand, the transition from the exploration phase to exploitation is a specific feature of the proposed algorithm, making it completely different from other metaheuristic algorithms. After focusing on exploring different search space solutions, more focus is on promising solutions and searches near promising solutions. The proposed

metaheuristic algorithm is evaluated using many mathematical problems and has been compared with other powerful metaheuristic algorithms such as PSO, DE and BBO, TFO, SSA, and GWO WOA, MFO, FFA. In this comparison, it was found that the proposed metaheuristic algorithm is very promising and powerful compared to the existing algorithms. Also, in terms of computational complexity and running time of this algorithm, it is much shorter than all the comparable algorithms and performs well in large-scale problems. Impressive Results of the proposed algorithm have made the proposed algorithm's details and its application to other functions a necessary topic for future research.

Further evaluation studies are needed to discover the extent of the algorithm's ability to solve optimization problems. Comparative studies with other meta-discoveries with complicated test functions and real-world problems will show the algorithm's complex strengths and weaknesses. Another research topic could be to study the sensitivity of the parameters and adjust the proposed algorithm's parameters and their effect on maintaining an optimal balance between the exploration and exploitation phases of the algorithm optimization process. Extending the improved version of the proposed algorithm for multi-objective or discrete optimization problems and various complex problems can be pursued as future research topics.

References

Abdollahzadeh, B., & Gharehchopogh, F. S. (2021). A multi-objective optimization algorithm for feature selection problems. *Engineering with Computers*, 1–19.

Abualigah, L., et al. (2020). The arithmetic optimization algorithm. *Computer Methods in Applied Mechanics and Engineering, 376*, Article 113609.

Abualigah, L., et al. (2021). Aquila optimizer: A novel meta-heuristic optimization algorithm. *Computers & Industrial Engineering*, Article 107250.

Anderson, D.J., Horwitz, R. J. (1979). Competitive interactions among vultures and their avian competitors. Ibis 121(4): p. 505-509.

Arora, J.S., Introduction to optimum design. 2004: Elsevier.

Askarzadeh, A. (2014). Bird mating optimizer: An optimization algorithm inspired by bird mating strategies. *Communications in Nonlinear Science and Numerical Simulation, 19*(4), 1213–1228.

Askarzadeh, A. (2016). A novel metaheuristic method for solving constrained engineering optimization problems: Crow search algorithm. *Computers & Structures, 169*, 1–12.

Attwell, G. R. (1963). Some observations on feeding habits, behaviour and inter-relationships of Northern Rhodesian vultures. *Ostrich, 34*(4), 235–247.

Balachandran, M., et al. (2012). Optimizing properties of nanoclay–nitrile rubber (NBR) composites using face centred central composite design. *Materials & Design, 35*, 854–862.

Bamford, A. J., Monadjem, A., & Hardy, I. C. (2009). An effect of vegetation structure on carcass exploitation by vultures in an African savanna. *Ostrich, 80*(3), 135–137.

Bansal, J. C., et al. (2014). Spider monkey optimization algorithm for numerical optimization. *Memetic Computing, 6*(1), 31–47.

Belegundu, A. D., & Arora, J. S. (1985). A study of mathematical programming methods for structural optimization. Part I: Theory. *International Journal for Numerical Methods in Engineering, 21*(9), 1583–1599.

Benyamin, A., Farhad, S. G., & Saeid, B. Discrete farmland fertility optimization algorithm with metropolis acceptance criterion for traveling salesman problems. International Journal of Intelligent Systems.

BosE, M., & Sarrazin, F. (2007). Competitive behaviour and feeding rate in a reintroduced population of Griffon Vultures Gyps fulvus. *Ibis, 149*(3), 490–501.

Boussaïd, I., Lepagnot, J., & Siarry, P. (2013). A survey on optimization metaheuristics. *Information Sciences, 237*, 82–117.

Buckley, N. J. (1996). Food finding and the influence of information, local enhancement, and communal roosting on foraging success of North American vultures. *The Auk, 113*(2), 473–488.

Cassioli, A., et al. (2012). Machine learning for global optimization. *Computational Optimization and Applications, 51*(1), 279–303.

Chou, J.-S., & Truong, D.-N. (2021). A novel metaheuristic optimizer inspired by behavior of jellyfish in ocean. *Applied Mathematics and Computation, 389*, Article 125535.

Coello, C. A. C. (2000). Use of a self-adaptive penalty approach for engineering optimization problems. *Computers in Industry, 41*(2), 113–127.

Coello, C. A. C., & Montes, E.n. M. (2002). Constraint-handling in genetic algorithms through the use of dominance-based tournament selection. *Advanced Engineering Informatics, 16*(3), 193–203.

Cuevas, E., et al. (2013). A swarm optimization algorithm inspired in the behavior of the social-spider. *Expert Systems with Applications, 40*(16), 6374–6384.

Deb, K. (1991). Optimal design of a welded beam via genetic algorithms. *AIAA journal, 29*(11), 2013–2015.

Derrac, J.n., et al. (2011). A practical tutorial on the use of nonparametric statistical tests as a methodology for comparing evolutionary and swarm intelligence algorithms. *Swarm and Evolutionary Computation, 1*(1), 3–18.

Dokeroglu, T., et al. (2019). A survey on new generation metaheuristic algorithms. *Computers & Industrial Engineering, 137*, Article 106040.

dos Santos Coelho, L. (2010). Gaussian quantum-behaved particle swarm optimization approaches for constrained engineering design problems. *Expert Systems with Applications, 37*(2), 1676–1683.

Erol, O. K., & Eksin, I. (2006). A new optimization method: Big bang–big crunch. *Advances in Engineering Software, 37*(2), 106–111.

Eskandar, H., et al. (2012). Water cycle algorithm–A novel metaheuristic optimization method for solving constrained engineering optimization problems. *Computers & Structures, 110*, 151–166.

Faramarzi, A., et al. (2020). Equilibrium optimizer: A novel optimization algorithm. *Knowledge-Based Systems, 191*, Article 105190.

Gandomi, A. H., et al. (2013). Bat algorithm for constrained optimization tasks. *Neural Computing and Applications, 22*(6), 1239–1255.

Gandomi, A. H., Yang, X.-S., & Alavi, A. H. (2013). Cuckoo search algorithm: A metaheuristic approach to solve structural optimization problems. *Engineering with Computers, 29*(1), 17–35.

Gautestad, A. O., & Mysterud, I. (2006). Complex animal distribution and abundance from memory-dependent kinetics. *ecological complexity, 3*(1), 44–55.

Geem, Z. W., Kim, J. H., & Loganathan, G. V. (2001). A new heuristic optimization algorithm: Harmony search. *Simulation, 76*(2), 60–68.

Gharehchopogh, F. S., & Gholizadeh, H. (2019). A comprehensive survey: Whale optimization algorithm and its applications. *Swarm and Evolutionary Computation, 48*, 1–24.

Gharehchopogh, F. S., Maleki, I., & Dizaji, Z. A. (2021). Chaotic vortex search algorithm: Metaheuristic algorithm for feature selection. *Evolutionary Intelligence*, 1–32.

Gharehchopogh, F. S., Shayanfar, H., & Gholizadeh, H. (2019). A comprehensive survey on symbiotic organisms search algorithms. *Artificial Intelligence Review*, 1–48.

Gong, W., Cai, Z., & Liang, D. (2014). Engineering optimization by means of an improved constrained differential evolution. *Computer Methods in Applied Mechanics and Engineering, 268*, 884–904.

Gupta, S., Tiwari, R., & Nair, S. B. (2007). Multi-objective design optimisation of rolling bearings using genetic algorithms. *Mechanism and Machine Theory, 42*(10), 1418–1443.

He, Q., & Wang, L. (2007). An effective co-evolutionary particle swarm optimization for constrained engineering design problems. *Engineering Applications of Artificial Intelligence, 20*(1), 89–99.

He, Q., & Wang, L. (2007). A hybrid particle swarm optimization with a feasibility-based rule for constrained optimization. *Applied Mathematics and Computation, 186*(2), 1407–1422.

Heidari, A. A., et al. (2019). Harris hawks optimization: Algorithm and applications. *Future Generation Computer Systems, 97*, 849–872.

Hoare, M. (1979). Structure and dynamics of simple microclusters. *Advances in Chemical Physics, 40*, 49–135.

Holland, J. H. (1992). Genetic algorithms. *Scientific American, 267*(1), 66–73.

Houston, D. (1974). Food searching in griffon vultures. *African Journal of Ecology, 12*(1), 63–77.

Houston, D. (1974). The role of griffon vultures Gyps africanus and Gyps ruppellii as scavengers. *Journal of Zoology, 172*(1), 35–46.

Houston, D. C. (1988). Competition for food between Neotropical vultures in forest. *Ibis, 130*(4), 402–417.

Huang, F.-Z., Wang, L., & He, Q. (2007). An effective co-evolutionary differential evolution for constrained optimization. *Applied Mathematics and computation, 186*(1), 340–356.

Hussain, K., et al. (2019). Metaheuristic research: A comprehensive survey. *Artificial Intelligence Review, 52*(4), 2191–2233.

Hussain, S. F., & Iqbal, S. (2018). Genetic ACCGA: Co-similarity based Co-clustering using genetic algorithm. *Applied Soft Computing, 72*, 30–42.

Izzo, D. (2010). Global optimization and space pruning for spacecraft trajectory design. *Spacecraft Trajectory Optimization, 1*, 178–200.

Jackson, A. L., Ruxton, G. D., & Houston, D. C. (2008). The effect of social facilitation on foraging success in vultures: A modelling study. *Biology Letters, 4*(3), 311–313.

Jia, H., et al. (2019). Dynamic harris hawks optimization with mutation mechanism for satellite image segmentation. *Remote Sensing, 11*(12), 1421.

Karaboga, D., & Basturk, B. (2007). Artificial bee colony (ABC) optimization algorithm for solving constrained optimization problems. *International fuzzy systems association world congress*. Springer.

Kashan, A. H. (2014). League Championship Algorithm (LCA): An algorithm for global optimization inspired by sport championships. *Applied Soft Computing, 16*, 171–200.

Kaur, S., et al. (2020). Tunicate Swarm Algorithm: A new bio-inspired based metaheuristic paradigm for global optimization. *Engineering Applications of Artificial Intelligence, 90*, Article 103541.

Kaveh, A., & Bakhshpoori, T. (2016). Water evaporation optimization: A novel physically inspired optimization algorithm. *Computers & Structures, 167*, 69–85.

Kaveh, A., & Dadras, A. (2017). A novel meta-heuristic optimization algorithm: Thermal exchange optimization. *Advances in Engineering Software, 110*, 69–84.

Kaveh, A., & Farhoudi, N. (2013). A new optimization method: Dolphin echolocation. *Advances in Engineering Software, 59*, 53–70.

Kaveh, A., & Ghazaan, M. I. (2017). Vibrating particles system algorithm for truss optimization with multiple natural frequency constraints. *Acta Mechanica, 228*(1), 307–322.

Kaveh, A., & Mahdavi, V. (2014). Colliding bodies optimization: A novel meta-heuristic method. *Computers & Structures, 139*, 18–27.

Kaveh, A., & Talatahari, S. (2010). A novel heuristic optimization method: Charged system search. *Acta Mechanica, 213*(3–4), 267–289.

Kendall, C., et al. (2012). Mechanisms of coexistence in vultures: Understanding the patterns of vulture abundance at carcasses in Masai Mara National Reserve. *Kenya. The Condor, 114*(3), 523–531.
Kirkpatrick, S., Gelatt, C. D., & Vecchi, M. P. (1983). Optimization by simulated annealing. *Science, 220*(4598), 671–680.
Krishnanand, K., & Ghose, D. (2009). Glowworm swarm optimization for simultaneous capture of multiple local optima of multimodal functions. *Swarm intelligence, 3*(2), 87–124.
Kumar, N., Singh, N., & Vidyarthi, D. P. (2021). Artificial lizard search optimization (ALSO): A novel nature-inspired meta-heuristic algorithm. *Soft Computing*, 1–23.
Lee, K. S., & Geem, Z. W. (2004). A new structural optimization method based on the harmony search algorithm. *Computers & Structures, 82*(9–10), 781–798.
Liang, J., Qu, B., & Suganthan, P. (2013). Problem definitions and evaluation criteria for the CEC 2014 special session and competition on single objective real-parameter numerical optimization. Computational Intelligence Laboratory, Zhengzhou University, Zhengzhou China and Technical Report, Nanyang Technological University, Singapore, 635.
Liu, H., Cai, Z., & Wang, Y. (2010). Hybridizing particle swarm optimization with differential evolution for constrained numerical and engineering optimization. *Applied Soft Computing, 10*(2), 629–640.
Manjarres, D., et al. (2013). A survey on applications of the harmony search algorithm. *Engineering Applications of Artificial Intelligence, 26*(8), 1818–1831.
Meteyer, C. U., et al. (2005). Pathology and proposed pathophysiology of diclofenac poisoning in free-living and experimentally exposed oriental white-backed vultures (Gyps bengalensis). *Journal of Wildlife Diseases, 41*(4), 707–716.
Mezura-Montes, E.n., et al. (2007). Multiple trial vectors in differential evolution for engineering design. *Engineering Optimization, 39*(5), 567–589.
Mezura-Montes, E.n., & Coello, C. A. C. (2005). A simple multimembered evolution strategy to solve constrained optimization problems. *IEEE Transactions on Evolutionary Computation, 9*(1), 1–17.
Mirjalili, S. (2015). Moth-flame optimization algorithm: A novel nature-inspired heuristic paradigm. *Knowledge-based Systems, 89*, 228–249.
Mirjalili, S., et al. (2017). Salp Swarm Algorithm: A bio-inspired optimizer for engineering design problems. *Advances in Engineering Software, 114*, 163–191.
Mirjalili, S., & Lewis, A. (2016). The whale optimization algorithm. *Advances in Engineering Software, 95*, 51–67.
Mirjalili, S., Mirjalili, S. M., & Hatamlou, A. (2016). Multi-verse optimizer: A nature-inspired algorithm for global optimization. *Neural Computing and Applications, 27*(2), 495–513.
Mirjalili, S., Mirjalili, S. M., & Lewis, A. (2014). Grey wolf optimizer. *Advances in Engineering Software, 69*, 46–61.
Mohammadi, A., & Zahiri, S. H. (2017). IIR model identification using a modified inclined planes system optimization algorithm. *Artificial Intelligence Review, 48*(2), 237–259.
Mohammadi, A., Zahiri, S. H., & Razavi, S. M. (2019). Infinite impulse response systems modeling by artificial intelligent optimization methods. *Evolving Systems, 10*(2), 221–237.
Mohmmadzadeh, H., & Gharehchopogh, F. S. (2021). An efficient binary chaotic symbiotic organisms search algorithm approaches for feature selection problems. *The Journal of Supercomputing*, 1–43.
Mokhlesi, O., et al. (2013). Improved gravitational search algorithm (GSA) using fuzzy logic. *Journal of Intelligent Procedures in Electrical Technology, 4*, 41–52.
Moloi, N., & Ali, M. (2005). An iterative global optimization algorithm for potential energy minimization. *Computational Optimization and Applications, 30*(2), 119–132.
Montemurro, M., Vincenti, A., & Vannucci, P. (2013). The automatic dynamic penalisation method (ADP) for handling constraints with genetic algorithms. *Computer Methods in Applied Mechanics and Engineering, 256*, 70–87.
Mozaffari, M. H., Abdy, H., & Zahiri, S. H. (2016). IPO: An inclined planes system optimization algorithm. *Computing and Informatics, 35*(1), 222–240.
Mozaffari, M. H., Abdy, H., Zahiri, S. H. (2013). Application of inclined planes system optimization on data clustering. in 2013 First Iranian Conference on Pattern Recognition and Image Analysis (PRIA). IEEE.
Mundy, P.J., The comparative biology of southern African vultures. Vol. 1. 1982: Vulture Study Group.
Mundy, P.J., The vultures of Africa. 1992: Acorn Books.
Muthiah-Nakarajan, V., & Noel, M. M. (2016). Galactic swarm optimization: A new global optimization metaheuristic inspired by galactic motion. *Applied Soft Computing, 38*, 771–787.
Nedić, N., et al. (2017). Simulation of hydraulic check valve for forestry equipment. *International Journal of Heavy Vehicle Systems, 24*(3), 260–276.
Ogada, D., & Buij, R. (2011). Large declines of the Hooded Vulture Necrosyrtes monachus across its African range. *Ostrich, 82*(2), 101–113.
Oualla, H., et al. (2021). Comparison of algorithms for identification of IIR systems from binary measurements on the output. in E3S Web of Conferences. EDP Sciences.
Petrides, G. A. (1959). Competition for food between five species of East African vultures. *The Auk, 76*(1), 104–106.
Prinzinger, R., et al. (2002). Energy metabolism and body temperature in the Griffon Vulture (Gyps fulvus) with comparative data on the Hooded Vulture (Necrosyrtes monachus) and the White-backed Vulture (Gyps africanus). *Journal für Ornithologie, 143*(4), 456–467.
Pršić, D., Nedić, N., & Stojanović, V. (2017). A nature inspired optimal control of pneumatic-driven parallel robot platform. *Proceedings of the Institution of Mechanical Engineers, Part C: Journal of Mechanical Engineering Science, 231*(1), 59–71.
Qi, X., Zhu, Y., & Zhang, H. (2017). A new meta-heuristic butterfly-inspired algorithm. *Journal of Computational Science, 23*, 226–239.
Ragsdell, K. and D. Phillips, Optimal design of a class of welded structures using geometric programming. 1976.
Rahnema, N., & Gharehchopogh, F. S. (2020). An improved artificial bee colony algorithm based on whale optimization algorithm for data clustering. *Multimedia Tools and Applications, 79*(43), 32169–32194.
Rao, R. V., Savsani, V. J., & Vakharia, D. (2011). Teaching–learning-based optimization: A novel method for constrained mechanical design optimization problems. *Computer-Aided Design, 43*(3), 303–315.
Rao, R. V., Savsani, V. J., & Vakharia, D. (2012). Teachingâ€“learning-based optimization: An optimization method for continuous non-linear large scale problems. *Information Sciences, 183*(1), 1–15.
Rashedi, E., Nezamabadi-Pour, H., & Saryazdi, S. (2009). GSA: A gravitational search algorithm. *Information Sciences, 179*(13), 2232–2248.
Ray, T., & Saini, P. (2001). Engineering design optimization using a swarm with an intelligent information sharing among individuals. *Engineering Optimization, 33*(6), 735–748.
Rosenbrock, H. (1960). An automatic method for finding the greatest or least value of a function. *The Computer Journal, 3*(3), 175–184.
Rosewell, J., Shorrocks, B., & Edwards, K. (1990). Competition on a divided and ephemeral resource: Testing the assumptions. I. Aggregation. *The Journal of Animal Ecology*, 977–1001.
Sadollah, A., et al. (2013). Mine blast algorithm: A new population based algorithm for solving constrained engineering optimization problems. *Applied Soft Computing, 13*(5), 2592–2612.
Salimi, H. (2015). Stochastic fractal search: A powerful metaheuristic algorithm. *Knowledge-Based Systems, 75*, 1–18.
Sang, H.-Y., Pan, Q.-K., & Duan, P.-Y. (2019). Self-adaptive fruit fly optimizer for global optimization. *Natural Computing, 18*(4), 785–813.
Saremi, S., Mirjalili, S., & Lewis, A. (2017). Grasshopper optimisation algorithm: Theory and application. *Advances in Engineering Software, 105*, 30–47.
Savsani, P., & Savsani, V. (2016). Passing vehicle search (PVS): A novel metaheuristic algorithm. *Applied Mathematical Modelling, 40*(5–6), 3951–3978.
Schlueter, M. (2012). *Nonlinear mixed integer based optimization technique for space applications*. University of Birmingham.
Shah-Hosseini, H. (2009). The intelligent water drops algorithm: A nature-inspired swarm-based optimization algorithm. *International Journal of Bio-Inspired Computation, 1*(1–2), 71–79.
Shah-Hosseini, H. (2011). Principal components analysis by the galaxy-based search algorithm: A novel metaheuristic for continuous optimisation. *International Journal of Computational Science and Engineering, 6*(1–2), 132–140.
Shahraki, N. S. Zahiri, S. -H. (2017). Inclined planes optimization algorithm in optimal architecture of MLP neural networks. in 2017 3rd International Conference on Pattern Recognition and Image Analysis (IPRIA). IEEE.
Shayanfar, H., & Gharehchopogh, F. S. (2018). Farmland fertility: A new metaheuristic algorithm for solving continuous optimization problems. *Applied Soft Computing, 71*, 728–746.
Sheikhpour, S., Sabouri, M., & Zahiri, S. -H. (2013). A hybrid Gravitational search algorithm—Genetic algorithm for neural network training. in 2013 21st Iranian Conference on Electrical Engineering (ICEE). IEEE.
Shlesinger, M. F. (1989). Levy flights: Variations on a theme. *Physica D: Nonlinear Phenomena, 38*(1–3), 304–309.
Simon, D. (2008). Biogeography-based optimization. *IEEE Transactions on Evolutionary Computation, 12*(6), 702–713.
Sims, D. W., et al. (2008). Scaling laws of marine predator search behaviour. *Nature, 451*(7182), 1098–1102.
Stojanovic, V., et al. (2016). Application of cuckoo search algorithm to constrained control problem of a parallel robot platform. *The International Journal of Advanced Manufacturing Technology, 87*(9), 2497–2507.
Stojanovic, V., He, S., & Zhang, B. (2020). State and parameter joint estimation of linear stochastic systems in presence of faults and non-Gaussian noises. *International Journal of Robust and Nonlinear Control, 30*(16), 6683–6700.
Stojanovic, V., & Nedic, N. (2016). A nature inspired parameter tuning approach to cascade control for hydraulically driven parallel robot platform. *Journal of Optimization Theory and Applications, 168*(1), 332–347.
Storn, R., & Price, K. (1997). Differential evolution–a simple and efficient heuristic for global optimization over continuous spaces. *Journal of global optimization, 11*(4), 341–359.
Sur, C., Sharma, S., & Shukla, A. (2013). Egyptian vulture optimization algorithmâ€“a new nature inspired meta-heuristics for knapsack problem. *The 9th International Conference on Computing and InformationTechnology (IC2IT2013)*. Springer.
Tilahun, S. L., & Ong, H. C. (2015). Prey-predator algorithm: A new metaheuristic algorithm for optimization problems. *International Journal of Information Technology & Decision Making, 14*(06), 1331–1352.
Tsai, J.-F. (2005). Global optimization of nonlinear fractional programming problems in engineering design. *Engineering Optimization, 37*(4), 399–409.
Vinkó, T., & Izzo, D. (2008). Global optimisation heuristics and test problems for preliminary spacecraft trajectory design. Advanced Concepts Team, ESATR ACT-TNT-MAD-GOHTPPSTD, Sept.
Viswanathan, G., et al. (2000). LÃ©vy flights in random searches. *Physica A: Statistical Mechanics and its Applications, 282*(1–2), 1–12.
Wang, Y., et al. (2009). Constrained optimization based on hybrid evolutionary algorithm and adaptive constraint-handling technique. *Structural and Multidisciplinary Optimization, 37*(4), 395–413.
Wang, L., & Li, L.-P. (2010). An effective differential evolution with level comparison for constrained engineering design. *Structural and Multidisciplinary Optimization, 41*(6), 947–963.

Xue, Y., et al. (2018). An evolutionary computation based feature selection method for intrusion detection. *Security and Communication Networks, 2018*.
Yang, X.-S. (2010). A new metaheuristic bat-inspired algorithm. In *Nature inspired cooperative strategies for optimization (NICSO 2010)* (pp. 65–74). Springer.
Yang, X. -S. (2008). Firefly algorithm. Nature-inspired metaheuristic algorithms 20: p. 79-90.
Yang, X. -S., (2010). Nature-inspired metaheuristic algorithms. Luniver Press.
Zahiri, S. H. (2012). Fuzzy gravitational search algorithm an approach for data mining. *Iranian Journal of Fuzzy Systems, 9*(1), 21–37.
Zhang, J., et al. (2018). Queuing search algorithm: A novel metaheuristic algorithm for solving engineering optimization problems. *Applied Mathematical Modelling, 63*, 464–490.
Zhang, M., Luo, W., & Wang, X. (2008). Differential evolution with dynamic stochastic selection for constrained optimization. *Information Sciences, 178*(15), 3043–3074.